Vol. 9, no. 2, 2025 eISSN 2587-8999
PEER-REVIEWED SCIENTIFIC AND THEORETICAL JOURNAL

Computational Mathematics and Information Technologies

Computational Mathematics

Mathematical Modelling

Information Technologies

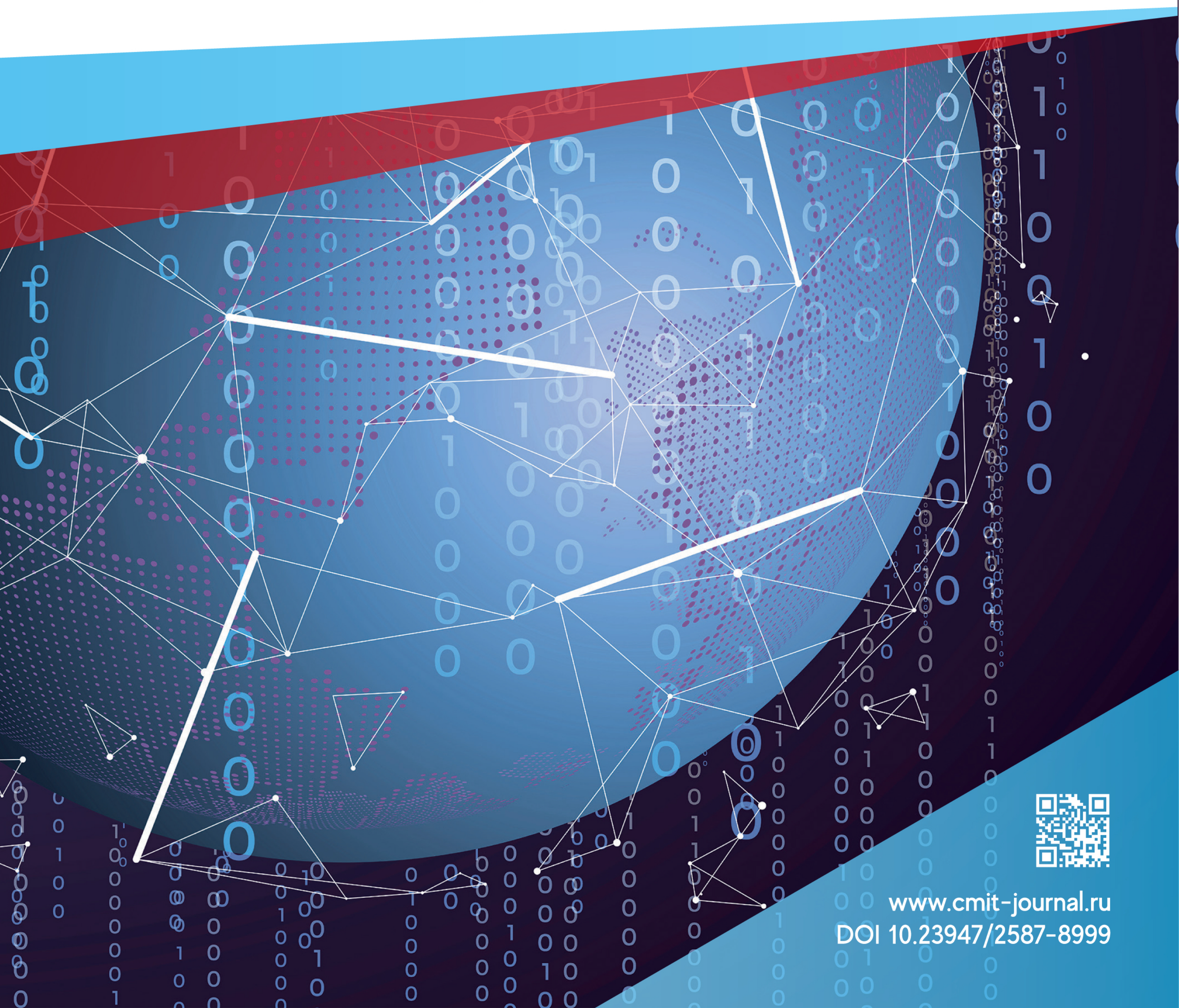

www.cmit-journal.ru
DOI 10.23947/2587-8999

Computational Mathematics and Information Technologies

Peer-reviewed scientific and theoretical journal

eISSN 2587–8999
Published since 2017
Periodicity — 4 issues per year
DOI: 10.23947/2587–8999

Founder and Publisher — Don State Technical University (DSTU), Rostov-on-Don, Russian Federation

The journal "Computational Mathematics and Information Technologies" publishes reviews, original articles and short reports on mathematical modeling, numerical methods and information technologies for solving complex and topical problems of science and modern technology. Research areas include continuum mechanics, fluid dynamics, Earth sciences, chemistry, biology, image processing and pattern recognition, parallel computing theory and its applications, big database and artificial intelligence technologies, etc.

The journal "Computational Mathematics and Information Technologies" accepts scientific and review articles for publication in accordance with the sections:

1. Computational Mathematics
2. Mathematical Modelling
3. Information Technologies

Registration:	Mass media registration certificate ЭЛ № ФС 77–66529 dated July 21, 2016 issued by the Federal Service for Supervision of Communications, Information Technology and Mass Media
Indexing and Archiving:	RISC, Crossref, Cyberleninka
Website:	https://cmit-journal.ru
Address of the Editorial Office:	1, Gagarin sq., Rostov-on-Don, 344003, Russian Federation
E-mail:	CMIT-EJ@yandex.ru
Telephone:	+7 (863) 273–85–14
Date of publication No. 2, 2025:	30.06.2025

Computational Mathematics and Information Technologies

Рецензируемый научно-теоретический журнал

eISSN 2587–8999

Издается с 2017 года

Периодичность — 4 выпуска в год

DOI: 10.23947/2587–8999

Учредитель и издатель — Федеральное государственное бюджетное образовательное учреждение высшего образования «Донской государственный технический университет» (ДГТУ), г. Ростов-на-Дону, Российская Федерация

Журнал «Computational Mathematics and Information Technologies» публикует обзоры, оригинальные статьи и краткие сообщения, посвященные математическому моделированию, численным методам и информационным технологиям для решения сложных и актуальных проблем науки и современной технологии. Область применения исследований — это механика сплошных сред, гидроаэродинамика, науки о Земле, химия, биология, обработка изображений и распознавание образов, теория параллельных вычислений и ее приложения, технологии больших баз данных и искусственного интеллекта и т. д.

Журнал «Computational Mathematics and Information Technologies» принимает к публикации научные и обзорные статьи в соответствии с разделами:

1. Вычислительная математика
2. Математическое моделирование
3. Информационные технологии

Регистрация:	Свидетельство о регистрации средства массовой информации ЭЛ № ФС 77 – 66529 от 21 июля 2016 г., выдано Федеральной службой по надзору в сфере связи, информационных технологий и массовых коммуникаций
Индексация и архивация:	РИНЦ, CrossRef, CyberLeninka
Сайт:	https://cmit-journal.ru
Адрес редакции:	344003, Российская Федерация, г. Ростов-на-Дону, пл. Гагарина, 1
E-mail:	CMIT-EJ@yandex.ru
Телефон:	+7 (863) 273–85–14
Дата выхода № 2, 2025 в свет:	30.06.2025

Contents

Содержание

COMPUTATIONAL MATHEMATICS
ВЫЧИСЛИТЕЛЬНАЯ МАТЕМАТИКА

UDC 519.63

Original Theoretical Research

https://doi.org/10.23947/2587-8999-2025-9-2-7-21

A Finite Difference Scheme with Improved Boundary Approximation for the Heat Conduction Equation with Third-Type Boundary Conditions

Alexander E. Chistyakov, Inna Yu. Kuznetsova
Don State Technical University, Rostov-on-Don, Russian Federation
✉ ikuznecova@donstu.ru

Abstract

Introduction. The development, analysis, and modification of finite difference schemes tailored to the specific features of the considered problem can significantly enhance the accuracy of modeling complex systems. In simulations of various processes, including hydrodynamic phenomena in shallow water bodies, it has been observed that for problems with third-type (Robin) boundary conditions, the theoretical error order of spatial discretization drops from second-order to first-order accuracy, which in turn decreases the overall accuracy of the numerical solution. The present study addresses the relevant issue of how the approximation of third-type boundary conditions affects the accuracy of the numerical solution to the heat conduction problem. It also proposes a finite difference scheme with improved boundary approximation for the heat conduction equation with third-type boundary conditions and compares the accuracy of the numerical solutions obtained by the authors with known benchmark solutions.

Materials and Methods. The paper considers the one-dimensional heat conduction equation with third-type boundary conditions, for which an analytical solution is available. The problem is discretized, and it is shown that under standard boundary approximation, the theoretical order of approximation error for the second-order differential operator in the diffusion equation is $O(h)$. To improve the accuracy of the numerical solution under specific third-type boundary conditions, a finite difference scheme is proposed. This scheme achieves second-order accuracy $O(h^2)$, for the differential operator not only at interior nodes but also at the boundary nodes of the computational domain.

Results. Test problems were used to compare the accuracy of numerical solutions obtained using the proposed scheme and those based on the standard boundary approximation.

Discussion and Conclusion. Numerical experiments demonstrate that the proposed scheme with enhanced boundary approximation for the heat conduction equation under specific third-type boundary conditions exhibits an effective accuracy order close to 2, which corresponds to the theoretical prediction. It is noteworthy that the scheme with standard boundary approximation also demonstrates an effective accuracy order close to 2, despite the lower theoretical order of boundary approximation. Importantly, the numerical error of the proposed scheme decreases significantly faster compared to the scheme with standard boundary treatment.

Keywords: heat conduction equation, third-type boundary conditions, numerical solution, approximation error

Funding. This research was supported by the Russian Science Foundation, grant no. 22–71–10102, https://rscf.ru/project/22-71-10102/

For Citation. Chistyakov A.E., Kuznetsova I.Yu. A Finite Difference Scheme with Improved Boundary Approximation for the Heat Conduction Equation with Third-Type Boundary Conditions. *Computational Mathematics and Information Technologies*. 2025;9(2):7–21. https://doi.org/10.23947/2587-8999-2025-9-2-7-21

Оригинальное теоретическое исследование

Разностная схема с улучшенной аппроксимацией на границе для уравнения теплопроводности с граничными условиями третьего рода

А.Е. Чистяков, И.Ю. Кузнецова
Донской государственный технический университет, г. Ростов-на-Дону, Российская Федерация
ikuznecova@donstu.ru

Аннотация
Введение. Построение разностных схем, их исследование и модификация с учетом специфики рассматриваемой задачи позволяет повысить точность моделирования сложных систем. При моделировании различных процессов, включая гидродинамические процессы в мелководных водоемах, было отмечено, что при решении задач с граничными условиями третьего рода теоретическая оценка порядка погрешности аппроксимации падает со второго порядка погрешности относительно пространственных шагов расчетной сетки до первого порядка, а, следовательно, падает и точность численного решения задачи. Настоящая работа посвящена актуальной проблеме исследования влияния аппроксимации граничных условий третьего рода на точность численного решения задачи теплопроводности, а также построению разностной схемы с улучшенной аппроксимацией граничных условий для уравнения теплопроводности с граничными условиями третьего рода и сравнению точности численных решений, полученных авторами, с известными решениями.
Материалы и методы. Рассматривается уравнение теплопроводности с граничными условиями третьего рода, для которого получено аналитическое решение. Проведена аппроксимация рассмотренной задачи и показано, что при стандартной аппроксимации задачи на границе расчетной области теоретическая оценка порядка погрешности аппроксимации дифференциального оператора второго порядка в уравнении диффузии составляет $O(h)$. Для повышения точности численного решения в случае граничных условий третьего рода специального вида предложена разностная схема, имеющая погрешность аппроксимации дифференциального оператора второго порядка $O(h^2)$, как во внутренних, так и в граничных узлах расчетной области.
Результаты исследования. На тестовых задачах проведено сравнение точности численных решений, полученных на основе предлагаемой схемы и схемы со стандартной аппроксимацией границы.
Обсуждение и заключение. Из проведенных численных экспериментов видно, что предложенная схема с улучшенной аппроксимацией на границе расчетной области для уравнения теплопроводности при граничных условиях третьего рода специального вида имеет эффективный порядок точности около 2, что соответствует полученной теоретической оценке. При этом стоит отметить, что разностная схема со стандартной аппроксимацией на границе расчетной области также имеет эффективный порядок точности, близкий к 2, несмотря на полученную теоретическую оценку порядка погрешности аппроксимации для граничных узлов. Важно отметить, что для предложенной схемы расчетная погрешность численного решения падает существенно быстрее, чем для решения на основе схемы со стандартной аппроксимацией на границе.

Ключевые слова: уравнение теплопроводности, граничные условия третьего рода, численное решение, погрешность аппроксимации

Финансирование. Исследование выполнено за счет гранта Российского научного фонда № 22–71–10102, https://rscf.ru/project/22-71-10102/

Для цитирования. Чистяков А.Е., Кузнецова И.Ю. Разностная схема с улучшенной аппроксимацией на границе для уравнения теплопроводности с граничными условиями третьего рода. *Computational Mathematics and Information Technologies*. 2025;9(2):7–21. https://doi.org/10.23947/2587-8999-2025-9-2-7-21

Introduction. The heat conduction equation is widely used to describe a broad class of problems related to the modeling of three-dimensional diffusion processes [1]. This diffusion equation has been extensively studied, and its solutions are broadly applied in practice to describe many physical phenomena. Analytical approaches to solving this equation are presented in [2, 3], while numerical methods for solving the heat conduction equation with first- and second-type boundary conditions are discussed in [4, 5].

When designing complex engineering structures, it is necessary to account for the impact of ambient temperature regimes. In many cases, heat propagation in such systems is described using the heat conduction equation with third-type (Robin) boundary conditions [6]. Therefore, the goal of this study is to develop a finite difference scheme with improved boundary condition approximation and to evaluate the performance of the proposed scheme on benchmark problems. This approach allows for a comparison of the accuracy of numerical solutions obtained from various finite difference schemes under different initial and boundary conditions. In [7, 8], the Burgers equation is used as a test case; in [9, 10], the transport equation; and in [11, 12], the convection-diffusion equation.

The problem of improving the accuracy of numerical solutions has been addressed by many prominent Russian and international researchers. Notably, P.N. Vabishchevich [13, 14] studied finite difference schemes for solving second-order parabolic-type equations involving specially structured non-self-adjoint operators. B.N. Chetverushkin has contributed significantly to the development, analysis, and parameter tuning of difference schemes for applied problems, particularly in the context of high-performance computing architectures [15, 16]. V.F. Tishkin explored the modification of discontinuous Galerkin methods for gas and hydrodynamic modeling [17, 18]. The use of a regularized finite difference scheme for hydrodynamic problems was discussed in [19], with its accuracy analyzed in [20]. Methods to improve the order of accuracy in the grid-characteristic method for two-dimensional linear elasticity problems are addressed in [21], and extended to three dimensions in [22]. A numerical approach for heat and mass transfer in two-phase fluids is presented in [23], while [24] proposes a finite difference scheme for single-phase filtration in fractured media, and [25] investigates two-phase filtration in complex environments.

Developing finite difference schemes and modifying existing ones with consideration of problem-specific features enables improved modeling accuracy of complex systems [26]. In simulations of various processes, including hydrodynamic flows in shallow water bodies, it has been observed that, for problems with third-type boundary conditions, the theoretical order of approximation error for spatial discretization drops from second order to first order. Consequently, the accuracy of the numerical solution is reduced. A.I. Sukhinov [27] recommended a more detailed study of the approximation of problems with third-type boundary conditions. Accordingly, this work is devoted to examining the impact of third-type boundary condition approximation on the accuracy of the numerical solution to the heat conduction problem. It also presents the construction of a finite difference scheme with improved boundary approximation and compares the accuracy of solutions obtained with the proposed scheme against those derived using a standard boundary approximation scheme on benchmark problems.

Materials and Methods

1. Analytical Solution of the Heat Conduction Equation

Let us consider the homogeneous heat conduction equation

$$\frac{\partial u}{\partial t} = a\frac{\partial^2 u}{\partial x^2},\ 0 < x < l,\ 0 < t < T, \tag{1}$$

subject to the initial condition

$$u(x,t)\big|_{t=0} = u_0(x) \tag{2}$$

and third-kind (Robin) boundary conditions

$$\left(\frac{\partial}{\partial x}u(x,t) - \alpha u(x,t)\right)\bigg|_{x=0} = \beta,\ \left(\frac{\partial}{\partial x}u(x,t) + \alpha u(x,t)\right)\bigg|_{x=l} = -\beta. \tag{3}$$

To find the analytical solution of the boundary value problem (1)–(3), we introduce a transformation $u(x,t) = v(x,t) - \beta/\alpha$, which reduces the problem to one with homogeneous third-kind boundary conditions:

$$\begin{gathered}\frac{\partial v}{\partial t} = a\frac{\partial^2 v}{\partial x^2},\ 0 < x < l,\ 0 < t < T,\ v(x,t)\big|_{t=0} = u_0(x) + \frac{\beta}{\alpha},\\ \left(\frac{\partial}{\partial x}v(x,t) - \alpha v(x,t)\right)\bigg|_{x=0} = 0,\ \left(\frac{\partial}{\partial x}v(x,t) + \alpha v(x,t)\right)\bigg|_{x=l} = 0.\end{gathered} \tag{4}$$

We seek the solution of (4) in the form:

$$v(x,t) = X(x)T(t). \tag{5}$$

Substituting (5) into the differential equation (4) and separating variables yields:

$$\frac{1}{a}\frac{T'(t)}{T(t)} = \frac{X''(x)}{X(x)} = -\lambda^2. \tag{6}$$

The boundary conditions in (4) transform into:

$$\left(X'(0) - \alpha X(0)\right)T(t) = 0,\ \left(X'(l) + \alpha X(l)\right)T(t) = 0. \tag{7}$$

Thus, taking (7) into account and assuming that $v(x,t) \neq 0$ we arrive at the Sturm–Liouville problem for the function $X(x)$:

$$\begin{gathered}X'' + \lambda^2 X = 0,\ 0 < x < l,\\ X'(0) - \alpha X(0) = 0,\ X'(l) + \alpha X(l) = 0.\end{gathered} \tag{8}$$

The general solution to (8) is:

$$X(x) = C_1 \cos\lambda x + C_2 \sin\lambda x. \tag{9}$$

Considering the boundary conditions in (8) and the general form (9), the eigenfunctions $X_k(x)$ are written as:

$$X_k(x) = \lambda_k \cos\lambda_k x + \alpha \sin\lambda_k x,\ k = 1,\ 2,\ldots\ , \tag{10}$$

where λ_k, $k = 1, 2,\ldots$ are the eigenvalues of the problem (8), which are the positive roots of the transcendental equation

$$2\ \text{ctg}\ \lambda l = \frac{\lambda}{\alpha} - \frac{\alpha}{\lambda}. \tag{11}$$

For the function $T(t)$ based on equation (6) and under the condition $\lambda = \lambda_k$ we arrive at the following problem:

$$T'(t) + a\lambda_k T(t) = 0,$$

the general solution of which is given by

$$T_k(t) = C_k \exp\left(-a\lambda_k^2 t\right),\ k = 1,\ 2,\ldots\ . \tag{12}$$

Then, taking into account equations (5), (10), and (12), the solution to problem (4) can be written in the form:

$$v(x,t) = \sum_{k=1}^{\infty} C_k \left(\lambda_k \cos\lambda_k x + \alpha \sin\lambda_k x\right) \exp\left(-a\lambda_k^2 t\right), \tag{13}$$

where λ_k, $k = 1, 2,\ldots$ are the positive roots of equation (11).

To determine the coefficients C_k we use the initial condition of problem (4):

$$\sum_{k=1}^{\infty} C_k \left(\lambda_k \cos\lambda_k x + \alpha \sin\lambda_k x\right) = u_0(x) + \beta/\alpha,$$

i. e., this represents the expansion of a function $f(x) = u_0(x) + \beta/\alpha$ for $0 \le x \le l$ into a Fourier series in terms of the eigenfunctions of the Sturm–Liouville problem (8). Then, assuming the eigenfunctions $X_k(x)$, $k = 1, 2,\ldots$ are orthogonal on the interval $0 \le x \le l$ the coefficients C_k are given by:

$$C_k = \frac{1}{\|X_k\|^2} \int_0^l f(x) \left(\lambda_k \cos\lambda_k x + \alpha \sin\lambda_k x\right) dx, \tag{14}$$

where $f(x) = u_0(x) + \beta/\alpha$,

$$\|X_k\|^2 = \int_0^l \left(\lambda_k \cos\lambda_k x + \alpha \sin\lambda_k x\right)^2 dx = \frac{\lambda_k^2 + \alpha^2}{2} + \frac{\lambda_k^2 - \alpha^2}{4\lambda_k} \sin 2\lambda_k l - \frac{\alpha}{2} \cos 2\lambda_k l + \frac{\alpha}{2}. \tag{15}$$

Taking into account the condition (11) for $\lambda = \lambda_k$, $k = 1, 2,\ldots$ and the trigonometric identities

$$\sin 2x = \frac{2\ \text{tg}\ x}{1 + \text{tg}^2 x},\ \cos 2x = \frac{1 - \text{tg}^2 x}{1 + \text{tg}^2 x}$$

the expression for the norm squared of the eigenfunctions $X_k(x)$ in (15) becomes:

$$\|X_k\|^2 = \frac{\left(\lambda_k^2 + \alpha^2\right) l + 2\alpha}{2}. \tag{16}$$

Thus, expression (14) for the coefficients C_k, $k = 1, 2,\ldots$ can be rewritten in the form:

$$C_k = \frac{2}{\left(\lambda_k^2 + \alpha^2\right) l + 2\alpha} \int_0^l \left(u_0(x) - \frac{\beta}{\alpha}\right) \left(\lambda_k \cos\lambda_k x + \alpha \sin\lambda_k x\right) dx = C_k^{(1)} + C_k^{(2)}, \tag{17}$$

where

$$C_k^{(1)} = \frac{2}{\left(\lambda_k^2 + \alpha^2\right) l + 2\alpha} \int_0^l u_0(x) \left(\lambda_k \cos\lambda_k x + \alpha \sin\lambda_k x\right) dx,$$

$$C_k^{(2)} = \frac{2\beta}{\left(\lambda_k^2 + \alpha^2\right)\alpha l + 2\alpha^2} \int_0^l \left(\lambda_k \cos\lambda_k x + \alpha \sin\lambda_k x\right) dx = \frac{2\beta}{\left(\lambda_k^2 + \alpha^2\right)\alpha l + 2\alpha^2} \left(\sin\lambda_k l - \frac{\alpha}{\lambda_k}\left(\cos\lambda_k l - 1\right)\right) = \tag{18}$$

$$=\frac{2\beta}{\left(\lambda_k^2+\alpha^2\right)\alpha l+2\alpha^2}\left(\frac{\alpha}{\lambda_k}+\sin\lambda_k l\left(1-\frac{\alpha}{\lambda_k}\mathrm{ctg}\lambda_k l\right)\right)=\frac{2\beta}{\left(\lambda_k^2+\alpha^2\right)\alpha l+2\alpha^2}\left(\frac{\alpha}{\lambda_k}+\frac{\lambda_k^2+\alpha^2}{2\lambda_k^2}\frac{(-1)^{k+1}}{\sqrt{1+\mathrm{ctg}^2\lambda_k l}}\right)=$$

$$=\frac{2\beta}{\lambda_k\left(\lambda_k^2+\alpha^2\right)l+2\lambda_k\alpha}\left(1+(-1)^{k+1}\right),$$

Thus, for $k = 2n$ the coefficients $C_k^{(2)} = 0$. Then the expression for the coefficients $C_k^{(2)}$ will be written as:

$$C_{2n}^{(2)}=0,\ C_{2n+1}^{(2)}=\frac{4\beta}{\lambda_{2n+1}\left(\lambda_{2n+1}^2+\alpha^2\right)l+2\lambda_{2n+1}\alpha},\ n=1,\ 2,\dots\ . \tag{19}$$

Then, the analytical solution of the original problem (1)–(3), taking into account the substitution and expressions (13), (18), and (19), can be written as:

$$u(x,t)=-\frac{\beta}{\alpha}+\sum_{k=1}^{\infty}C_k\left(\lambda_k\cos\lambda_k x+\alpha\sin\lambda_k x\right)\exp\left(-a\lambda_k^2 t\right), \tag{20}$$

where $C_k = C_k^{(1)} + C_k^{(2)}$, the coefficients $C_k^{(1)}$ and $C_k^{(2)}$ are defined by expressions (18) and (19), respectively, and λ_k, $k = 1, 2,\dots$ are the positive roots of equation (11).

In the case of solving the nonhomogeneous analog of the heat conduction equation (1):

$$\frac{\partial u}{\partial t}=a\frac{\partial^2 u}{\partial x^2}+f(x,t),\ 0<x<l,\ 0<t<T \tag{21}$$

with the initial and boundary conditions (2)–(3), the solution will be sought in the form $u(x,t)=v(x,t)+w(x,t)-\beta/\alpha$, where $v(x,t)$ is the solution to problem (4), defined by formula (13) with coefficients (18)–(19), and $w(x,t)$ is the solution to the following problem:

$$\begin{gathered}\frac{\partial w}{\partial t}=a\frac{\partial^2 w}{\partial x^2}+f,\ 0<x<l,\ 0<t<T,\ w(x,t)\big|_{t=0}=0,\\ \left.\left(\frac{\partial}{\partial x}w(x,t)-\alpha w(x,t)\right)\right|_{x=0}=0,\ \left.\left(\frac{\partial}{\partial x}w(x,t)+\alpha w(x,t)\right)\right|_{x=l}=0.\end{gathered} \tag{22}$$

The function $w(x,t)$ is sought as an expansion in terms of the eigenfunctions of the corresponding homogeneous Sturm–Liouville problem:

$$w(x,t)=\sum_{k=1}^{\infty}C_k^{(w)}(t)\left(\lambda_k\cos\lambda_k x+\alpha\sin\lambda_k x\right). \tag{23}$$

We also expand the function $f(x,t)$ over the considered interval as $0 \le x \le l$:

$$f(x,t)=\sum_{k=1}^{\infty}C_k^{(f)}(t)\left(\lambda_k\cos\lambda_k x+\alpha\sin\lambda_k x\right), \tag{24}$$

where

$$C_k^{(f)}(t)=\frac{1}{\|X_k\|^2}\int_0^l f(x,t)\left(\lambda_k\cos\lambda_k x+\alpha\sin\lambda_k x\right)dx, \tag{25}$$

where $\|X_k\|^2$ is defined by formula (16).

Substituting (23) and (24) into (22), we obtain:

$$\sum_{k=1}^{\infty}\left(\left(C_k^{(w)}(t)\right)'+a\lambda_k^2C_k^{(w)}(t)\right)\left(\lambda_k\cos\lambda_k x+\alpha\sin\lambda_k x\right)=\sum_{k=1}^{\infty}C_k^{(f)}(t)\left(\lambda_k\cos\lambda_k x+\alpha\sin\lambda_k x\right). \tag{26}$$

Due to the completeness of the orthogonal system of eigenfunctions $X_k(x)$, $k = 1, 2,\dots$, equality (26) holds if and only if:

$$\left(C_k^{(w)}(t)\right)'+a\lambda_k^2C_k^{(w)}(t)=C_k^{(f)}(t). \tag{27}$$

Given (23) and the homogeneous initial conditions in (22), we have:

$$C_k^{(w)}(0)=0. \tag{28}$$

Thus, we obtain a Cauchy problem for an ordinary differential equation (27) with the initial condition (28). The solution to this problem can be found, for example, by the method of variation of arbitrary constant (Lagrange method):

$$C_k^{(w)}(t) = \int_0^t C_k^{(f)}(\tau)\exp\left(a\lambda_k^2(\tau - t)\right)d\tau, \tag{29}$$

where $C_k^{(f)}(\tau)$ is defined by formula (25).

Thus, the solution to the nonhomogeneous heat equation (21) with third-kind boundary conditions (3) can be written as:

$$u(x,t) = -\frac{\beta}{\alpha} + \sum_{k=1}^{\infty} C_k\left(\lambda_k \cos\lambda_k x + \alpha\sin\lambda_k x\right)\exp\left(-a\lambda_k^2 t\right) + \sum_{k=1}^{\infty} C_k^{(w)}(t)\left(\lambda_k \cos\lambda_k x + \alpha\sin\lambda_k x\right), \tag{30}$$

where $C_k = C_k^{(1)} + C_k^{(2)}$, the coefficients $C_k^{(1)}$, $C_k^{(2)}$ and $C_k^{(w)}(t)$ are defined by formulas (18), (19), and (29), respectively, and λ_k, $k = 1, 2,...$ are the positive roots of equation (11).

2. Approximation of the Second-Order Differential Operator in the Diffusion Equation

Assume we need to consider the approximation of the nonhomogeneous heat conduction (diffusion) equation:

$$\frac{\partial u}{\partial t} = a\frac{\partial^2 u}{\partial x^2} + f(x,t),\ 0 < x < l,\ 0 < t < T, \tag{31}$$

with the following initial condition:

$$u(x,t)\big|_{t=0} = u_0(x) \tag{32}$$

and third-kind (Robin) boundary conditions:

$$\left(\frac{\partial}{\partial x}u(x,t) - \alpha u(x,t)\right)\bigg|_{x=0} = 0,\ \left(\frac{\partial}{\partial x}u(x,t) + \alpha u(x,t)\right)\bigg|_{x=l} = 0. \tag{33}$$

To obtain a numerical solution to the problem (31)–(33), we divide the computational domain using a uniform grid $\overline{\omega} = \overline{\omega}_t \times \overline{\omega}_h$, where

$$\overline{\omega}_t = \left\{t^n = n\tau,\ n = \overline{0..N_t},\ N_t\tau = T\right\},\ \ \overline{\omega}_h = \left\{x_i = ih,\ i = \overline{0..N_x},\ N_x h = l\right\}, \tag{34}$$

where τ is the time step size; N_t is the number of time steps; h is the spatial step size; N_x is the number of spatial nodes.

The analytical solution of the problem (31)–(33), according to equation (30), can be written as:

$$u(x,t) = \sum_{k=1}^{\infty}\left(C_k^{(1)}\exp\left(-a\lambda_k^2 t\right) + C_k^{(w)}(t)\right)\left(\lambda_k\cos\lambda_k x + \alpha\sin\lambda_k x\right), \tag{35}$$

where the coefficients $C_k^{(1)}$ and $C_k^{(w)}(t)$ are defined by expressions (18) and (29), respectively, and λ_k, $k = 1, 2,...$ are the positive roots of equation (11).

To simplify further calculations, let us introduce the following notation:

$$C_k^{(u)}(t) = C_k^{(1)}\exp\left(-a\lambda_k^2 t\right) + C_k^{(w)}(t). \tag{36}$$

We now write the approximation of equation (31) at the interior nodes of the computational grid (34) as:

$$\frac{u_i^{n+1} - u_i^n}{\tau} = a\frac{u_{i+1}^n - 2u_i^n + u_{i-1}^n}{h^2} + f_i^n, \tag{37}$$

where $u_{i\pm1}^n = u(t^n, x_{i\pm1}),\ u_i^n = u(t^n, x_i)$.

Then, taking into account expressions (24), (35), and (36), the approximation (37) can be written in the form:

$$\begin{gathered}\frac{1}{\tau}\sum_{k=1}^{N-1}\left(C_k^{(u)}(t^{n+1}) - C_k^{(u)}(t^n)\right)\left(\lambda_k\cos\lambda_k x + \alpha\sin\lambda_k x\right) = \\ = \frac{a}{h^2}\sum_{k=1}^{N-1}C_k^{(u)}(t^n)\left(\lambda_k\cos\left(\lambda_k(x_i + h)\right) + \alpha\sin\left(\lambda_k(x_i + h)\right) - 2\lambda_k\cos\lambda_k x_i - 2\alpha\sin\lambda_k x_i + \right. \\ \left. + \lambda_k\cos\left(\lambda_k(x_i - h)\right) + \alpha\sin\left(\lambda_k(x_i - h)\right)\right) + \sum_{k=1}^{N-1}C_k^{(f)}(t^n)\left(\lambda_k\cos\lambda_k x_i + \alpha\sin\lambda_k x_i\right).\end{gathered} \tag{38}$$

Using the transformations

$$\lambda_k\cos\left(\lambda_k(x_i + h)\right) + \lambda_k\cos\left(\lambda_k(x_i - h)\right) = 2\lambda_k\cos\lambda_k x_i\cos\lambda_k h,$$

$$\alpha\sin\left(\lambda_k(x_i + h)\right) + \alpha\sin\left(\lambda_k(x_i - h)\right) = 2\alpha\sin\lambda_k x_i\cos\lambda_k h,$$

expression (38) becomes:

$$\frac{1}{\tau}\sum_{k=1}^{N-1}\left(C_k^{(u)}(t^{n+1})-C_k^{(u)}(t^n)\right)\left(\lambda_k\cos\lambda_k x+\alpha\sin\lambda_k x\right)=a\frac{2}{h^2}\sum_{k=1}^{N-1}C_k^{(u)}(t^n)\left(\cos\lambda_k h-1\right)\left(\lambda_k\cos\lambda_k x_i+\alpha\sin\lambda_k x_i\right)+$$
$$+\sum_{k=1}^{N-1}C_k^{(f)}(t^n)\left(\lambda_k\cos\lambda_k x_i+\alpha\sin\lambda_k x_i\right).$$

Taking into account the orthogonality of the basis functions $X_k(x)$, $k=1,2,...$, defined in (10), the final expression can be written as:

$$\frac{C_k^{(u)}(t^{n+1})-C_k^{(u)}(t^n)}{\tau}=a\frac{2\left(\cos\lambda_k h-1\right)}{h^2}C_k^{(u)}(t^n)+C_k^{(f)}(t^n). \tag{39}$$

Let us find the second derivative of the function $u(x,t)$ with respect to the spatial variable:

$$\frac{\partial^2 u}{\partial x^2}=\frac{\partial^2}{\partial x^2}\left(\sum_{k=1}^{\infty}C_k^{(u)}(t)\left(\lambda_k\cos\lambda_k x+\alpha\sin\lambda_k x\right)\right)=\frac{\partial}{\partial x}\left(\sum_{k=1}^{\infty}C_k^{(u)}(t)\left(-\lambda_k^2\sin\lambda_k x+\alpha\lambda_k\cos\lambda_k x\right)\right)=$$
$$=-\sum_{k=1}^{\infty}\lambda_k^2C_k^{(u)}(t)\left(\lambda_k\cos\lambda_k x+\alpha\sin\lambda_k x\right). \tag{40}$$

From formulas (39) and (40), it follows that in the approximation of problem (31)–(33) on the computational grid (34) using scheme (37), the obtained solution for each harmonic deviates from the exact value by the quantity $\alpha^*=1-2\left(1-\cos\lambda_k h\right)/\left(\lambda_k h\right)^2$.

Let's consider the resulting value separately α^*:

$$\alpha^*=1-\frac{2\left(1-\cos\lambda_k h\right)}{\left(\lambda_k h\right)^2}=1-\frac{2\left(\frac{\left(\lambda_k h\right)^2}{2}-\frac{\left(\lambda_k h\right)^4}{24}+O\left(h^6\right)\right)}{\left(\lambda_k h\right)^2}=\frac{\left(\lambda_k h\right)^2}{12}+O\left(h^4\right). \tag{41}$$

From (41), we can conclude that when approximating the spatial variable using scheme (37), the numerical solution at the interior grid nodes (34) deviates from the exact solution by $O(h^2)$.

Let us now consider the approximation of the function $u(x,t)$ with respect to the spatial variable at the boundary nodes of the spatial grid (34). We construct this approximation based on the integro-interpolation method (the balance method). Without loss of generality, let us consider the approximation of $u(x,t)$ on the left boundary of the computational grid (i. e., at $x=0$):

$$2\frac{u_1^n-u_0^n}{h^2}-2\frac{\alpha u_0^n}{h}=2\sum_{k=1}^{N-1}C_k^{(u)}(t^n)\frac{\lambda_k\cos\lambda_k h+\alpha\sin\lambda_k h-\lambda_k}{h^2}-2\sum_{k=1}^{N-1}C_k^{(u)}(t^n)\frac{\alpha\lambda_k}{h}=$$
$$=2\sum_{k=1}^{N-1}C_k^{(u)}(t^n)\frac{\lambda_k\left(\cos\lambda_k h-1\right)+\alpha\left(\sin\lambda_k h-\lambda_k h\right)}{h^2}=\frac{2\lambda_k}{h^2}\sum_{k=1}^{N-1}C_k^{(u)}(t^n)\left(1-\frac{\left(\lambda_k h\right)^2}{2}+\frac{\left(\lambda_k h\right)^4}{24}+O\left(h^6\right)-1\right)+ \tag{42}$$
$$+\frac{2\alpha}{h^2}\sum_{k=1}^{N-1}C_k^{(u)}(t^n)\left(\lambda_k h-\frac{\left(\lambda_k h\right)^3}{6}+\frac{\left(\lambda_k h\right)^5}{120}+O\left(h^7\right)-\lambda_k h\right)=\sum_{k=1}^{N-1}C_k^{(u)}(t^n)\left(-\lambda_k^3-\lambda_k^3\frac{\alpha h}{3}+O\left(h^2\right)\right).$$

To increase the order of approximation error for the spatial derivative of the function $u(x,t)$ at the boundary nodes of the grid (34), we consider the following approximation:

$$2\frac{u_1^n-u_0^n}{h^2}-2\alpha\frac{\gamma_1u_0^n+\gamma_2u_1^n}{h}=2\sum_{k=1}^{N-1}C_k^{(u)}(t^n)\frac{\lambda_k\cos\lambda_k h+\alpha\sin\lambda_k h-\lambda_k}{h^2}-2\alpha\sum_{k=1}^{N-1}C_k^{(u)}(t^n)\frac{\gamma_1\lambda_k+\gamma_2\lambda_k\cos\lambda_k h+\gamma_2\alpha\sin\lambda_k h}{h}=$$
$$=\frac{2}{h^2}\sum_{k=1}^{N-1}C_k^{(u)}(t^n)\left(1-\gamma_2\alpha h\right)\left(\lambda_k\cos\lambda_k h+\alpha\sin\lambda_k h\right)-\frac{2}{h^2}\sum_{k=1}^{N-1}C_k^{(u)}(t^n)\lambda_k\left(1+\gamma_1\alpha h\right)=$$
$$=\frac{2}{h^2}\left(1-\gamma_2\alpha h\right)\sum_{k=1}^{N-1}C_k^{(u)}(t^n)\left(\lambda_k-\frac{\lambda_k^3h^2}{2}+\frac{\lambda_k^5h^4}{24}+\alpha\lambda_k h-\alpha\frac{\lambda_k^3h^3}{6}+\alpha\frac{\lambda_k^5h^5}{120}+O\left(h^6\right)\right)- \tag{43}$$
$$-\frac{2}{h^2}\left(1+\gamma_1\alpha h\right)\sum_{k=1}^{N-1}C_k^{(u)}(t^n)\lambda_k=\frac{2\alpha}{h}\left(\gamma_2+1-\gamma_2\alpha h-\gamma_1\right)\sum_{k=1}^{N-1}C_k^{(u)}(t^n)\lambda_k-\sum_{k=1}^{N-1}C_k^{(u)}(t^n)\lambda_k^3+$$
$$+\frac{2}{h^2}\left(\gamma_2\alpha\frac{h^3}{2}-\alpha\frac{h^3}{6}+\gamma_2\alpha^2\frac{h^4}{6}\right)\sum_{k=1}^{N-1}C_k^{(u)}(t^n)\lambda_k^3+\frac{h^2}{12}\sum_{k=1}^{N-1}C_k^{(u)}(t^n)\lambda_k^5+O\left(h^3\right).$$

The coefficients γ_1 and γ_2 in (43) are found as a solution to the system:

$$\begin{cases} \gamma_2 + 1 - \gamma_2 \alpha h - \gamma_1 = 0, \\ \gamma_2 - \dfrac{1}{3} + \gamma_2 \alpha \dfrac{h}{3} = 0, \end{cases}$$

from which we obtain the values of the coefficients $\gamma_1 = 2/(3 + \alpha h)$ and $\gamma_2 = 1/(3 + \alpha h)$.

Thus, we obtain the following approximation for the spatial derivative of the function $u(x,t)$ at the boundary nodes of the grid (34):

$$2\frac{u_1^n - u_0^n}{h^2} - \frac{4\alpha}{h(3+\alpha h)} u_0^n - \frac{2\alpha}{h(3+\alpha h)} u_1^n = \sum_{k=1}^{N-1} C_k^{(u)}(t^n)\left(-\lambda_k^3 + \frac{\lambda_k^5 h^2}{12} + O\left(h^3\right)\right). \quad (44)$$

Results. Assume we need to compare the computational accuracy of the spatial approximations (42) and (44) by solving test problems. We consider three test problems. The first is a steady-state problem with a constant right-hand side. The second is also a steady-state problem, but with a harmonic right-hand side corresponding to an eigenvalue λ_k. The third problem involves solving the heat conduction equation with a stepwise right-hand side.

Test Problem 1. Find the solution to the following problem:

$$\frac{\partial u}{\partial t} = \frac{\partial^2 u}{\partial x^2} + 2, \ 0 < x < 2, \quad (45)$$

with the initial condition:

$$u(x,t)\big|_{t=0} = 0 \quad (46)$$

and boundary conditions of the third kind

$$\left(\frac{\partial}{\partial x} u(x,t) - 2u(x,t)\right)\bigg|_{x=0} = 0, \ \left(\frac{\partial}{\partial x} u(x,t) + 2u(x,t)\right)\bigg|_{x=2} = 0. \quad (47)$$

Problem (45)–(47) is a steady-state problem.

The analytical solution to problem (45)–(47) can be written in the form: $u(x,t) = -x^2 + 2x + 1$.

Figure 1 shows the analytical solution of problem (45)–(47), as well as numerical solutions of Test Problem 1 obtained using: the first-order finite difference scheme in space (42), and the second-order finite difference scheme in space (44), for different spatial step sizes.

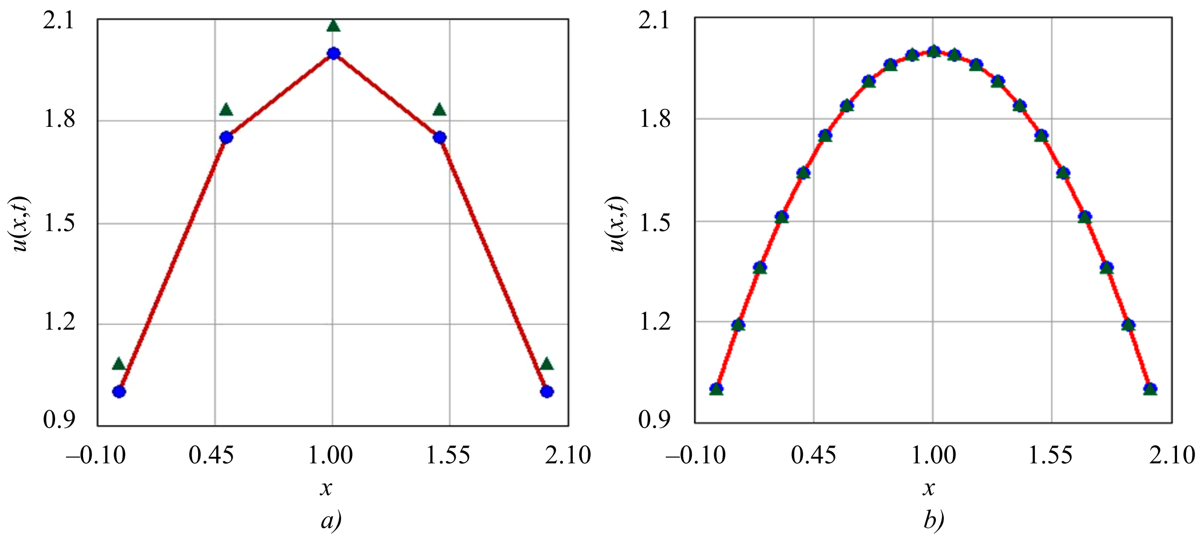

Fig. 1. Results of solving Test Problem 1:
red line — exact solution; blue dots — numerical solution using the first-order spatial approximation scheme (42);
green triangles — numerical solution using the second-order spatial approximation scheme (44);
a — spatial step size $h = 0.5$; *b* — spatial step size $h = 0.1$

In addition to the approximation error, we compute the effective order of accuracy of the scheme [28]:

$$p^{eff} = \log_r \left|\frac{R_N}{R_{rN}}\right|, \quad (48)$$

where R_N is the error of the numerical solution on the grid with step size h, R_{rN} is the error on the grid with step size h/r.

Table 1 presents the computational error of the numerical solution for Test Problem 1 based on schemes (42) and (44) for different spatial step sizes. The error was measured in the grid space norm $\Psi^n = \sum_{i=1}^{N} \left|u(x_i,t^n) - u_i^n\right| \cdot h,$ where $u(x_i,t^n)$ is the analytical solution, and u_i^n is the numerical solution.

Based on the data in Table 1, we can conclude that the proposed scheme (44), with improved boundary approximation for the heat conduction equation under third-kind boundary conditions (33), exhibits an effective order of accuracy equal to 2, which agrees with the theoretical estimate.

Table 1

Computed errors of the numerical solution for Test Problem 1 for various spatial step sizes

	The error value of the numerical solution			
	h = 1.00	h = 0.50	h = 0.25	h = 0.10
Finite difference scheme with standard boundary approximation (42)	0.000	0.000	0.000	3.286×10^{-15}
Finite difference scheme with improved boundary approximation (44)	1.000	0.208	0.047	0.007
Effective accuracy order of scheme (44)	–	2.263	2.152	2.075

Test Problem 2. Let us consider the solution of the following problem:

$$\frac{\partial u}{\partial t} = \frac{\partial^2 u}{\partial x^2} + X_k,\ 0 < x < 5, \quad (49)$$

with the following initial condition:

$$u(x,t)\big|_{t=0} = 0 \quad (50)$$

and third-kind boundary conditions:

$$\left(\frac{\partial}{\partial x}u(x,t) - 0{,}1u(x,t)\right)\Bigg|_{x=0} = 0,\ \left(\frac{\partial}{\partial x}u(x,t) + 0{,}1u(x,t)\right)\Bigg|_{x=5} = 0, \quad (51)$$

where X_k is an eigenfunction corresponding to an eigenvalue λ_k, which is determined by equation (11). Problem (49)–(51) is a steady-state problem.

The analytical solution to problem (49)–(51) in the steady-state formulation can be expressed in the following form:

$$u(x,t) = \frac{1}{\sqrt{\alpha^2 + \lambda_k^2}} \sin\left(\lambda_k x + \arccos\left(\frac{\alpha}{\sqrt{\alpha^2 + \lambda_k^2}}\right)\right).$$

According to the conditions of the problem (49)–(51), α = 0.1. Let us determine λ_k.

We now consider the numerical algorithm for solving equation (11) to determine the eigenvalues λ_k. Let us assume we need to find the roots of the nonlinear equation $f(\lambda) = 0$, where $f(\lambda) = 2\ \mathrm{ctg}\ \lambda l - \frac{\lambda}{\alpha} + \frac{\alpha}{\lambda}$.

Step 1. Introduce two auxiliary functions $f_1(\lambda) = 2\ \mathrm{ctg}\ \lambda l$ and $f_2(\lambda) = \frac{\lambda}{\alpha} - \frac{\alpha}{\lambda}$.

Step 2. Define the number of iterations K, which also determines the number of eigenvalues to be computed.

Step 3. For each eigenvalue λ_k define the initial guess using the following expression:

$$w_k = \frac{(2k+1)\pi}{2l} - \frac{1}{l} \cdot \mathrm{arctg}\left(\frac{1}{2} \cdot f_2\left(\frac{(2k+1)\pi}{2l}\right)\right),$$

where k is the iteration index or the index of the corresponding eigenvalue λ_k.

Step 4. At each iteration, apply Newton's method to find the solution of the nonlinear equation $f(\lambda) = 0$. For this, define the function

$$g(\lambda) = f'(\lambda) = -\frac{2l}{\sin^2(\lambda l)} - \frac{1}{\alpha} - \frac{\alpha}{\lambda^2}.$$

Step 5. Use x_0 as the initial approximation w_k.

Step 6. Compute the value $x_{i+1} = x_i - f(x_i)/g(x_i)$.

Step 7. If $|x_{i+1} - x_i| > \varepsilon$, where ε is a predefined small tolerance, return to Step 6.

Step 8. Assign the computed value λ_k define equal x_{i+1}.

Step 9. If $k < K$, proceed to Step 4. Otherwise, terminate the eigenvalue computation algorithm λ_k.

Figure 2 presents the results of the algorithm described above. The points in the figure indicate the values λ_k, that correspond to the solution of the equation $f(\lambda) = 0$.

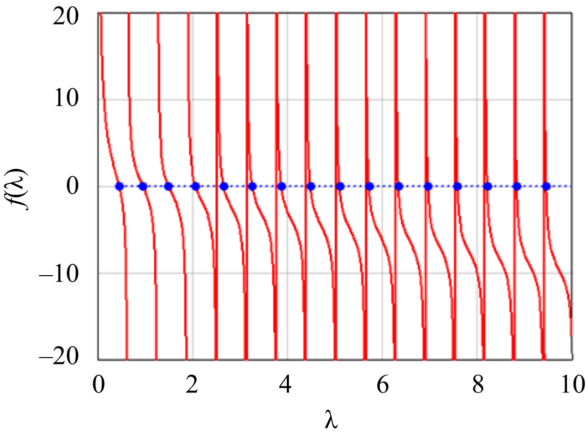

Fig. 2. Results of the eigenvalue λ_k computation algorithm: the red line represents the graph of the function $f(\lambda)$; the blue dots indicate the computed values λ_k, which correspond to the roots of the equation $f(\lambda) = 0$

Figure 3 presents the analytical solution of problem (49)–(51), as well as the numerical solutions of Test Problem 2 obtained using the first-order finite difference scheme in space (42) and the second-order finite difference scheme in space (44) for various spatial step sizes. The eigenvalue was taken for $k = 4$ and is equal to $\lambda_4 \approx 2{,}529$.

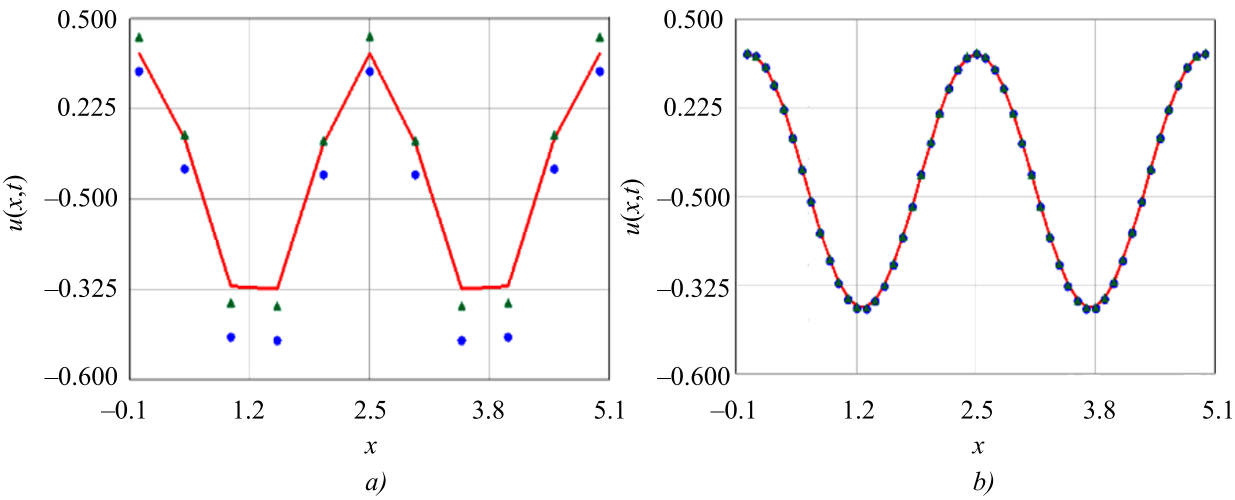

Fig. 3. Results of solving Test Problem 2 for $k = 4$: the red line represents the exact solution; blue dots represent the numerical solution based on the first-order spatial approximation scheme (42); green triangles represent the numerical solution based on the second-order spatial approximation scheme (44); *a* — spatial step size $h = 0.5$; *b* — spatial step size $h = 0.1$

Table 2 presents data on the computed error of the numerical solution of Test Problem 2 obtained using schemes (42) and (44) for various spatial step sizes.

Table 2

Computed Error Values of the Numerical Solution of Test Problem 2 for Various Spatial Step Sizes

	Values of the Numerical Solution Error			
	h = 1.00	h = 0.50	h = 0.25	h = 0.10
Finite Difference Scheme (42)	2.916	0.581	0.136	0.021
Effective Order of Accuracy of Scheme (42)	–	2.327	2.094	2.028
Finite Difference Scheme with Improved Boundary Approximation (44)	1.126	0.206	0.047	6.964×10^{-3}
Effective Order of Accuracy of Scheme (44)	–	2.455	2.133	2.080

Based on the data in Table 2, it can be observed that the proposed scheme (44), which incorporates improved boundary approximation for the heat conduction equation with third-kind boundary conditions (33), demonstrates an effective order of accuracy equal to 2, which is consistent with the theoretical estimate. The finite difference scheme (42), employing standard boundary approximation, also exhibits an effective order of accuracy close to 2, despite the lower theoretical approximation error order at the boundary nodes. It is worth noting that the proposed scheme (44) reduces the numerical solution error by approximately 2.5 to 3 times, depending on the spatial step size. As the spatial step size decreases, the difference in accuracy between schemes (42) and (44) becomes more pronounced.

Test Problem 3. Let us find the solution to the following problem:

$$\frac{\partial u}{\partial t}=\frac{\partial^2 u}{\partial x^2}-\theta(x-1)+\theta(x-3),\ 0<x<5,\ 0<T<10 \tag{52}$$

with the following initial condition

$$u(x,t)\big|_{t=0}=0 \tag{53}$$

and third-order boundary conditions

$$\left(\frac{\partial}{\partial x}u(x,t)-u(x,t)\right)\Bigg|_{x=0}=0,\ \left(\frac{\partial}{\partial x}u(x,t)+u(x,t)\right)\Bigg|_{x=5}=0, \tag{54}$$

where $\theta(x)$ is a piecewise-defined Heaviside function.

According to (30), the analytical solution to the problem (52)–(54) can be written in the following form:

$$u(x,t)=\sum_{k=1}^{\infty}C_k^{(w)}(t)\left(\lambda_k\cos\lambda_k x+\alpha\sin\lambda_k x\right),$$

where $C_k^{(w)}(t)$ is determined based on (29), while taking into account the type of the right-hand side (52)

$$C_k^{(f)}(t)=C_k^{(f)}=-\frac{2}{5\left(\lambda_k^2+1\right)+2}\int_1^3\left(\lambda_k\cos\lambda_k x+\alpha\sin\lambda_k x\right)dx=\frac{2}{5\left(\lambda_k^2+1\right)+2}\left(\frac{1}{\lambda_k}\left(\cos3\lambda_k-\cos\lambda_k\right)+\sin\lambda_k-\sin3\lambda_k\right). \tag{55}$$

Taking into account (29) and (55), we obtain the following form for the exact solution of the problem (52)–(54):

$$u(x,t)=\sum_{k=1}^{\infty}\frac{\exp\left(-\lambda_k^2 t\right)-1}{\lambda_k^2}C_k^{(f)}\left(\lambda_k\cos\lambda_k x+\alpha\sin\lambda_k x\right).$$

The eigenvalues λ_k are determined using the algorithm described in Test Problem 2.

In Figure 4*a*, the numerical solution to Test Problem 3, obtained using the difference scheme with improved boundary approximation (44) for a spatial step of h = 0.5. is presented. In these calculations, 1000 eigenvalues λ_k were used. Visually, no significant difference was observed between the numerical solutions obtained using difference schemes (42) and (44).

In Figure 4*b*, difference between the analytical and numerical solutions, calculated using formula (56) for k from 1 to 1000, is shown.

Figure 5 presents the analytical solution of the problem (52)–(54) at a fixed time $t = 2$, as well as the numerical solutions of Test Problem 3 obtained using the first-order spatial approximation scheme (42) and the second-order spatial approximation scheme (44) for different spatial step sizes. The calculations accounted for the sum of the first 1000 eigenvalues λ_k.

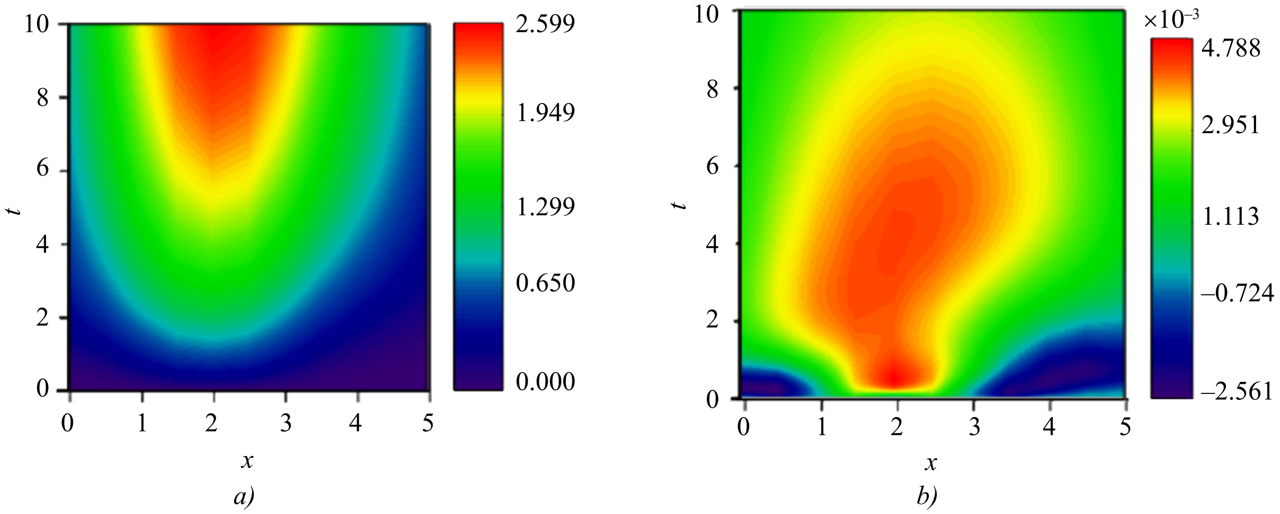

Fig. 4. Results of solving Test Problem 3 considering 1000 λ_k and time steps $\tau = 0.001$ and spatial steps $h = 0.5$:
a — numerical solution based on the second-order spatial approximation scheme (42);
b — difference between the analytical and numerical solutions based on (44)

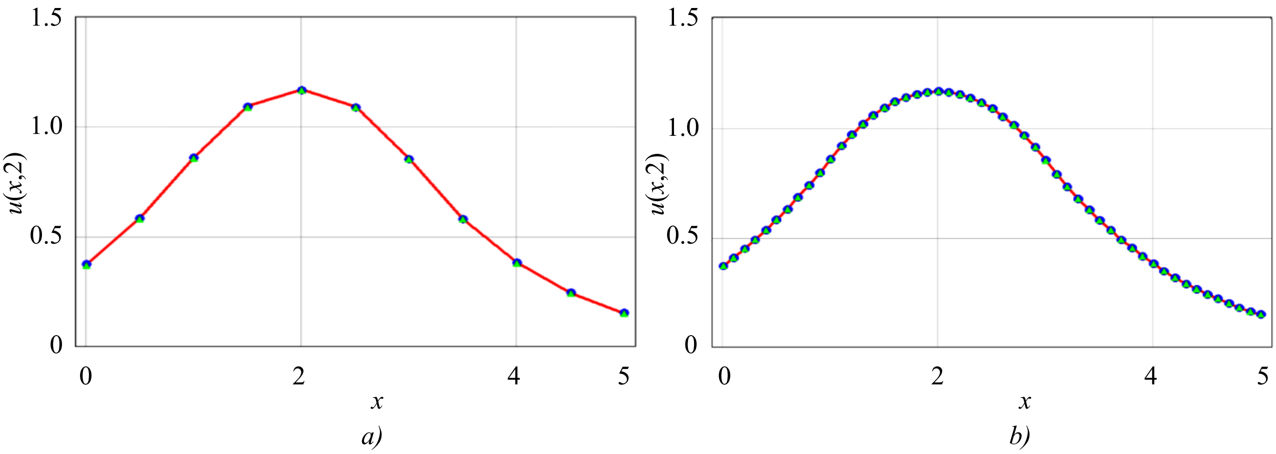

Fig. 5. Results of solving Test Problem 3 at $t = 2$:
red line — analytical solution; blue dots — numerical solution based on the first-order spatial approximation scheme (42); green triangles — numerical solution based on the second-order spatial approximation scheme (44);
a — spatial step $h = 0.5$; b — spatial step $h = 0.1$

Table 3 presents information on the computational error of the numerical solution of Test Problem 3 based on schemes (42) and (44) for different spatial step sizes.

Table 3

Computed values of the error for the numerical solution of Test Problem 3 at $t = 2$ for different spatial step sizes

	Error values of the numerical solution			
	$h = 1.00$	$h = 0.50$	$h = 0.25$	$h = 0.10$
Solution based on the first-order spatial approximation scheme (42)	0.0503	0.0102	0.002	2.6797×10^{-4}
Effective order of accuracy of scheme (42)	–	2.3010	2.231	2.2860
Solution based on the second-order spatial approximation scheme (44)	0.0530	0.0130	2.914×10^{-3}	2.0397×10^{-4}
Effective order of accuracy of scheme (44)	–	2.0570	2.132	2.9020

From the data in Table 3 (similarly to Test Problem 2), it can be observed that the proposed scheme (44) with improved boundary approximation for the heat conduction equation under third-kind boundary conditions (33) exhibits an effective order of accuracy equal to 2, which is consistent with the theoretical estimate. The difference scheme (42) with standard boundary approximation also demonstrates an effective order of accuracy close to 2, despite the theoretical estimate of the approximation error order at the boundary nodes. At the same time, for the proposed scheme (44), the numerical solution error decreases significantly faster than for the solution based on scheme (42).

Discussion and Conclusion. This study examined the heat conduction equation with third-kind boundary conditions, for which an exact solution was obtained. The problem was discretized, and it was shown that under standard boundary approximation, the theoretical order of approximation error for the second-order differential operator in the diffusion equation is $O(h)$. Based on this estimate, it follows that for the heat conduction equation with third-kind boundary conditions, the standard discretization yields a first-order accurate scheme. To improve the accuracy of the numerical solution, a finite difference scheme was proposed that provides an approximation error of $O(h^2)$, for the second-order differential operator, both at interior and boundary nodes of the computational domain. This scheme is applicable to third-kind boundary conditions of a specific form.

Numerical experiments demonstrate that the proposed scheme, featuring enhanced boundary approximation for the heat conduction equation with third-kind boundary conditions of a specific type, achieves an effective order of accuracy close to 2, which aligns with the theoretical estimate. It is also worth noting that the finite difference scheme with standard boundary approximation exhibits an effective order of accuracy close to 2, despite the theoretical approximation error estimate at the boundary nodes. The observed discrepancy between the theoretical approximation error and the achieved numerical accuracy calls for further investigation. Importantly, the numerical error of the proposed scheme decreases significantly faster than that of the scheme with standard boundary approximation.

References

1. Tikhonov A.N., Samarskii A.A. *Equations of mathematical physics*. 7th ed. Moscow: Nauka; 2004. 798 p. (In Russ.)

2. Cannon J.R. *The one-dimensional heat equation (Encyclopedia of Mathematics and Its Applications*, vol. 23). Cambridge: Addison-Wesley Publishing Company/Cambridge University Press; 1984. XXV + 483 p.

3. Evans L.C. *Partial differential equations*. American Mathematical Society; 1998. 662 p.

4. Samarskii A.A., Gulin A.V. *Numerical methods*. Moscow: Nauka; 1989. 432 p. (In Russ.)

5. Crank J., Nicolson P. A practical method for numerical evaluation of solutions of partial differential equations of the heat-conduction type. *Mathematical Proceedings of the Cambridge Philosophical Society*. 1947;43(1):50–67. https://doi.org/10.1017/S0305004100023197

6. Smetannikov O.Y. (2010). Optimization of the residual bending flexure of round polymer plate with glass transition at non-uniform cooling. *Computational Continuum Mechanics*. 2010;3(1):81–92. https://doi.org/10.7242/1999-6691/2010.3.1.9 (In Russ.)

7. Guzhev D.S., Kalitkin N.N. Burgers equation as a test for numerical methods. *Mathematical Models and Computer Simulations*. 1995;7(4):99–127. (In Russ.)

8. Markov V.V., Utesinov V.N. Difference scheme for the numerical solution of the Burgers equation. *Computational Mathematics and Mathematical Physics*. 2020;60(12):1985–1989. https://doi.org/10.1134/S0965542520120106 (In Russ.)

9. Kovyrkina O.A., Ostapenko V.V. On the accuracy of finite-difference schemes in calculations of centered rarefaction waves. *Mathematical Models and Computer Simulations*. 2023;15(Suppl. 1):S54–S63. https://doi.org/10.1134/S2070048223070104

10. Aristova E.N., Rogov B.V., Chikitkin A.V. Optimal monotonization of a high-order accurate bicompact scheme for the nonstationary multidimensional transport equation. *Computational Mathematics and Mathematical Physics*. 2016;56(6):962–976. https://doi.org/10.1134/S0965542516060038 (In Russ.)

11. Sukhinov A.I., Kuznetsova I.Yu., Chistyakov A.E., Protsenko E.A., Belova Yu.V. Studying the accuracy and applicability of the finite difference scheme for solving the diffusion–convection problem at large grid Péclet numbers. *Journal of Applied Mechanics and Technical Physics*. 2021;62:1255–1266. https://doi.org/10.1134/S002189442107018X (In Russ.)

12. Sukhinov A.I., Chistyakov A.E., Sidoryakina V.V., Kuznetsova I.Yu., Atayan A.M. Using parallel computing to evaluate the transport of pollutants in shallow waters. *Izvestiya of Saratov University. Mathematics. Mechanics. Informatics*. 2024;24(2):298–315. https://doi.org/10.18500/1816-9791-2024-24-2-298-315 (In Russ.)

13. Afanas'eva N.M., Vabishchevich P.N. Stable difference schemes for certain parabolic equations. *Computational Mathematics and Mathematical Physics*. 2014;54:1159–1166. https://doi.org/10.1134/S0965542514040034 (In Russ.)

14. Vabishchevich P.N. Monotone schemes for convection–diffusion problems with convective transport in different forms. *Computational Mathematics and Mathematical Physics*. 2021;61(1):90–102. https://doi.org/10.1134/S0965542520120155 (In Russ.)

15. Chetverushkin B.N., Gulin A.V. Explicit schemes and numerical simulation using ultrahigh-performance computer systems. *Doklady Mathematics*. 2012;86(2):681–683. https://doi.org/10.1134/S1064562412050213

16. Chetverushkin B.N., Olkhovskaya O.G., Gasilov V.A. An explicit difference scheme for a nonlinear heat conduction equation. *Mathematical Models and Computer Simulations*. 2023;15(3):529–538. https://doi.org/10.1134/S2070048223030031 (In Russ.)

17. Kriksin Y.A., Tishkin V.F. Entropic regularization of the discontinuous Galerkin method for two-dimensional euler equations in triangulated domains. *Mathematical Models and Computer Simulations.* 2023;15(5):781–791. https://doi.org/10.1134/S2070048223050058 (In Russ.)

18. Ladonkina M.E., Neklyudova O.A., Ostapenko V.V., Tishkin V.F. On the accuracy of discontinuous Galerkin method calculating gas-dynamic shock waves. *Doklady Mathematics*. 2023;107(2):120–125. https://doi.org/10.1134/S1064562423700746 (In Russ.)

19. Sukhinov A.I., Chistyakov A.E., Kuznetsova I.Yu., Atayan A.M., Nikitina A.V. Regularized difference scheme for solving hydrodynamic problems. *Mathematical Models and Computer Simulations*. 2022;14:745–754. https://doi.org/10.1134/S2070048222050155 (In Russ.)

20. Chistyakov A.E., Nikitina, A.V., Kuznetsova I.Yu., Rakhimbaeva E.O., Porksheyan M.V. Investigation of the approximation error of the difference scheme for the mathematical model of hydrodynamics. *Lobachevskii Journal of Mathematics*. 2023;44(5):1839–1846. https://doi.org/10.1134/S1995080223050128

21. Golubev V.I., Shevchenko A.V., Petrov I.B. Raising convergence order of grid-characteristic schemes for 2D linear elasticity problems using operator splitting. *Computer Research and Modeling*. 2022;14(4):899–910. https://doi.org/10.20537/2076-7633-2022-14-4-899-910 (In Russ.)

22. Vasyukov A.V., Petrov I.B. Increase in approximation order of calculations of wave processes in a composite sample when using an unstructured computational grid. *Journal of Applied Mechanics and Technical Physics*. 2024;65(3):528–535. https://doi.org/10.1134/S0021894424030143 (In Russ.)

23. Bobreneva Yu.O., Poveshchenko Yu., PodrygaV.O., Polyakov S.V., Uzyunbaev R.M., Rahimly P.I. et al. One approach to numerical modeling of the heat and mass transfers of two-phase fluids in fractured-porous reservoirs. *Mathematics*. 2023;11(18):3991. https://doi.org/10.3390/math11183991

24. Vasil'ev V.I. et al. Numerical solution of a fluid filtration problem in a fractured medium by using the domain decomposition method. *Journal of Applied and Industrial Mathematics.* 2018;12(4):785–796. https://doi.org/10.1134/S199047891804018X (In Russ.)

25. Uzyanbaev R.M., Bobreneva Yu.O., Poveshchenko Yu.A., Podryga V.O., Polyakov S.V., Gubaydullin I.M. Numerical modeling of piezoconductive processes in a two-dimensional formulation for a fractured-pore type reservoir. *Preprints of the Keldysh Institute of Applied Mathematics of the Russian Academy of Sciences*. 2024;35:1–17. https://doi.org/10.20948/prepr-2024-35 (In Russ.)

26. Litvinov V.N., Chistyakov A.E., Nikitina A.V., Atayan A.M., Kuznetsova I.Yu. Mathematical modeling of hydrodynamics problems of the Azov Sea on a multiprocessor computer system. *Computer Research and Modeling*. 2024;16(3):647–672. https://doi.org/10.20537/2076-7633-2024-16-3-647-672 (In Russ.)

27. Sukhinov A.I., Kuznetsova I.Yu. Mathematical model of three-component suspension transport. *Computational Mathematics and Information Technologies*. 2023;7(3):39–48. https://doi.org/10.23947/2587-8999-2023-7-3-39-48 (In Russ.)

28. Popov I.V. Construction of a difference scheme of increased order of approximation for a nonlinear transport equation using adaptive artificial viscosity. *Preprints of the Keldysh Institute of Applied Mathematics of the Russian Academy of Sciences*. 2017;68:1–22. https://doi.org/10.20948/prepr-2017-68 (In Russ.)

About the Authors:

Alexander E. Chistyakov, Professor at the Department of Software for Computer Engineering and Automated Systems, Don State Technical University (1, Gagarin Sq., Rostov-on-Don, Russian Federation, 344003), ORCID, ScopusID, SPIN-code, cheese_05@mail.ru

Inna Yu. Kuznetsova, Senior Lecturer at the Department of Mathematics and Informatics, Don State Technical University (344003, Russian Federation, Rostov-on-Don, Gagarin Square, 1), ORCID, ScopusID, SPIN-code, ikuznecova@donstu.ru

Contributions of the authors:

A.E. Chistyakov: problem statement; eigenvalue determination algorithm; numerical experiments.

I.Yu. Kuznetsova: derivation of the analytical solution; development of the difference scheme with improved boundary approximation for the heat conduction equation with third-kind boundary conditions; numerical experiments.

Conflict of Interest Statement: **the authors declare no conflict of interest.**

All authors have read and approved the final manuscript.

Об авторах:

Александр Евгеньевич Чистяков, профессор кафедры программного обеспечения вычислительной техники и автоматизированных систем Донского государственного технического университета (344003, Российская Федерация, г. Ростов-на-Дону, пл. Гагарина, 1), ORCID, ScopusID, SPIN-код, cheese_05@mail.ru

Инна Юрьевна Кузнецова, старший преподаватель кафедры математики и информатики Донского государственного технического университета (344003, Российская Федерация, г. Ростов-на-Дону, пл. Гагарина, 1), ORCID, ScopusID, SPIN-код, ikuznecova@donstu.ru

Заявленный вклад авторов:

А.Е. Чистяков: постановка задачи; алгоритм определения собственных значений; численные эксперименты.

И.Ю. Кузнецова: получение аналитического решения задачи; получение разностной схемы с улучшенной аппроксимацией на границе для уравнения теплопроводности с граничными условиями третьего рода, численные эксперименты.

Конфликт интересов: ***авторы заявляют об отсутствии конфликта интересов.***

Все авторы прочитали и одобрили окончательный вариант рукописи.

Received / Поступила в редакцию 27.02.2025
Revised / Поступила после рецензирования 19.03.2025
Accepted / Принята к публикации 22.04.2025

COMPUTATIONAL MATHEMATICS
ВЫЧИСЛИТЕЛЬНАЯ МАТЕМАТИКА

UDC 519.6

Original Theoretical Research

https://doi.org/10.23947/2587-8999-2025-9-2-22-33

Comparison of Solutions to a Hydrodynamic Problem in a Rectangular Cavity Using Initial Velocity Field Damping and Acceleration Methods

Natalya K. Volosova[1], **Konstantin A. Volosov**[2], **Aleksandra K. Volosova**[2], **Mikhail I. Karlov**[3], **Dmitriy F. Pastukhov**[4] ✉, **Yuriy F. Pastukhov**[4]

[1] MGTU named after. N.E. Bauman, Moscow, Russian Federation

[2] Russian University of Transport, Moscow, Russian Federation

[3] Moscow Institute of Physics and Technology (National Research University), Dolgoprudny, Russian Federation

[4] Polotsk State University named after Euphrosyne of Polotsk, Novopolotsk, Republic of Belarus

✉ dmitrij.pastuhov@mail.ru

Abstract

Introduction. This study investigates the numerical solution of a two-dimensional hydrodynamic problem in a rectangular cavity using the method of initial velocity field damping and the method of accelerating the initial conditions in terms of stream function and vorticity variables. The damping method was applied at Reynolds numbers Re $\leq$ 3000, and the acceleration method was used for Re = 8000.

Materials and Methods. To speed up the numerical solution of the problem using an explicit finite-difference scheme for the vorticity dynamics equation, the method of initial condition damping and the method of n-fold splitting of the explicit difference scheme (with $n = 100$) were used. Compared to the traditional method of accelerating from stationary fluid, the initial velocity field damping method reduced the computation time by a factor of 57. The splitting method used a maximum time step proportional to the square of the spatial step, while maintaining spectral stability of the explicit scheme in the vorticity equation. The majority of computation time was spent solving the Poisson equation in the "stream function — vorticity" variables. By freezing the velocity field and solving only the vorticity dynamics equation, computation time was further reduced in the splitting method. The inverse matrix for solving the Poisson equation using a finite number of elementary operations were computed using the Msimsl library.

Results. Numerical solutions demonstrated the equivalence of the damping and acceleration methods for the initial velocity field at low Reynolds numbers (up to 3000). The equivalence of solutions obtained using the "stream function — vorticity" algorithm and the implicit iterated polyneutic recurrent method for accelerated initial conditions was numerically confirmed. For the first time, an initial horizontal velocity field was proposed, smooth at internal points and composed of two sine waves, with a stationary center of mass for the fluid in the rectangular cavity.

Discussion and Conclusion. An algorithm for numerically solving a two-dimensional hydrodynamic problem in a rectangular cavity using "stream function — vorticity" variables is proposed. The approximation of the equations in system (1) has sixth-order accuracy at internal grid points and fourth-order accuracy at boundary points. A novel damping method is introduced using an initial horizontal velocity field formed by smoothly connecting two sine waves. The proposed algorithms enhance the efficiency of solving hydrodynamic problems using an explicit finite-difference scheme for the vorticity equation.

Keywords: hydrodynamics, numerical methods, partial differential equations, initial-boundary value problem, boundary conditions, initial conditions

For Citation. Volosova N.K., Volosov K.A., Volosova A.K., Karlov M.I., Pastukhov D.F., Pastukhov Yu.F. Comparison of Solutions to a Hydrodynamic Problem in a Rectangular Cavity Using Initial Velocity Field Damping and Acceleration Methods. *Computation Mathematics and Information Technologies*. 2025;9(2):22–33. https://doi.org/10.23947/2587-8999-2025-9-2-22-33

Оригинальное теоретическое исследование

Сравнение решений гидродинамической задачи в прямоугольной каверне методами торможения и разгона начального поля скорости

Н.К. Волосова[1], К.А. Волосов[2], А.К. Волосова[2], М.И. Карлов[3], Д.Ф. Пастухов[4]✉, Ю.Ф. Пастухов[4]

[1] Московский государственный технический университет им. Н.Э. Баумана, г. Москва, Российская Федерация

[2] Российский университет транспорта, г. Москва, Российская Федерация

[3] Московский физико-технический институт (национальный исследовательский университет), г. Долгопрудный, Российская Федерация

[4] Полоцкий государственный университет им. Евфросинии Полоцкой, г. Новополоцк, Республика Беларусь

✉ dmitrij.pastuhov@mail.ru

Аннотация

Введение. Исследуется численное решение двумерной гидродинамической задачи в прямоугольной каверне методом торможения и методом разгона начальных условий в переменных «функция тока — вихрь». Метод торможения применялся при числах Рейнольдса Re ≤ 3000, а метод разгона при числах Re = 8000.

Материалы и методы. Для ускорения численного решения задачи с явной разностной схемой уравнения динамики вихря использовался метод торможения начальных условий и метод n-кратного расщепления явной разностной схемы (n = 100). Метод торможения начальных условий поля скорости по сравнению с методом разгона неподвижной жидкости позволил сократить время счета задачи в 57 раз. Метод расщепления использовал максимальный шаг времени, пропорциональный квадрату координатного шага, не нарушая при этом спектральной устойчивости явной схемы в уравнении вихря. Наибольшее время программа затратила на решение уравнения Пуассона с переменными «функция тока — вихрь». Используя замороженное поле скоростей и решая только динамическое уравнение вихря, было сокращено время счета в методе расщепления. Обратная матрица для решения уравнения Пуассона за конечное число элементарных операций вычислялась библиотекой Msimsl.

Результаты исследования. Численное решение задачи показало эквивалентность методов торможения и разгона начального поля скорости при небольших числах Рейнольдса (до 3000). Численно доказана эквивалентность решения гидродинамической задачи алгоритмом в переменных «функция тока — вихрь» и алгоритмом с неявным полилинейным рекуррентным методом в случае разгона начальных условий. Впервые предложено начальное горизонтальное поле скорости, гладкое во внутренних точках и состоящее из двух синусоид с неподвижным центром масс всей жидкости в прямоугольной каверне.

Обсуждение и заключение. Предложен алгоритм численного решения двухмерной гидродинамической задачи в прямоугольной каверне в переменных «функция тока — вихрь». Аппроксимация уравнений в системе (1) имеет шестой порядок погрешности во внутренних узлах и четвертый в граничных узлах. Впервые предложен метод торможения с начальным полем горизонтальной скорости посредством гладкого соединения двух синусоид. Предложенные алгоритмы позволяют более эффективно решать задачи гидродинамики с явной разностной схемой уравнения вихря.

Ключевые слова: гидродинамика, численные методы, уравнения в частных производных, начально-краевая задача, граничные условия, начальные условия

Для цитирования. Волосова Н.К., Волосов К.А., Волосова А.К., Карлов М.И., Пастухов Д.Ф., Пастухов Ю.Ф. Сравнение решений гидродинамической задачи в прямоугольной каверне методами торможения и разгона начального поля скорости. *Computational Mathematics and Information Technologies*. 2025;9(2):22–33. https://doi.org/10.23947/2587-8999-2025-9-2-22-33

Introduction. This paper examines a two-dimensional hydrodynamic problem in a rectangular cavity with a moving upper lid, formulated in the “stream function — vorticity” variables [1]. The velocity field features two singular points in the upper corners of the cavity—both in magnitude and direction—making this problem a benchmark for testing numerical algorithms designed to solve various hydrodynamic problems [2]. For instance, studies [3–5] focus on exact or highly accurate approximate solutions to hydrodynamic problems. Problems involving large velocity field gradients at singular points are presented in [6, 7], while flows in viscous fluids are addressed in [8, 9]. Several approaches to formulating initial and boundary conditions in hydrodynamics are discussed in [10, 11].

The present work builds upon the method of n-fold splitting of the vorticity equation using an explicit finite-difference scheme (n = 100), as described in [11], and employs a uniform grid $n_1 \times n_2 = 100 \times 100$.

Materials and Methods

Problem Statement. We consider the classical hydrodynamic problem in a rectangular domain (cavity), described by a system of partial differential equations along with initial and boundary conditions for the physical fields [1], formulated in the "stream function — vorticity" variables. Let ($u(x,y)$, $v(x,y)$) denote the velocity vector of a fluid particle. On the solid boundaries — the lateral and bottom sides of the rectangular cavity — the velocity is zero (no-slip condition for fluid particles). The normal component of the velocity is also zero along the entire rectangular boundary. We position the origin of the coordinate system at the lower left corner of the rectangle, with the y-axis directed upward and the x-axis to the right. Let L be the width of the rectangular cavity and H its height.

In this hydrodynamic problem within a closed cavity, the moving upper lid translates to the right with a constant velocity $u_{\max}$. We define the characteristic scales: length scale: L, time scale: $\frac{L}{u_{\max}}$, velocity scale: $u_{\max}$, stream function scale: $Lu_{\max}$, vorticity scale: $\frac{u_{\max}}{L}$, Reynolds number: Re. We introduce the following dimensionless variables: $\bar{x}$ is the horizontal coordinate, $\bar{y}$ is the vertical coordinate, $\bar{\psi}$, $\bar{w}$ are the stream function and vorticity, respectively, $(\bar{u},\ \bar{v})$ is the dimensionless velocity vector, $\bar{t}$ is the dimensionless time:

$$0 \le \bar{x} = \frac{x}{L} \le 1,\ 0 \le \bar{y} = \frac{y}{L} \le k = \frac{H}{L}, \bar{\psi} = \frac{\psi}{\psi_{\max}}, \psi_{\max} = Lu_{\max},$$

$$\bar{u} = \frac{u}{u_{\max}}, \bar{v} = \frac{v}{u_{\max}} \bar{w} = \frac{w}{w_{\max}}, w_{\max} = \frac{u_{\max}}{L},$$

$$\bar{t} = \frac{t}{T}, T = \frac{L}{u_{\max}}, \mathrm{Re} = \frac{u_{\max}L}{\nu}.$$

Let us write the system of hydrodynamic equations using the dimensionless variables and functions [1, 5, 11]:

$$\begin{cases} \bar{\psi}_{\bar{x}\bar{x}} + \bar{\psi}_{\bar{y}\bar{y}} = -\bar{w}(\bar{x},\bar{y}),\ 0 < \bar{x} = \dfrac{x}{L} < 1,\ 0 < \bar{y} < k_{\max}, \\ \bar{w} = \bar{v}_{\bar{x}} - \bar{u}_{\bar{y}}, \\ \bar{u} = \bar{\psi}_{\bar{y}}; \bar{v} = -\bar{\psi}_{\bar{x}}, \\ \bar{w}_{\bar{t}} + \bar{u}\cdot\bar{w}_{\bar{x}} + \bar{v}\cdot\bar{w}_{\bar{y}} = \dfrac{1}{\mathrm{Re}}\left(\bar{w}_{\bar{x}\bar{x}} + \bar{w}_{\bar{y}\bar{y}}\right), 0 < \bar{t} = \dfrac{t}{T}, \\ \bar{\psi}\big|_{\Gamma} \equiv 0, \bar{v}\big|_{\Gamma} \equiv 0, \bar{u}\big|_{\Gamma_1} = 0, \bar{u}\big|_{\Gamma\backslash\Gamma_1} = 1. \end{cases} \tag{1}$$

Here Γ_1 denotes the union of the side walls and the bottom segment of the rectangular boundary, $\Gamma\backslash\Gamma_1$ represents the upper segment of the rectangle. The first equation in system (1) is the Poisson equation for the stream function and vorticity. The two-dimensional Poisson equation on a rectangular domain is solved in matrix form using a finite number of arithmetic operations with sixth-order accuracy [5, 12]. From this point forward, we will omit the overbars above the dimensionless functions, time, and coordinates for convenience.

The second line of system (1) describes the vorticity function, which is computed through the spatial derivatives of the velocity field. The third line calculates the velocity components as partial derivatives of the stream function. The fourth line is the vorticity dynamics equation, the only one in system (1) that explicitly depends on time. On the left-hand side is the total (convective) time derivative. On the boundary of the rectangle, the vertical component of velocity is zero; the horizontal component is equal to one on the upper segment and zero on the bottom and side segments.

In addition to the two mentioned singular points of the velocity field, for testing the algorithm in the method of initial velocity field damping, a highly unsteady and vortical initial velocity field was used. This field should, by its parameters, be close to a steady-state velocity field, satisfy the continuity equation for incompressible flow, and—as numerical experiments show—be continuously differentiable at all points in the domain.

For the first time in this work, an initial horizontal velocity field on a uniform rectangular grid is proposed, defined by formula (2). The horizontal velocity profile on the upper segment of the rectangular cavity is constructed by smoothly stitching together two cubic polynomials:

$$u(x_n, y_m) = \begin{cases} u_-(x_n, y_m) = -\dfrac{u_0(x_n)}{\sqrt{2}}\sin\left(\dfrac{\pi y_m}{k_1}\right) = -\dfrac{u_0(x_n)}{\sqrt{2}}\sin\left(\dfrac{\left(1+\sqrt{2}\right)\pi y_m}{k\sqrt{2}}\right), 0 \le y_m \le \dfrac{\sqrt{2}}{1+\sqrt{2}}k, \\ u_+(x_n, y_m) = u_0(x_n)\sin\left(\dfrac{\pi(y_m - k_1)}{2k_2}\right) = u_0(x_n)\sin\left(\dfrac{\pi}{2}\dfrac{\left(y_m - \dfrac{\sqrt{2}k}{1+\sqrt{2}}\right)}{\dfrac{k}{1+\sqrt{2}}}\right), \dfrac{\sqrt{2}}{1+\sqrt{2}}k < y_m \le k, \\ x_n = nh_1, y_m = mh_2, h_1 = \dfrac{1}{n_1}, h_2 = \dfrac{k}{n_2}, k_1 = \dfrac{\sqrt{2}k}{1+\sqrt{2}}, k_2 = \dfrac{k}{1+\sqrt{2}}, k_1 + k_2 = k, k_1 = \sqrt{2}k_2, \\ n = \overline{0,n_1}, m = \overline{0,n_2}, n_1 = n_2 = 100. \end{cases} \tag{2}$$

In formula (2), the lower part of the fluid moves to the left, the upper part moves to the right, and the horizontal component of the velocity is bounded by $u_0(x_n)$, i. e., it does not exceed unity. The profile of the horizontal velocity is continuous with respect to the variable y: $u_-(x_n,0)=u_-(x_n,k_1)=u_+(x_n,k_1)=0, u_+(x_n,k)=u_0(x_n)$. At the boundary point, the sine curve graphs are tangent to each other:

$$u_{-y}(x_n,k_1)=u_{+y}(x_n,k_1)\Leftrightarrow -\frac{u_0(x_n)}{\sqrt{2}}\frac{\pi}{k_1}\cos\left(\frac{\pi k_1}{k_1}\right)=\frac{u_0(x_n)}{\sqrt{2}}\frac{\pi}{k_1}=u_0(x_n)\frac{\pi}{2k_2}\cos\left(\frac{\pi(k_1-k_1)}{2k_2}\right)=u_0(x_n)\frac{\pi}{2k_2}=u_0(x_n)\frac{\pi}{\sqrt{2}k_1}.$$

Integrating the profile (2) with respect to y from 0 to k while keeping the variable x, constant, and denoting the integral by $\overline{y}\big|_0^1=\frac{y\big|_0^{k_1}}{k_1}, \overline{\overline{y}}\big|_0^1=\frac{(y-k_1)\big|_{k_1}^{k=k_1+k_2}}{k_2}$ we get:

$$\int_0^k u(x,y)dy=\int_0^{k_1}u_-(x,y)dy+\int_{k_1}^{k_1+k_2}u_+(x,y)dy=u_0(x)\left(-\frac{k_1}{\sqrt{2}}\int_0^1\sin(\pi\overline{y})d\overline{y}+k_2\int_0^1\sin\left(\frac{\pi}{2}\overline{\overline{y}}\right)d\overline{\overline{y}}\right)=$$

$$=u_0(x)\left(\frac{k_1}{\sqrt{2}\pi}\cos(\pi\overline{y})\Big|_0^1-\frac{2k_2}{\pi}\cos\left(\frac{\pi}{2}\overline{\overline{y}}\right)\Big|_0^1\right)=u_0(x)\left(\frac{-2k_1}{\sqrt{2}\pi}+\frac{2k_2}{\pi}\right)=u_0(x)\left(\frac{-\sqrt{2}k_1}{\pi}+\frac{\sqrt{2}k_1}{\pi}\right)=0.$$

This last integral shows that, at the initial moment in time, the center of mass of each sufficiently thin vertical column of fluid lies on the x-axis. Thus, according to the law of conservation of momentum, the center of mass of the entire fluid does not move along the x-axis either initially or at any subsequent moment in time.

The profile of the horizontal velocity component (3) on the upper segment of the cavity ($y = k = 1$) had the form of a smooth and continuous symmetric curved trapezoid without singular points in the velocity field:

$$u(x,k)\equiv u_0(x)=\begin{cases}3z^2\text{-}2z^3, z=\frac{x}{\tau}\in[0,1], 0\le x\le\tau, \tau=\frac{n_0}{n_1}=\frac{1}{10},\\ 1, \tau\le x\le 1-\tau,\\ 3z^2\text{-}2z^3, z=\frac{1-x}{\tau}\in[0,1], 1-\tau\le x\le 1.\end{cases} \tag{3}$$

Note that $u(0)=u'(0)=(6z-6z^2)_{z=0}=0, u(1)=1, u'(1)=(6z-6z^2)_{z=1}=0$, i. e., at the two junction points $x=\tau$, $x = 1 - \tau$ the profile of the horizontal component of velocity on the upper segment of the rectangular cavity is smooth.

The vertical component of the fluid particle velocity at the initial moment, according to the continuity equation, was calculated using the trapezoidal rule $m=\overline{1,n_2-1}, n=\overline{1,n_1-1}$:

$$v(x_n,y_m)=-h_2\left(\frac{u_x(x_n,y_m)}{2}+\sum_{i=1}^{m-1}u_x(x_n,y_i)\right)=-h_2\left(\frac{u(x_{n+1},y_m)-u(x_{n-1},y_m)}{4h_1}+\sum_{i=1}^{m-1}\frac{u(x_{n+1},y_i)-u(x_{n-1},y_i)}{2h_1}\right). \tag{4}$$

According to the algorithm described in [1], the first equation to be solved in system (1) is the Poisson equation, which is computed using a finite number of elementary operations [5]. The Poisson equation is approximated with sixth-order accuracy at all internal points.

To approximate the Laplace operator, we expand the nodal values of the stream function $\psi(x, y)$ in a Taylor series around the central node on a 3×3 rectangular stencil. Due to symmetry, the odd-order partial derivatives of the stream function vanish. When expanding in a Taylor series, we also take into account the Poisson equation:

$$\Delta\psi=\psi_{xx}+\psi_{yy}=f(x,y)=-w\Leftrightarrow \psi_{xx}\big|_{(x_i,y_j)}+\psi_{yy}\big|_{(x_i,y_j)}=f(x_i,y_j)=f_{i,j}, i=\overline{1,n_2-1}, j=\overline{1,n_1-1}, \tag{5}$$

$$\Delta\psi=\frac{1}{h^2}\big(C_0\psi_{0,0}+C_1(\psi_{-1,0}+\psi_{0,-1}+\psi_{1,0}+\psi_{0,1})+C_2(\psi_{-1,-1}+\psi_{1,-1}+\psi_{-1,1}+\psi_{1,1})\big)=\frac{1}{h^2}\big(\psi_{0,0}(C_0+4C_1+4C_2)+$$
$$+C_1\left(h^2(\psi_{xx}+\psi_{yy})+\frac{h^4}{12}(\psi_x^{(4)}+\psi_y^{(4)})+\frac{h^6}{360}(\psi_x^{(6)}+\psi_y^{(6)})+O(h^8)\right)+$$
$$+C_2\left(2h^2(\psi_{xx}+\psi_{yy})+\frac{h^4}{6}(\psi_x^{(4)}+\psi_y^{(4)}+6\psi_{xxyy}^{(4)})+\frac{h^6}{180}(\psi_x^{(6)}+\psi_y^{(6)}+15(\psi_{xxxxyy}^{(6)}+\psi_{xxyyyy}^{(6)}))+O(h^8)\right)= \tag{6}$$
$$=\frac{\psi_{0,0}(C_0+4C_1+4C_2)}{h^2}+(C_1+2C_2)(\psi_{xx}+\psi_{yy})+\frac{h^2}{12}\big((\psi_x^{(4)}+\psi_y^{(4)})C_1+2C_2(\psi_x^{(4)}+\psi_y^{(4)}+6\psi_{xxyy}^{(4)})\big)+$$
$$+h^4\left((\psi_x^{(6)}+\psi_y^{(6)})\frac{C_1}{360}+(\psi_x^{(6)}+\psi_y^{(6)}+15(\psi_{xxxxyy}^{(6)}+\psi_{xxyyyy}^{(6)}))\frac{C_2}{180}\right)+O(h^6)=\Delta\psi=\psi_{xx}+\psi_{yy}.$$

Using equation (5) for equation (6), as well as the boundedness of the solution at each node of the rectangular grid, we get that

$$\begin{cases} C_0 + 4C_1 + 4C_2 = 0, \\ C_1 + 2C_2 = 1. \end{cases}$$

Note that

$$\Delta f = \Delta\left(\psi_{xx} + \psi_{yy}\right) = \left(\frac{\partial^2}{\partial x^2} + \frac{\partial^2}{\partial y^2}\right)\left(\psi_{xx} + \psi_{yy}\right) = \psi_x^{(4)} + \psi_y^{(4)} + 2\psi_{xxyy}^{(4)} = f_{xx} + f_{yy},$$

$$\Delta^2 f = \Delta\left(\psi_x^{(4)} + \psi_y^{(4)} + 2\psi_{xxyy}^{(4)}\right) = \psi_x^{(6)} + \psi_y^{(6)} + 3\left(\psi_{xxxxyy}^{(6)} + \psi_{xxyyyy}^{(6)}\right), f_{xxyy}^{(4)} = \left(\psi_{xx} + \psi_{yy}\right)_{xxyy} = \psi_{xxyyyy}^{(6)} + \psi_{yyxxxx}^{(6)}.$$

Considering the transformations above, we can rewrite formula (6) as:

$$\Delta\psi = \psi_{xx} + \psi_{yy} + \frac{h^2}{12}\left(\left(\psi_x^{(4)} + \psi_y^{(4)}\right)\left(C_1 + 2C_2\right) + 12C_2\psi_{xxyy}^{(4)}\right) +$$
$$+ h^4\left(\left(\psi_x^{(6)} + \psi_y^{(6)}\right)\frac{C_1}{360} + \left(\psi_x^{(6)} + \psi_y^{(6)} + 15\left(\psi_{xxxxyy}^{(6)} + \psi_{xxyyyy}^{(6)}\right)\right)\frac{C_2}{180}\right) + O\left(h^6\right).$$

We require that the coefficient of $\frac{h^2}{12}$ becomes an operator Δf acting on the function f. Therefore, we have:

$$12C_2 = 2,$$

$$\begin{cases} C_0 + 4C_1 + 4C_2 = 0 \\ C_1 + 2C_2 = 1 \\ 12C_2 = 2 \end{cases} \Leftrightarrow C_2 = \frac{1}{6}, C_1 = 1 - 2C_2 = \frac{2}{3}, C_0 = -4C_1 - 4C_2 = -\frac{10}{3},$$

$$\Delta\psi = f + \frac{h^2}{12}\Delta f + \frac{h^4}{360}\left(C_1 + 2C_2\right)\left(\psi_x^{(6)} + \psi_y^{(6)}\right) + \frac{h^4\left(\psi_{xxxxyy}^{(6)} + \psi_{xxyyyy}^{(6)}\right)}{72} + O\left(h^6\right) \Leftrightarrow$$
$$\Leftrightarrow \frac{1}{h^2}\left(-\frac{10}{3}\psi_{0,0} + \frac{2}{3}\left(\psi_{-1,0} + \psi_{0,-1} + \psi_{1,0} + \psi_{0,1}\right) + \frac{1}{6}\left(\psi_{-1,-1} + \psi_{1,-1} + \psi_{-1,1} + \psi_{1,1}\right)\right) =$$
$$= f + \frac{h^2}{12}\Delta f + \frac{h^4}{360}\left(\psi_x^{(6)} + \psi_y^{(6)} + 3\left(\psi_{xxxxyy}^{(6)} + \psi_{xxyyyy}^{(6)}\right)\right) + \left(\psi_{xxxxyy}^{(6)} + \psi_{xxyyyy}^{(6)}\right)\left(\frac{5}{360} - \frac{1}{120}\right) + O\left(h^6\right) =$$
$$= f + \frac{h^2}{12}\Delta f + \frac{h^4}{360}\Delta^2 f + \frac{h^4 f_{xxyy}^{(4)}}{180} + O\left(h^6\right) = f + \frac{h^2}{12}\left(f_{xx} + f_{yy}\right) + \frac{h^4}{360}\left(f_x^{(4)} + f_y^{(4)}\right) + \frac{h^4 f_{xxyy}^{(4)}}{90} + O\left(h^6\right). \quad (7)$$

To use the Poisson equation (7) for the stream function in the system of equations (1) with an accuracy of $O(h^6)$ it is necessary $f = -w$, the derivatives f_{xx}, f_{yy} be represented with an accuracy of $O(h^4)$, and $f_x^{(4)}, f_y^{(4)}, f_{xxyy}^{(4)}$ with an accuracy of $O(h^2)$.

Using the method of undetermined coefficients [12], formulas for the internal nodes of the function f with indices $n = \overline{2, n_1 - 2}, m = \overline{2, n_2 - 2}$ were obtained:

$$\begin{cases} f_{xx} + f_{yy} = \frac{1}{h^2}\left(-5f_{0,0} + \frac{4}{3}\left(f_{-1,0} + f_{0,-1} + f_{1,0} + f_{0,1}\right) - \frac{1}{12}\left(f_{-2,0} + f_{0,-2} + f_{2,0} + f_{0,2}\right)\right) + O\left(h^4\right), \\ f_x^{(4)} + f_y^{(4)} = \frac{1}{h^4}\left(12f_{0,0} - 4\left(f_{-1,0} + f_{0,-1} + f_{1,0} + f_{0,1}\right) + f_{-2,0} + f_{0,-2} + f_{2,0} + f_{0,2}\right) + O\left(h^2\right), \\ f_{xxyy}^{(4)} = \frac{1}{h^4}\left(4f_{0,0} - 2\left(f_{-1,0} + f_{0,-1} + f_{1,0} + f_{0,1}\right) + f_{-1,-1} + f_{-1,1} + f_{1,-1} + f_{1,1}\right) + O\left(h^2\right). \end{cases} \quad (8)$$

Thus, formulas (7) and (8) together approximate the Poisson equation for the stream function and the vorticity function in (1) with sixth-order accuracy at the interior nodes of the rectangle.

In [5], an algorithm for the matrix method of solving the difference Poisson equation (7) is described, which involves a finite number of elementary arithmetic operations using the vector sweep method.

Consider the difference equation (9):

$$\frac{1}{h^2}\left(\frac{-10}{3}\psi_{m,n} + \frac{2}{3}\left(\psi_{m-1,n} + \psi_{m+1,n} + \psi_{m,n-1} + \psi_{m,n+1}\right) + \frac{1}{6}\left(\psi_{m-1,n-1} + \psi_{m+1,n-1} + \psi_{m-1,n+1} + \psi_{m+1,n+1}\right)\right) = f_{m,n} + \frac{h^2}{12}\left(f_{xx} + f_{yy}\right) +$$
$$+ h^4\left(\frac{1}{360}\left(f_x^{(4)} + f_y^{(4)}\right) + \frac{1}{90}f_{xxyy}^{(4)}\right) + O\left(h^6\right) \equiv F_{m,n}, \quad n = \overline{1, n_1 - 1}, m = \overline{1, n_2 - 1}. \quad (9)$$

We define square matrices A, B of dimension $(n_1-1)\times(n_1-1)$:

$$a_{m,n}=\begin{cases}-\dfrac{10}{3}, m=n; m=\overline{1,n_1-1}, n=\overline{1,n_1-1},\\ \dfrac{2}{3}, m=n+1\vee m=n-1,\\ 0, m\ge n+2\vee m\le n-2,\end{cases}\qquad b_{m,n}=\begin{cases}\dfrac{2}{3}, m=n; m=\overline{1,n_1-1}, n=\overline{1,n_1-1},\\ \dfrac{1}{6}, m=n+1\vee m=n-1,\\ 0, m\ge n+2\vee m\le n-2.\end{cases}\tag{10}$$

Let us briefly write the matrix algorithm for solving the difference equation (9) [5]:

1. Using the formula:

$$F^T{}_{m,n}=f_{m,n}h^2+\frac{h^4}{12}\left(f_{xx}+f_{yy}\right)+h^6\left(\frac{1}{360}\left(f_x^{(4)}+f_y^{(4)}\right)+\frac{1}{90}f_{xxyy}^{(4)}\right)+O\left(h^8\right)\Big|_{x=x_n,y=y_m}$$

compute the right-hand side of the Poisson equation at all interior nodes of the uniform grid of the rectangle ($m=1,\ldots,n_2-1$; $n=1,\ldots,n_1-1$).

2. Modify the right-hand side of the system of equations (11) using formulas (12) and (13) at the nodes of the rectangular contour adjacent to the boundary contour, i. e., calculate $\overline{F_{m,n}}$ based on the values $F_{m,n}$ from step 1:

$$\begin{cases}A\psi_1^T+B\psi_2^T=\overline{F_1^T},\\ B\psi_{m-1}^T+A\psi_m^T+B\psi_{m+1}^T=\overline{F_m^T}, m=\overline{2,n_2-2},\\ B\psi_{n_2-2}^T+A\psi_{n_2-1}^T=\overline{F_{n_2-1}^T}.\end{cases}\tag{11}$$

$$\begin{cases}\dfrac{-10}{3}\psi_{1,n_1-1}+\dfrac{2}{3}\left(\psi_{2,n_1-1}+\psi_{1,n_1-2}+\psi_{1,n_1}+\psi_{0,n_1-1}\right)+\dfrac{1}{6}\left(\psi_{2,n_1-2}+\psi_{0,n_1-2}+\psi_{2,n_1}+\psi_{0,n_1}\right)=F_{1,n_1-1},\\ \overline{F_{1,n_1-1}}\equiv F_{1,n_1-1}-\dfrac{2}{3}\left(\psi_{1,n_1}+\psi_{0,n_1-1}\right)-\dfrac{1}{6}\left(\psi_{0,n_1-2}+\psi_{2,n_1}+\psi_{0,n_1}\right),\\ \dfrac{-10}{3}\psi_{n_2-1,1}+\dfrac{2}{3}\left(\psi_{n_2-2,1}+\psi_{n_2-1,2}+\psi_{n_2-1,0}+\psi_{n_2,1}\right)+\dfrac{1}{6}\left(\psi_{n_2-2,2}+\psi_{n_2,2}+\psi_{n_2-2,0}+\psi_{n_2,0}\right)=F_{n_2-1,1},\\ \overline{F_{n_2-1,1}}\equiv F_{n_2-1,1}-\dfrac{2}{3}\left(\psi_{n_2-1,0}+\psi_{n_2,1}\right)-\dfrac{1}{6}\left(\psi_{n_2,2}+\psi_{n_2-2,0}+\psi_{n_2,0}\right),\\ \dfrac{-10}{3}\psi_{n_2-1,n_1-1}+\dfrac{2}{3}\left(\psi_{n_2-2,n_1-1}+\psi_{n_2-1,n_1-2}+\psi_{n_2-1,n_1}+\psi_{n_2,n_1-1}\right)+\dfrac{1}{6}\left(\psi_{n_2-2,n_1-2}+\psi_{n_2,n_1-2}+\psi_{n_2-2,n_1}+\psi_{n_2,n_1}\right)=F_{n_2-1,n_1-1},\\ \overline{F_{n_2-1,n_1-1}}\equiv F_{n_2-1,n_1-1}-\dfrac{2}{3}\left(\psi_{n_2-1,n_1}+\psi_{n_2,n_1-1}\right)-\dfrac{1}{6}\left(\psi_{n_2,n_1-2}+\psi_{n_2-2,n_1}+\psi_{n_2,n_1}\right),\\ \dfrac{-10}{3}\psi_{1,1}+\dfrac{2}{3}\left(\psi_{2,1}+\psi_{1,2}+\psi_{1,0}+\psi_{0,1}\right)+\dfrac{1}{6}\left(\psi_{2,2}+\psi_{0,2}+\psi_{2,0}+\psi_{0,0}\right)=F_{1,1},\\ \overline{F_{1,1}}\equiv F_{1,1}-\dfrac{2}{3}\left(\psi_{1,0}+\psi_{0,1}\right)-\dfrac{1}{6}\left(\psi_{0,2}+\psi_{2,0}+\psi_{0,0}\right).\end{cases}\tag{12}$$

$$\begin{cases}-\dfrac{10}{3}\psi_{1,n}+\dfrac{2}{3}\left(\psi_{1,n-1}+\psi_{2,n}+\psi_{1,n+1}+\psi_{0,n}\right)+\dfrac{1}{6}\left(\psi_{2,n-1}+\psi_{2,n+1}+\psi_{0,n-1}+\psi_{0,n+1}\right)=F_{1,n}, n=\overline{2,n_1-2},\\ \overline{F_{1,n}}=F_{1,n}-\dfrac{2}{3}\psi_{0,n}-\dfrac{1}{6}\left(\psi_{0,n-1}+\psi_{0,n+1}\right), n=\overline{2,n_1-2},\\ -\dfrac{10}{3}\psi_{n_2-1,n}+\dfrac{2}{3}\left(\psi_{n_2-1,n-1}+\psi_{n_2-2,n}+\psi_{n_2-1,n+1}+\psi_{n_2,n}\right)+\dfrac{1}{6}\left(\psi_{n_2-2,n-1}+\psi_{n_2-2,n+1}+\psi_{n_2,n-1}+\psi_{n_2,n+1}\right)=F_{n_2-1,n}, n=\overline{2,n_1-2},\\ \overline{F_{n_2-1,n}}=F_{n_2-1,n}-\dfrac{2}{3}\psi_{n_2,n}-\dfrac{1}{6}\left(\psi_{n_2,n-1}+\psi_{n_2,n+1}\right), n=\overline{2,n_1-2},\\ -\dfrac{10}{3}\psi_{m,1}+\dfrac{2}{3}\left(\psi_{m-1,1}+\psi_{m,2}+\psi_{m+1,1}+\psi_{m,0}\right)+\dfrac{1}{6}\left(\psi_{m-1,2}+\psi_{m+1,2}+\psi_{m-1,0}+\psi_{m+1,0}\right)=F_{m,1}, m=\overline{2,n_2-2},\\ \overline{F_{m,1}}=F_{m,1}-\dfrac{2}{3}\psi_{m,0}-\dfrac{1}{6}\left(\psi_{m-1,0}+\psi_{m+1,0}\right), m=\overline{2,n_2-2},\\ -\dfrac{10}{3}\psi_{m,n_1-1}+\dfrac{2}{3}\left(\psi_{m-1,n_1-1}+\psi_{m,n_1-2}+\psi_{m+1,n_1-1}+\psi_{m,n_1}\right)+\dfrac{1}{6}\left(\psi_{m-1,n_1-2}+\psi_{m+1,n_1-2}+\psi_{m-1,n_1}+\psi_{m+1,n_1}\right)=F_{m,n_1-1}, m=\overline{2,n_2-2},\\ \overline{F_{m,n_1-1}}=F_{m,n_1-1}-\dfrac{2}{3}\psi_{m,n_1}-\dfrac{1}{6}\left(\psi_{m-1,n_1}+\psi_{m+1,n_1}\right), m=\overline{2,n_2-2},\\ \overline{F_{m,n}}=F_{m,n},\ \forall m\in\overline{2,n_2-2}, n\in\overline{2,n_1-2}.\end{cases}\tag{13}$$

3. Find the matrix coefficients for the forward sweep using formulas (14) and (15) $m=\overline{1,n_2-2}$:

$$\lambda_1=-A^{-1}B, \nu_1=A^{-1}\overline{F_1^T}, \tag{14}$$

$$\lambda_m=-\left(B\lambda_{m-1}+A\right)^{-1}B, \nu_m=\left(B\lambda_{m-1}+A\right)^{-1}\left(\overline{F_m^T}-B\nu_{m-1}\right), m=\overline{2,n_2-2}. \tag{15}$$

4. Find the vector-row $\psi^T_{n_2-1}$ using formula (16):

$$\psi^T_{n_2-1}=\left(B\lambda_{n_2-2}+A\right)^{-1}\left(\overline{F^T_{n_2-1}}-B\nu_{n_2-2}\right). \tag{16}$$

5. Find the remaining rows of the solution matrix $\psi^T{}_m$ using formulas (17):

$$m=\overline{n_2-2,1}\ \psi^T_m=\lambda_m\psi^T_{m+1}+\nu_m, m=\overline{n_2-2,1}, \nu_{n_2-1}=\psi^T_{n_2-1}. \tag{17}$$

The matrix algorithm for the sweep (9)–(17) preserves sixth-order accuracy according to formulas (7) and (8) for the Poisson equation.

The second and third equations of the system (1) $\overline{w}=\overline{v}_{\bar{x}}-\overline{u}_{\bar{y}}, \overline{u}=\overline{\psi}_{\bar{y}}, \overline{v}=-\overline{\psi}_{\bar{x}}$ are linear with respect to the first partial derivatives, which can be calculated independently. Let us present the quadrature formulas for the first derivative with different stencil centers.

For example, for the equation $\overline{u}=\overline{\psi}_{\bar{y}}$ we obtain:

$$\begin{cases} u_{(i,j)}=\dfrac{1}{h}\left(\dfrac{3}{4}\left(\psi_{i+1,j}-\psi_{i-1,j}\right)-\dfrac{3}{20}\left(\psi_{i+2,j}-u_{i-2,j}\right)+\dfrac{1}{60}\left(\psi_{i+3,j}-\psi_{i-3,j}\right)\right)+O\left(h^6\right), i=\overline{3,n_2-3}, j=\overline{1,n_1-1},\\ u_{(1,j)}=\dfrac{1}{h}\left(-\dfrac{\psi_{0,j}}{5}-\dfrac{13}{12}\psi_{1,j}+2\psi_{2,j}-\psi_{3,j}+\dfrac{\psi_{4,j}}{3}-\dfrac{\psi_{5,j}}{20}\right)+O\left(h^4\right), j=\overline{1,n_1-1},\\ u_{(2,j)}=\dfrac{1}{12h}\left(8\left(\psi_{3,j}-\psi_{1,j}\right)-\left(\psi_{4,j}-\psi_{0,j}\right)\right)+O\left(h^4\right), j=\overline{1,n_1-1},\\ u_{(n_2-1,j)}=-\dfrac{1}{h}\left(-\dfrac{\psi_{n_2,j}}{5}-\dfrac{13}{12}\psi_{n_2-1,j}+2\psi_{n_2-2,j}-\psi_{n_2-3,j}+\dfrac{\psi_{n_2-4,j}}{3}-\dfrac{\psi_{n_2-5,j}}{20}\right)+O\left(h^4\right), j=\overline{1,n_1-1},\\ u_{(n_2-2,j)}=-\dfrac{1}{12h}\left(8\left(\psi_{n_2-3,j}-\psi_{n_2-1,j}\right)-\left(\psi_{n_2-4,j}-\psi_{n_2,j}\right)\right)+O\left(h^4\right), j=\overline{1,n_1-1}. \end{cases} \tag{18}$$

Similar formulas can be written for the equations $\overline{v}=-\overline{\psi}_{\bar{x}}, \overline{w}=\overline{v}_{\bar{x}}-\overline{u}_{\bar{y}}$. Consider the vortex dynamics equation in the system of equations (1). To accelerate the numerical solution of the problem (1), the splitting method [11] was used.

Analytically, the method of *n*-fold splitting of the vortex equation for the time interval $\tau_0\cdot n$ can be written as:

$$\frac{w^{k+i+1}-w^{k+i}}{\tau_0}+u^k\cdot w_x^{k+i}+v^k\cdot w_y^{k+i}=\frac{1}{\mathrm{Re}}\left(w_{xx}^{k+i}+w_{yy}^{k+i}\right), i=\overline{0,n-1}. \tag{19}$$

The system of recurrence equations (19) for the vortex with a frozen velocity field $\left(u^k(x,y),v^k(x,y)\right), i=\overline{0,n-1}, k=const, k=1,2,...$ consists of n intermediate steps $i=\overline{0,n-1}$, where the upper index *i* indicates the number of the intermediate time layer in the vortex equation (19), and the index k is the number of the multiple time layer in the system (19) (if *k* is a multiple of *n*). The velocity fields and stream functions are constant in equations (19) for given values of *k* = *const* and the change in index $i=\overline{0,n-1}$. In this system of equations, only the vortex field changes $w^{k+i}, i=\overline{0,n-1}$. The velocity field changes abruptly in systems (1) and (19) when the time index of the vortex function increases by *n* from *k* to *k* + *n* in the vortex equation system (19).

The idea of splitting the system of equations (19) is to reduce the accumulation of rounding errors and the computational time when solving it. Differential operators with respect to the coordinate in (19) are approximated in the internal nodes with accuracy $O(h^6)$, as are all the equations in the system (1), boundary conditions with accuracy $O(h^4)$, and the time with accuracy $O(\tau)$.

Thus, by solving equation (19) $\tau_0\cdot n$, *n* times in time we get a time jump $\tau_0\cdot n$ (which is *n* times larger than the sequential solution of the system of equations (1)) and reduce the rounding error without solving the other equations in the system (1) inside the system (19).

Equation (19) is linear with respect to the coordinate derivatives $w_x^i, w_y^i, w_{xx}^i, w_{yy}^i$. In work [11], it is shown that for spectral stability of the vortex dynamics equation (19), it is enough to choose the ratio of the time and spatial steps in the form of the inequality $\tau_0\le\frac{3}{16}h^2\,\mathrm{Re}$. This maximum time step was set by the authors in the program.

For the first partial derivatives of equation (19), approximation formulas were used, for example, for w_y ((formulas for the derivative with respect to w_x are similar):

$$\begin{cases} w_{y(i,j)} = \dfrac{1}{h}\left(\dfrac{3}{4}\left(w_{i+1,j} - w_{i-1,j}\right) - \dfrac{3}{20}\left(w_{i+2,j} - w_{i-2,j}\right) + \dfrac{1}{60}\left(w_{i+3,j} - w_{i-3,j}\right)\right) + O\left(h^6\right), i = \overline{3, n_2 - 3}, j = \overline{1, n_1 - 1}, \\ w_{y(1,j)} = \dfrac{1}{h}\left(-\dfrac{w_{0,j}}{5} - \dfrac{13}{12}w_{1,j} + 2w_{2,j} - w_{3,j} + \dfrac{w_{4,j}}{3} - \dfrac{w_{5,j}}{20}\right) + O\left(h^4\right), j = \overline{1, n_1 - 1}, \\ w_{y(2,j)} = \dfrac{1}{12h}\left(8\left(w_{3,j} - w_{1,j}\right) - \left(w_{4,j} - w_{0,j}\right)\right) + O\left(h^4\right), j = \overline{1, n_1 - 1}, \\ w_{y(n_2-1,j)} = -\dfrac{1}{h}\left(-\dfrac{w_{n_2,j}}{5} - \dfrac{13}{12}w_{n_2-1,j} + 2w_{n_2-2,j} - w_{n_2-3,j} + \dfrac{w_{n_2-4,j}}{3} - \dfrac{w_{n_2-5,j}}{20}\right) + O\left(h^4\right), j = \overline{1, n_1 - 1}, \\ w_{y(n_2-2,j)} = -\dfrac{1}{12h}\left(8\left(w_{n_2-3,j} - w_{n_2-1,j}\right) - \left(w_{n_2-4,j} - w_{n_2,j}\right)\right) + O\left(h^4\right), j = \overline{1, n_1 - 1}. \end{cases} \quad (20)$$

The second partial derivatives w_{yy} in equation (19) are given by:

$$\begin{cases} w_{yy(i,j)} = \dfrac{1}{h^2}\left(-\dfrac{49}{18}w_{i,j} + \dfrac{3}{2}\left(w_{i+1,j} + w_{i-1,j}\right) - \dfrac{3}{20}\left(w_{i+2,j} + w_{i-2,j}\right) + \dfrac{1}{90}\left(w_{i+3,j} + w_{i-3,j}\right)\right) + O\left(h^6\right), i = \overline{3, n_2 - 3}, j = \overline{1, n_1 - 1}, \\ w_{yy(1,j)} = \dfrac{1}{h^2}\left(\dfrac{137}{180}w_{0,j} - \dfrac{49}{60}w_{1,j} - \dfrac{17}{12}w_{2,j} + \dfrac{47}{18}w_{3,j} - \dfrac{19}{12}w_{4,j} + \dfrac{31}{60}w_{5,j} - \dfrac{13}{180}w_{6,j}\right) + O\left(h^4\right), j = \overline{1, n_1 - 1}, \\ w_{yy(2,j)} = \dfrac{1}{h^2}\left(-\dfrac{5}{2}w_{2,j} + \dfrac{4}{3}\left(w_{1,j} + w_{3,j}\right) - \dfrac{1}{12}\left(w_{0,j} + w_{4,j}\right)\right) + O\left(h^4\right), j = \overline{1, n_1 - 1}, \\ w_{yy(n_2-1,j)} = \dfrac{1}{h^2}\left(\dfrac{137}{180}w_{n_2,j} - \dfrac{49}{60}w_{n_2-1,j} - \dfrac{17}{12}w_{n_2-2,j} + \dfrac{47}{18}w_{n_2-3,j} - \dfrac{19}{12}w_{n_2-4,j} + \dfrac{31}{60}w_{n_2-5,j} - \dfrac{13}{180}w_{n_2-6,j}\right) + O\left(h^4\right), j = \overline{1, n_1 - 1}, \\ w_{yy(n_2-2,j)} = \dfrac{1}{h^2}\left(-\dfrac{5}{2}w_{n_2-2,j} + \dfrac{4}{3}\left(w_{n_2-1,j} + w_{n_2-3,j}\right) - \dfrac{1}{12}\left(w_{n_2 j} + w_{n_2-4,j}\right)\right) + O\left(h^4\right), j = \overline{1, n_1 - 1}. \end{cases} \quad (20)$$

Similar to formulas (20), formulas for the derivative with respect to w_{xx} are written.

According to the algorithm of A. Salih [1], it is necessary first to update the values of the vortex function w at the boundary of the rectangle and only then solve the vortex equation (19) in the internal points of the cavity.

Let's expand the stream function at the first coordinate node at a distance h from the left wall along the x-axis, which is normal to the left wall:

$$\psi_1 = \psi_0 + \psi_x h + \psi_{xx}\frac{h^2}{2} + \psi_{xxx}\frac{h^3}{6} + \psi_{xxxx}\frac{h^4}{24} + \psi_{xxxxx}\frac{h^5}{120} + O\left(h^6\right). \quad (21)$$

From the equation $\bar{u} = \bar{\psi}_{\bar{y}} = 0$ it follows that on the lateral walls the stream function does not change, and from the equation $\bar{v} = -\bar{\psi}_{\bar{x}} = 0$ it follows that the stream function does not change on the bottom and top segments of the cavity. Therefore, on all four sides of the rectangular cavity, we set the stream function to be equal to zero.

Considering that on the left wall of the cavity $\psi_0 = 0, \psi_x = -v, \psi_{xx} = -w$ we rewrite equation (21) as:

$$\psi_1 = -vh - w\frac{h^2}{2} + \psi_{xxx}\frac{h^3}{6} + \psi_{xxxx}\frac{h^4}{24} + \psi_{xxxxx}\frac{h^5}{120} + O\left(h^6\right) \Leftrightarrow w = -\frac{2}{h}v - \frac{2\psi_1}{h^2} + \psi_{xxx}\frac{h}{3} + \psi_{xxxx}\frac{h^2}{12} + \psi_{xxxxx}\frac{h^3}{60} + O\left(h^4\right). \quad (22)$$

From equation (22), it can be seen that it is sufficient to approximate the derivatives of the stream function ψ_{xxx}, ψ_{xxxx}, ψ_{xxxxx} at the left boundary with the 3rd, 2nd, and 1st orders of accuracy, respectively. Equation (22) has an invariant form since the order of the derivative and the step size h have the same parity. For example, for ψ_{xxxxx}, h^3 the 3rd and 5th orders, respectively, the product of the difference operator applied to ψ_{xxxxx} by h^3 does not change the sign and has the same form relative to both the right and left walls.

The program used the following approximation of derivatives for the formula (22) (in each formula (23), the index j changes within the range $j = \overline{1, n_1 - 1}$):

$$\begin{cases} w^{(3)}_{y(0,j)}h = \dfrac{1}{h^2}\left(-\dfrac{49}{8}w_{0,j} + 29w_{1,j} - \dfrac{461}{8}w_{2,j} + 62w_{3,j} - \dfrac{307}{8}w_{4,j} + 13w_{5,j} - \dfrac{15}{8}w_{6,j}\right) + O\left(h^4\right), \\ w^{(4)}_{y(0,j)}h^2 = \dfrac{1}{h^2}\left(\dfrac{35}{6}w_{0,j} - 31w_{1,j} + \dfrac{137}{2}w_{2,j} - \dfrac{242}{3}w_{3,j} + \dfrac{107}{2}w_{4,j} - 19w_{5,j} + \dfrac{17}{6}w_{6,j}\right) + O\left(h^4\right), \\ w^{(5)}_{y(0,j)}h^3 = \dfrac{1}{h^2}\left(-\dfrac{7}{2}w_{0,j} + 20w_{1,j} - \dfrac{95}{2}w_{2,j} + 60w_{3,j} - \dfrac{85}{2}w_{4,j} + 16w_{5,j} - \dfrac{5}{2}w_{6,j}\right) + O\left(h^4\right), \\ w^{(3)}_{y(n_2,j)}h = \dfrac{1}{h^2}\left(-\dfrac{49}{8}w_{n_2,j} + 29w_{n_2-1,j} - \dfrac{461}{8}w_{n_2-2,j} + 62w_{n_2-3,j} - \dfrac{307}{8}w_{n_2-4,j} + 13w_{n_2-5,j} - \dfrac{15}{8}w_{n_2-6,j}\right) + O\left(h^4\right), \\ w^{(4)}_{y(n_2,j)}h^2 = \dfrac{1}{h^2}\left(\dfrac{35}{6}w_{n_2,j} - 31w_{n_2-1,j} + \dfrac{137}{2}w_{n_2-2,j} - \dfrac{242}{3}w_{n_2-3,j} + \dfrac{107}{2}w_{n_2-4,j} - 19w_{n_2-5,j} + \dfrac{17}{6}w_{n_2-6,j}\right) + O\left(h^4\right), \\ w^{(5)}_{y(n_2,j)}h^3 = \dfrac{1}{h^2}\left(-\dfrac{7}{2}w_{n_2,j} + 20w_{n_2-1,j} - \dfrac{95}{2}w_{n_2-2,j} + 60w_{n_2-3,j} - \dfrac{85}{2}w_{n_2-4,j} + 16w_{n_2-5,j} - \dfrac{5}{2}w_{n_2-6,j}\right) + O\left(h^4\right). \end{cases} \quad (23)$$

In the work by A. Salih [1], it is pointed out that the stability of the numerical solution to problem (1) depends on the order of approximation of the boundary values of the vortex function in an equation analogous to equation (23). For example, he claims that approximating the boundary conditions of the vortex with the first order is more stable than with the second order. Using the method of splitting the vortex equation (19) with an explicit finite difference scheme, the authors did not notice any influence of the order of approximation of the vortex boundary conditions on the stability of the problem, even with a fourth-order approximation. The stability of the solution to the general problem (1) depended only on the Reynolds number Re and the choice of initial conditions.

Similarly to equation (22), for the vortex at the lower (upper) wall, we have:

$$w = \frac{2}{h}u - \frac{2\psi_1}{h^2} + \psi_{yyy}\frac{h}{3} + \psi_{yyyy}\frac{h^2}{12} + \psi_{yyyyy}\frac{h^3}{60} + O\left(h^4\right). \qquad (24)$$

The profile of the initial horizontal velocity component (2), (3) and the vertical velocity component (4) refers to the deceleration method and is stable for a Reynolds number Re ≤ 3000. The acceleration method assumes initially stationary fluid in the cavity and was first proposed by A.A. Fomin and L.N. Fomina in their work [2]. The upper cover of the cavity, slowly accelerating from the stationary state, drags the fluid along with it inside the closed cavity. In work [2], the Fomins proposed the velocity of the upper cover as a function of time, according to the formula:

$$v(x,k) = 0, u(x,k) = \begin{cases} \frac{1}{2}\left(\sin\left(\frac{\pi}{2}(2t/t_1 - 1)\right) + 1\right), 0 \le t \le t_1, \\ 1, t > t_1. \end{cases}$$

In this work, the acceleration method used a similar formula:

$$v(x,k) = 0, u(x,k) = \begin{cases} \sin\left(\frac{\pi}{2}\frac{t}{t_1}\right), 0 \le t \le t_1, \\ 1, t > t_1. \end{cases} \qquad (25)$$

```
horosho!                  24045 u  2.398584847328107E-003
-0.117589460964839
uu                  24045   1.26213918814584      -0.407936688073471
vv                  24045  0.241397444300957      -0.663734592934930
ww                  24045  104.601518805320        -103.604719388108
wwi0=          94 j0=         100
wwil=         100 j1=           9
```

a)

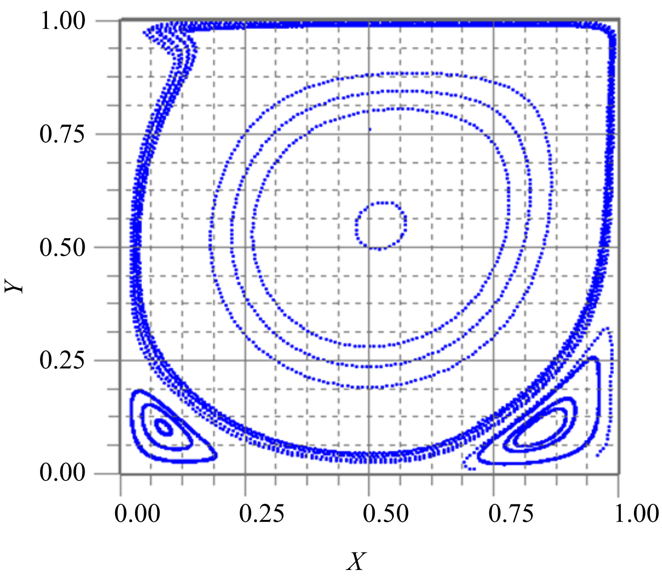

b)

Fig. 1. Results of the solution: *a* — Re = 2000, deceleration method, lower boundary of the stream function (first number), boundaries of horizontal and vertical velocity components, and vortex function at time *t* = 24000; *b* — the limiting field of streamlines in the deceleration method Re = 2000, $n_1 \times n_2 = 100 \times 100$

```
-0.117589460964840
uu               1260159   1.26213918814584        -0.407936688073472
vv               1260159  0.241397444300959        -0.663734592934934
ww               1260159   104.601518805320         -103.604719388108
wwi0=                          94 j0=                  100
wwi1=                         100 j1=                    9
```

a)

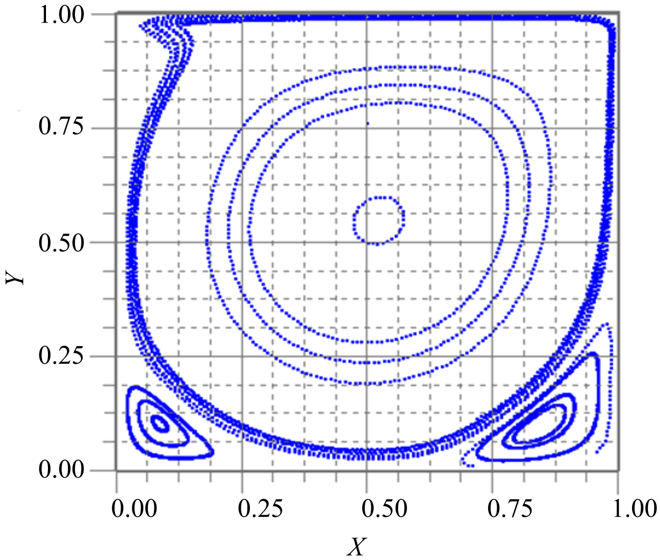

b)

Fig. 2. Results of the solution: *a* — Re = 2000, acceleration method, lower boundary of the stream function (first number), boundaries of horizontal and vertical velocity components, and vortex function at time t = 1260000; *b* — the limiting field of streamlines in the acceleration method Re = 2000, $n_1 \times n_2 = 100 \times 100$

By comparing the intervals of variation of the stream function values, the fields of horizontal and vertical velocities, and the vortex function in Figures 1 and 2, we see that they coincide with an accuracy of up to 16 significant digits. Therefore, the fields of streamlines in Figures 1 and 2 also coincide.

Thus, the acceleration and deceleration methods for the initial velocity field (2), (3), (4) are equivalent for Reynolds numbers Re ≤ 3000. However, the time required to establish steady fields in the deceleration method is tens of times (57 times) shorter than the time required to solve problem (1) using the acceleration method.

```
-9.807891140697904E-002
uu               1044968   1.00000000000000        -0.362267751647030
vv               1044968  0.222611083056212        -0.543539677038107
ww               1044968   120.628076257385         -133.907927009122
wwi0=                          89 j0=                  100
wwi1=                         100 j1=                    9
```

a)

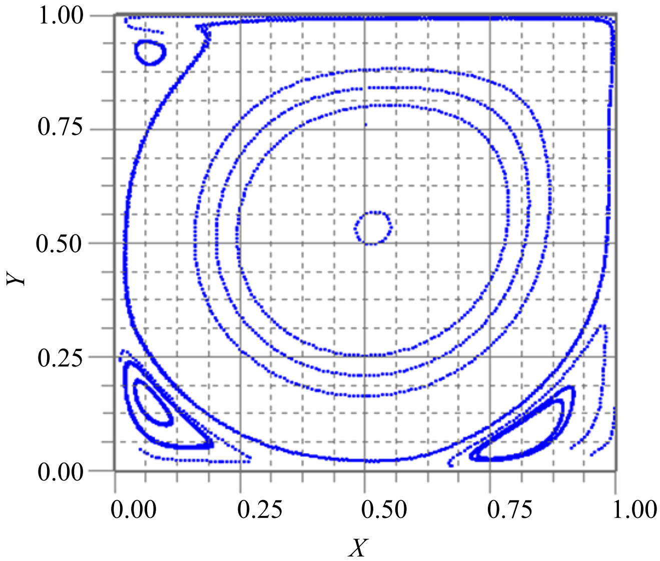

b)

Fig. 3. Results of the solution: *a* — Re = 8000, acceleration method, lower boundary of the stream function (first number), boundaries of horizontal and vertical velocity components, and vortex function at time t = 1044000; *b* — the limiting field of streamlines in the acceleration method Re = 8000, $n_1 \times n_2 = 100 \times 100$

The field of streamlines in Figure 3*b* shows three second-order vortices located at the corners of the cavity and fully coincides with the streamlines field presented in work [13, p. 22] for Re = 8000. From Figures 1, 2, and 3, it is evident that the maximum values of the vortex function occur at nodes on the upper and right walls of the cavity, near the points where the velocity profile joins or near special velocity points at the upper corners of the cavity [14].

Discussion and Conclusion. A numerical solution algorithm for a two-dimensional hydrodynamic problem in a rectangular cavity, in terms of "stream function — vortex", is proposed. The approximation of the equations in the system (1) has a sixth-order error in the interior nodes and fourth-order error in the boundary nodes. For the first time, a deceleration method with an initial horizontal velocity field is proposed using a smooth connection of two sinusoids. The initial conditions in the deceleration method are suitable for Reynolds numbers $Re \leq 3000$. The numerical equivalence of solutions using the acceleration and deceleration methods is demonstrated, with final fields of the stream function, horizontal and vertical velocity components, and the vortex field coinciding up to 15 significant digits. The problem in terms of "stream function — vortex" has been numerically solved for Re = 8000 and its solution and the structure of the primary and secondary vortices qualitatively match the results of other authors.

References

1. Salih A. *Streamfunction — Vorticity Formulation*. Department of Aerospace Engineering Indian Institute of Space Science and Technology, Thiruvananthapuram; 2013:10 p.

2. Fomin A.A., Fomina L.N. The implisit iterated polynetic recurrent method in application to solving the problems of the dynamics of inconsistent fluid. *Computation research and modelling*. 2015;7(1): 35–50. (In Russ.)

3. Petrov A.G. High-precision numerical schemes for solving plane boundary value problems for a polyharmonic equation and their application to problems of hydrodynamics. *Applied Mathematics and Mechanics*. 2023;87(3):343–368 (In Russ.) https://doi.org/10.31857/S0032823523030128

4. Sukhinov A.I., Kolgunova O.V., Girmay M.Z., Nakhom O.S. A two-dimensional hydrodynamic model of coastal systems, taking into account evaporation. *Computation Mathematics and Information Technologies*. 2023;7(4):9–21. https://doi.org/10.23947/2587-8999-2023-7-4-9-21

5. Volosova N.K., Volosov K.A., Volosova A.K., Pastukhov D.F., Pastukhov Yu.F., Basarab M.A. *Collection of articles on hydrodynamics. 2nd edition*. Moscow: Moscow State Transport University of Emperor Nicholas II; 2023. 231 p. (In Russ.)

6. Ershova T.Ya. Boundary value problem for a third-order differential equation with a strong boundary layer. *Bulletin of Moscow University. Episode 15: Computational mathematics and cybernetics*. 2020;1:30–39. (In Russ.) https://doi.org/10.3103/S0278641920010057

7. Sitnikova M.A., Skulsky O.I. Flow of momentary anisotropic fluid in thin layers. *Bulletin of Perm University. Mathematics. Mechanics. Informatics*. 2015;28(1): 56–62. (In Russ.)

8. Volosov K.A., Vdovina E.K., Pugina L.V. Modeling of "pulsatile" modes of blood coagulation dynamics. *Math modeling*. 2014;26(12):14–32. (In Russ.)

9. Buzmakova M.M., Gilev V.G., Rusakov S.V. Experimental study of the rheokinetics of an epoxy binder modified with C60 fullerenes. *Bulletin of Perm University. Physics*. 2019;2:35–40. (In Russ.) https://doi.org/10.17072/1994-3598-2019-2-35-40

10. Sidoryakina V.V., Solomaha D.A. Symmetrized versions of the Seidel and upper relaxation methods for solving two-dimensional difference problems of elliptic. *Computational Mathematics and Information Technologies*. 2023;7(3):12–19. (In Russ.) https://doi.org/10.23947/2587-8999-2023-7-3-12-19

11. Volosova N.K., Volosov K.A., Volosova A.K., Karlov M.I., Pastukhov D.F., Pastukhov Yu.F. The N-fold distribution of the obvious variable scheme for the equalization of the vortex in the viscous incompatible fluid. *Bulletin of the Perm University. Mathematics. Mechanics. Informatics*. 2023;63(4):12–21. (In Russ.) https://doi.org/10.17072/1993-0550-2023-4-12-21

12. Bahvalov N.S., Zhidkov N.P., Kobelkov G.M. *Numerical methods: a textbook for students of physics and mathematics specialties of higher educational institutions.* Moscow: Binom. lab. Knowledge; 2011. 636 p. (In Russ.)

13. Kuhlmann H.C., Romano F. The Lid-Driven cavety. In book: Gelfgat A. (ed.) C*omputational Modelling of Bifurcations and Instabilities in Fluid Dynamics. Computational Methods in Applied Sciences*. Springer, Cham. 2018;50:233–309. https://doi.org/10.1007/978-3-319-91494-7_8

14. Speranskaya A.A. *Border layers in geophysical hydrodynamics:* dissertation Doctor of Physical and Mathematical Sciences. Moscow; 1982. 345 p. (In Russ.)

About the Authors:

Natalya K. Volosova, Post-graduate Student of Bauman Moscow State Technical University (2nd Baumanskaya St. 5–1, Moscow, 105005, Russian Federation), ORCID, navalosova@yandex.ru

Konstantin A. Volosov, Doctor of Physical and Mathematical Sciences, Professor of the Department of Applied Mathematics of the Russian University of Transport (Obraztsova St. 9–9, Moscow, GSP-4, 127994, Russian Federation), ORCID, SPIN-code, konstantinvolosov@yandex.ru

Aleksandra K. Volosova, Candidate of Physical and Mathematical Sciences, Chief Analytical Department “Tramplin” LLC, Russian University of Transport (Obraztsova St. 9–9, Moscow, GSP-4, 127994, Russian Federation), ORCID, SPIN-code, alya01@yandex.ru

Mikhail I. Karlov, Candidate of Physical and Mathematical Sciences, Associate Professor of the Department of Mathematics, Moscow Institute of Physics and Technology (9, Institutsky Lane, GSP-4, Dolgoprudny, 141701, Russian Federation), SPIN-code, karlov.mipt@gmail.com

Dmitriy F. Pastukhov, Candidate of Physical and Mathematical Sciences, Associate Professor of Polotsk State University (Blokhin St. 29, Novopolotsk, 211440, Republic of Belarus), ORCID, SPIN-code, dmitrij.pastuhov@mail.ru

Yuriy F. Pastukhov, Candidate of Physical and Mathematical Sciences,Associate Professor of Polotsk State University (Blokhin St. 29, Novopolotsk, 211440, Republic of Belarus), ORCID, SPIN-code, pulsar1900@mail.ru

Contributions of the authors:

N.K. Volosova: setting the task; writing a draft of the manuscript; formulation of research ideas, goals and objectives.

K.A. Volosov: scientific guidance; methodology development.

A.K. Volosova: translation; study of the history of the task; literature.

M.I. Karlov: formal analysis.

D.F. Pastukhov: visualization; validation; software.

Yu.F. Pastukhov: testing of existing code components.

Conflict of Interest Statement: **the authors declare no conflict of interest.**

All authors have read and approved the final manuscript.

Об авторах:

Наталья Константиновна Волосова, аспирант Московского государственного технического университета им. Н.Э. Баумана (105005, Российская Федерация, г. Москва, ул. 2-я Бауманская, 5, стр. 1), ORCID, navalosova@yandex.ru

Константин Александрович Волосов, доктор физико-математических наук, профессор кафедры прикладной математики Российского университета транспорта (127994, ГСП-4, Российская Федерация, г. Москва, ул. Образцова, 9, стр. 9), ORCID, SPIN-код, konstantinvolosov@yandex.ru

Александра Константиновна Волосова, кандидат физико-математических наук, начальник аналитического отдела ООО «Трамплин» Российского университета транспорта (127994, ГСП-4, Российская Федерация, г. Москва, ул. Образцова, 9, стр. 9), ORCID, SPIN-код, alya01@yandex.ru

Михаил Иванович Карлов, кандидат физико-математических наук, доцент кафедры математики Московского физико-технического института (141701, ГСП-4, Российская Федерация, г. Долгопрудный, Институтский переулок, 9), SPIN-код, karlov.mipt@gmail.com

Дмитрий Феликсович Пастухов, кандидат физико-математических наук, доцент кафедры технологий программирования Полоцкого государственного университета (211440, Республика Беларусь, г. Новополоцк, ул. Блохина, 29), ORCID, SPIN-код, dmitrij.pastuhov@mail.ru

Юрий Феликсович Пастухов, кандидат физико-математических наук, доцент кафедры технологий программирования Полоцкого государственного университета (211440, Республика Беларусь, г. Новополоцк, ул. Блохина, 29), ORCID, SPIN-код, pulsar1900@mail.ru

Заявленный вклад авторов:

Н.К. Волосова: постановка задачи; написание черновика рукописи; формулировка идей исследования, целей и задач.

К.А. Волосов: научное руководство; разработка методологии.

А.К. Волосова: перевод; изучение истории задачи; поиск литературы.

М.И. Карлов: формальный анализ.

Д.Ф. Пастухов: визуализация; валидация; разработка программного обеспечения.

Ю.Ф. Пастухов: тестирование существующих компонентов кода.

Конфликт интересов: **авторы заявляют об отсутствии конфликта интересов.**

Все авторы прочитали и одобрили окончательный вариант рукописи.

Received / Поступила в редакцию 12.02.2025

Revised / Поступила после рецензирования 19.03.2025

Accepted / Принята к публикации 28.04.2025

MATHEMATICAL MODELLING
МАТЕМАТИЧЕСКОЕ МОДЕЛИРОВАНИЕ

UDC 534.11

https://doi.org/10.23947/2587-8999-2025-9-2-34-43

Check for updates

Original Empirical Research

Study of the Influence of Boundary Motion on the Oscillatory and Resonance Properties of Mechanical Systems with Variable Length

Alexey L. Semenov[1], **Vladimir L. Litvinov**[2], **Maxim V. Shamolin**[3] ✉

[1, 3] Lomonosov Moscow State University, Moscow, Russian Federation

[2] Samara State Technical University, Samara, Russian Federation

✉ shamolin@rambler.ru

Abstract

Introduction. The widespread use of technical systems with moving boundaries necessitates the development of mathematical modelling methods and algorithmic software for their analysis. This paper presents a systematic review of studies examining the oscillatory and resonance properties of mechanical systems with moving boundaries, such as hoisting cables, flexible transmission mechanisms, strings, rods, beams with variable length, and others.

Materials and Methods. A problem statement is formulated, and numerical methods are developed for solving nonlinear problems that describe wave processes and the resonance properties of systems with moving boundaries.

Results. An analysis is conducted on wave reflection from moving boundaries, including changes in their energy and frequency. It is shown that the energy of the system increases when the boundary moves toward the waves and decreases when moving in the same direction as the waves. Criteria are obtained to determine the conditions under which the boundary motion must be considered for accurate calculation of oscillation amplitudes. Numerical results demonstrate the influence of boundary speed and damping on the system dynamics.

Discussion and Conclusion. The findings have practical significance for the design and operation of mechanical systems with variable geometry. The results make it possible to prevent large-amplitude oscillations in mechanical objects with moving boundaries at the design stage. These problems have not been sufficiently studied and require further research.

Keywords: resonance properties, vibrations of systems with moving boundaries, wave processes, damping, vibration amplitude

For Citation. Semenov A.L., Litvinov V.L., Shamolin M.V. Study of the Influence of Boundary Motion on the Oscillatory and Resonance Properties of Mechanical Systems with Variable Length. *Computational Mathematics and Information Technologies*. 2025;9(2):34–43. https://doi.org/10.23947/2587-8999-2025-9-2-34-43

Оригинальное эмпирическое исследование

Исследование влияния движения границ на колебательные и резонансные свойства механических систем переменной длины

А.Л. Семенов[1], **В.Л. Литвинов**[2], **М.В. Шамолин**[3] ✉

[1, 3] Московский государственный университет им. М.В. Ломоносова, г. Москва, Российская Федерация

[2] Самарский государственный технический университет, г. Самара, Российская Федерация

✉ shamolin@rambler.ru

Аннотация

Введение. Широкое распространение в технике объектов с движущимися границами обусловливает необходимость развития методов математического моделирования и создания алгоритмического программного обеспечения для соответствующего анализа. Настоящая работа представляет собой систематизированный обзор материалов, в которых исследуются колебательные и резонансные свойства механических систем с движущимися границами, таких как канаты подъемных устройств, гибкие передаточные механизмы, струны, стержни, балки переменной длины и т. д.

Материалы и методы. Сформулирована постановка и разработаны численные методы решения нелинейных задач, описывающих волновые процессы и резонансные свойства объектов с движущимися границами.
Результаты исследования. Проведен анализ отражения волн от движущихся границ, включая изменение их энергии и частоты. Показано, что энергия системы возрастает при движении границы навстречу волнам и убывает при совпадении направлений. Получены критерии, определяющие условия, при которых необходимо учитывать движение границ для корректного расчета амплитуд колебаний. Численные результаты демонстрируют влияние скорости движения границ и демпфирования на динамику системы.
Обсуждение и заключение. Результаты работы имеют практическое значение для проектирования и эксплуатации механических систем с переменной геометрией. Приведенные результаты позволяют на стадии проектирования предотвратить возможность возникновения колебаний большой амплитуды в механических объектах с движущимися границами. Данные задачи мало изучены и требуют дальнейшего исследования.

Ключевые слова: резонансные свойства, колебания систем с движущимися границами, волновые процессы, демпфирование, амплитуда колебаний

Для цитирования. Семенов А.Л., Литвинов В.Л., Шамолин М.В. Исследование влияния движения границ на колебательные и резонансные свойства механических систем переменной длины. *Computational Mathematics and Information Technologies*. 2025;9(2):34–43. https://doi.org/10.23947/2587-8999-2025-9-2-34-43

Introduction. In the field of elastic system dynamics, particular practical interest is drawn to problems involving vibrations of structures whose geometric parameters change over time. Typical examples of such systems include hoisting ropes [1–8], flexible transmission elements [4, 6, 9], drilling rigs [10], and others. Numerous studies on the dynamics of hoisting ropes have revealed the need to develop new approaches to analyzing the behavior of one-dimensional objects with variable geometric characteristics.

Similar problems involving moving boundaries also arise in the context of heat transfer, thermal conductivity, and diffusion equations (notably, the Stefan problem). Such issues have been addressed in the works of L.A. Uvarova [11], V.A. Kudinov [12], and other researchers.

A related class of problems—devoted to constructing two- and three-dimensional mathematical models of marine and coastal systems, shallow water bodies, wave hydrodynamics and geophysics, and the correctness of problem formulations described by elliptic-type equations—has been investigated by A.I. Sukhinov and his students [13, 14]. These authors study the development and analysis of two-dimensional-one-dimensional splitting schemes and methods for solving grid-based diffusion-convection-reaction problems, which form the basis for efficient parallel algorithms.

The results of A.I. Sukhinov, A.M. Atayan, A.V. Nikitina, A.E. Chistyakov, V.V. Sidoryakina [15], and others form the foundation for studying forecasting problems of adverse and hazardous phenomena, including wave processes at boundaries in natural and man-made systems; mass transfer across moving boundaries such as storm surges, coastal flooding, and the formation of hypoxic zones in marine and coastal systems using precision models; as well as for remote sensing and artificial intelligence applications. These authors have examined the existence and uniqueness of solutions to linearized initial-boundary value problems for the developed models.

The problem of vibrations in systems with moving boundaries is related to obtaining solutions of systems of partial differential equations in time-varying domains, as well as integro-differential equations with time-dependent integration limits and kernels. It involves introducing the concepts of "eigenvalues" and "eigenfunctions" for variable-length objects and developing a general framework for studying boundary value problems of this class based on the synthesis of integral equation theory and asymptotic methods. Characteristic model boundary value problems are solved in the context of the dynamics of hoisting ropes, beams, rods, and strings with variable length, and their resonance properties are analyzed. These problems have not been sufficiently studied. Traditional methods of mathematical physics are mainly limited to problems with fixed boundaries.

The difficulties encountered in formulating and solving such problems stem from the fact that, to date, no sufficiently general approach exists for analyzing the dynamic behavior of such systems. Existing results are limited to qualitative descriptions of dynamic phenomena, while little attention has been given in the literature to obtaining quantitative characteristics with practical value.

The theoretical significance of this study lies in the development and investigation of new mathematical models describing the vibrations of objects with moving boundaries in the form of partial differential equations.

The practical significance consists in the generalization of modelling techniques and numerical analysis of the resonance properties of objects described by boundary value problems with moving boundaries. The emergence of large-amplitude oscillations in such systems is often unacceptable, making resonance analysis a key focus.

From a mathematical perspective, these problems require solving hyperbolic-type equations in domains with moving boundaries. The considerable challenges in describing such systems justify the predominant use of approximate analytical methods. Among the analytical approaches, the most effective are those based on special variable transformations [16, 17], as well as methods employing the principle of superposition of counter-propagating wave processes [18]. Of particular interest is the approach proposed in [19], which involves using complex variable substitutions to reduce the original problem to the analysis of the Laplace equation.

However, the capabilities of exact analytical methods are significantly limited [1–3, 20–21]. Among approximate methods, special attention should be given to the Kantorovich-Galerkin method [10, 22], as well as approaches based on constructing solutions to integro-differential equations [23].

In systems with moving boundaries, two types of resonance phenomena are observed [4]: steady-state resonance and passage through resonance.

If a system with time-varying dimensions is subjected to an external force whose variation is synchronized with the changing natural frequency, the phenomenon of continuous amplitude growth is referred to as steady-state (or generalized) resonance. Passage through resonance refers to the sharp increase in amplitude over a finite time interval, during which the instantaneous natural frequency of one of the modes coincides with the excitation frequency.

Passage through resonance occurs over a limited time interval and typically does not reach the amplitude levels characteristic of steady-state resonance. However, when damping is high and boundary motion is slow, the amplitude values of both resonance types are close. In such situations, to estimate the vibration amplitude during passage through resonance, it is sufficient to fix the boundaries at the resonance point and compute the amplitude of the steady-state oscillations, which will approximate the maximum amplitude observed during the passage through resonance. Thus, the amplitude in the fixed-boundary case provides an upper bound estimate for the desired quantity.

Consequently, there is a need to expand the range of problems related to modelling vibrations in systems with moving boundaries and to develop new solution methods and corresponding software tools. This need constitutes the main objective of the present work. The study explores the patterns of wave reflection from moving boundaries in systems whose vibrations are described by the wave equation, as well as the interaction of longitudinal waves with moving boundaries. The influence of damping forces on vibration amplitudes during resonance passage in systems with moving boundaries is analyzed. Inequalities are derived that define the domains in which boundary motion must be accounted for. The paper presents a systematized review of materials previously presented by the authors at scientific conferences [24–26], which examine the vibrational and resonance properties of mechanical systems with moving boundaries.

Materials and Methods

Investigation of wave reflection patterns from moving boundaries. Let the oscillatory processes of the system be described by the wave equation:

$$U_{tt}(x,t) - a^2 U_{xx}(x,t) = 0. \tag{1}$$

Here $U(x,t)$ is the function representing longitudinal or transverse displacement of the object from the equilibrium position; t is the time; x is the spatial coordinate.

The oscillating object (string, rod) is unbounded on one side, while the other boundary moves according to a law $x = l(t)$. A sinusoidal wave $g(x + at)$ is incident on the moving boundary, where

$$g(z) = A\sin(wz + \gamma), \tag{2}$$

and a reflected wave $q(x - at)$ emerges from the boundary.

The task is to determine the change in energy of the reflected wave compared to the incident wave under uniform and periodic boundary motion. The solution to equation (1) is written in the form:

$$U(x,t) = g(x + at) + q(x - at). \tag{3}$$

The energy of the segment of the object ($x \in [a;b]$) is given by the formula:

$$W = \frac{1}{2}\rho\int_a^b (a^2 U_x^2(x,t) + U_t^2(x,t))dx, \tag{4}$$

where ρ is the linear mass density of the object.

Substituting expression (3) into (4), we obtain:

$$W = \frac{1}{2}\rho a^2 \int_a^b ((g'(x+at))^2 + (q'(x-at))^2)dx.$$

Thus, the system's energy consists of two parts — the energy of the incident wave and the energy of the reflected wave:

$$W_{пад.} = \frac{1}{2}\rho a^2 \int_a^b (g'(x+at))^2 dx, \tag{5}$$

$$W_{отр.} = \frac{1}{2}\rho a^2 \int_a^b (q'(x-at))^2 dx. \tag{6}$$

We will also use the dimensionless characteristic

$$W_0 = \frac{W_{отр.}}{W_{пад.}} \tag{7}$$

and the dimensionless variables:

$$U(x,t) = AY(\xi,\tau),\ \ \tau = wat,\ \ \xi = wx,\ \ p = wz,\ \ q(z) = AQ(p),\ \ g(z) = AG(p).$$

Then expressions (1)–(3), (5), and (6) will take the following form:

$$Y_{\tau\tau}(\xi,\tau) - Y_{\xi\xi}(\xi,\tau) = 0, \tag{8}$$

$$G(p) = \sin(p+\gamma), \tag{9}$$

$$Y(\xi,\tau) = G(\xi+\tau) + Q(\xi-\tau), \tag{10}$$

$$W_{пад.} = C\int_{a_0}^{b_0} (G'(\xi+\tau))^2 d\xi,\ \ W_{отр.} = C\int_{a_0}^{b_0} (Q'(\xi-\tau))^2 d\xi,$$

where $C = \frac{1}{2}\rho a^2 A^2 w,\ \ a_0 = wa,\ \ b_0 = wb.$

Consider the boundary condition at the moving boundary of the form:

$$U(l(t),t) = 0 \tag{11}$$

for uniform boundary motion $l(t)=Vt$.

In dimensionless variables, the boundary condition will have the form:

$$Y(L(\tau),\tau) = 0, \tag{12}$$

where

$$L(\tau) = \alpha\tau,\ \ \alpha = V/a\ \ (\alpha < 1). \tag{13}$$

Substitute the solution (10) into the boundary condition (12). As a result, we obtain:

$$G(L(\tau)+\tau) + Q(L(\tau)-\tau) = 0. \tag{14}$$

Let us denote this equation $P = (L(\tau) - \tau)$ and find from it the relation for τ: $\tau = \varphi(P)$:

Express: $L(\tau)+\tau = P + 2\varphi(P)$. When the boundary moves according to the law $\varphi(P) = \frac{z}{\alpha - 1}$ equation (14) becomes: $Q(P) = -G\left(\frac{\alpha+1}{\alpha-1}P\right)$.

Given that the incident wave is defined by expression (9), the reflected wave will have the form:

$$Q(P) = -\sin\left(-\frac{1+\alpha}{1-\alpha}P + \gamma\right). \tag{15}$$

Analysis of equation (15) shows that the amplitude of the wave does not change upon reflection from a moving boundary, while the frequency changes in accordance with the Doppler effect by a factor of $\frac{1+\alpha}{1-\alpha}$. When the boundary moves toward the wave, the frequency increases ($\alpha > 0$), when the boundary moves in the same direction as the wave, the frequency decreases ($\alpha < 0$).

Let us now calculate the energy change of a single incident wave upon reflection.

The wavelength of the incident wave (from equation (9)) is 2π. The wavelength of the reflected wave is $\frac{1-\alpha}{1+\alpha}2\pi$, therefore the ratio of the energies becomes

$$W_{пад.} = C\int_0^{2\pi} \cos^2(P+\gamma)dP = C\pi, \tag{16}$$

$$W_{отр.} = C\int_0^{2\pi\frac{1-\alpha}{1+\alpha}} \left(\frac{1+\alpha}{1-\alpha}\right)^2 \cos^2\left(\frac{1+\alpha}{1-\alpha}P + \gamma\right)dP = C\pi\left(\frac{1+\alpha}{1-\alpha}\right),$$

$$W_0 = \frac{W_{отр.}}{W_{пад.}} = \frac{1+\alpha}{1-\alpha}.$$

The energy of the system increases when the boundary moves toward the wave. The energy decreases when the boundary moves in the same direction as the wave.

Now consider periodic boundary motion:

$$l(t) = B\sin(\omega t). \tag{17}$$

Let us synchronize the motion of the boundary with the incident waves in such a way that during the time it takes for one wave to arrive ($T = 2\pi/wa$) the boundary completes an integer number of oscillations, denoted by n. In this case

$$\omega = wan. \tag{18}$$

Expression (17) in dimensionless variables $L(\tau) = wl(t), \tau = wat,\ \xi = wx$ taking into account (18) takes the form:

$$L(\tau) = \beta\sin(n\tau), \tag{19}$$

where $\beta = Bw$.

For subsonic boundary motion, the condition $(|L'(\tau)| < 1)$ must be satisfied $\beta n < 1$. Substituting (19) into the boundary condition (15) for the reflected wave yields:

$$Q(P) = -\sin(P + 2\varphi(P) + \gamma). \tag{20}$$

The function $\varphi(P)$ is defined implicitly and determined by the equation:

$$\beta\sin(n\varphi(P)) - \varphi(P) = P. \tag{21}$$

To determine the energy of the reflected wave, we find from (21) $\varphi'(P)$ and from (20) $Q'(P)$:

$$\varphi'(P) = 1/(\beta n\cos(\varphi(P)) - 1), \tag{22}$$

$$Q'(P) = -(1 + 2\varphi'(P))\cos(P + 2\varphi(P) + \gamma). \tag{23}$$

The energy of the incident wave is defined by expression (16).

Taking into account (22) and (23), the energy of the reflected wave is given by:

$$W_{omp.} = C\int_0^{2\pi} \left(\frac{\beta n\cos\varphi + 1}{\beta n\cos\varphi - 1}\cos(P + 2\varphi(P) + \gamma)\right)^2 dP. \tag{24}$$

Results. We analyze expression (24) using the developed software package [27] to find its maximum with respect to β and γ for different values of n.

As a result of the numerical analysis, it was established that for any values of β the maximum energy of the reflected wave is achieved at $n = 2$ when $\gamma = \pi / 2$. For other values of n the maximum is reached at different values of $\gamma = 0$. It was also found that the function $W_0(\gamma)$ is periodic with period π for any values of n.

The dependence of W_0 on β on γ for $n = 2$, is presented in Table 1.

Table 1

Dependence of W_0 on β and γ for $n = 2$

γ \ β	0.000	0.045	0.090	0.135	0.180	0.225	0.270	0.315	0.360	0.405
0.00	1.000	0.955	0.989	1.096	1.280	1.559	1.973	2.608	3.658	5.661
0.31	1.000	0.969	1.015	1.132	1.325	1.615	2.043	2.695	3.764	5.773
0.63	1.000	1.008	1.082	1.224	1.443	1.762	2.226	2.924	4.047	6.089
0.94	1.000	1.055	1.165	1.338	1.588	1.943	2.453	3.208	4.398	6.488
1.26	1.000	1.093	1.232	1.430	1.706	2.090	2.636	3.438	4.683	6.818
1.57	1.000	1.108	1.258	1.465	1.750	2.146	2.706	3.526	4.794	6.952
1.88	1.000	1.093	1.232	1.430	1.706	2.090	2.637	3.439	4.688	6.840
2.20	1.000	1.055	1.165	1.338	1.588	1.944	2.453	3.210	4.405	6.524
2.51	1.000	1.008	1.082	1.224	1.443	1.762	2.227	2.926	4.054	6.125
2.83	1.000	0.969	1.015	1.132	1.325	1.616	2.044	2.696	3.769	5.795
3.13	1.000	0.955	0.989	1.096	1.280	1.559	1.973	2.608	3.658	5.661

Features of Longitudinal Wave Interaction with a Moving Boundary. Let us consider the propagation of longitudinal waves in a semi-infinite rod, where the left boundary moves between two rollers rotating with a circumferential speed v and simultaneously translating along the x-axis with the same speed.

Until now, in the formulation of similar problems, the fact that deformed sections of the rod pass through the boundary has been neglected, and the boundary condition in the absence of slip was written as:

$$U_t(l(t), t) = 0;\ l(t) = \nu t.$$

In cases where the deformations are significant, this can lead to substantial errors.

Let $U(x,t)$ be the longitudinal displacement of the cross-section of the rod at coordinate x at time t which satisfies the wave equation (1). If deformations are taken into account, the boundary condition remains the same:

$$U_t(l(t),t) = 0, \tag{25}$$

however, the law of boundary motion becomes coupled with $U(x,t)$ by the relation:

$$l'(t) = \nu / (1 + U_x(l(t),t)). \tag{26}$$

This dependence of the boundary's motion law on the oscillatory process makes the problem nonlinear. Problems of this kind are currently poorly studied. A similar problem was first considered in [21].

We study the influence of the deformation magnitude and the boundary's speed on the process of reflection of a harmonic wave:

$$\varphi(x + at) = A \sin \omega(x + at) \tag{27}$$

from a moving boundary.

Let us introduce the following dimensionless variables into the problem (1), (25)–(27):

$$U(x,t) = AV(\xi,\tau),\ l(t) = L(\tau) / \omega,$$
$$\xi = \omega x,\ \tau = a\omega t,\ \varphi(x + at) = Ag(\xi + \tau).$$

As a result, we obtain:

$$V_{\tau\tau}(\xi,\tau) - V_{\xi\xi}(\xi,\tau) = 0,\ V_\tau(L(\tau),\tau) = 0,$$
$$L'(\tau) = \varepsilon / (1 + \alpha V_\xi(L(\tau),\tau)),\ g(\xi + \tau) = \sin(\xi + \tau),\ \varepsilon = \nu / a,\ \alpha = A\omega.$$

We seek the solution in the form:

$$V(\xi,\tau) = \sin(\xi + \tau) + G(\xi - \tau).$$

As a result, to determine the functions G and L we obtain the following system:

$$L'(\tau) = \varepsilon / (1 + 2\alpha \cos(L(\tau) + \tau)),\ G'(L(\tau) - \tau) = \cos(L(\tau) + \tau).$$

From the second equation of the system, it follows that the amplitude of the deformation waves does not change. A comparison of the system's solution (the system was solved numerically using the developed software package [27]) with the solution that does not account for the change in $L(\tau)$ due to deformation, namely:

$$L(\tau) = \varepsilon\tau,\ G'(z) = \cos((\varepsilon + 1)z / (\varepsilon - 1)),\ z = \tau(\varepsilon - 1),$$

shows that there is a constant phase shift over time between the solutions. The wavelength in the first case is shorter. The phase shift per unit time, depending on the parameters ε and α deformation magnitude, is presented in Table 2.

Table 2

Phase shift per unit time depending on ε and deformation magnitude α

ε \ α	0.1	0.2	0.3	0.4
0.1	0.004	0.008	0.034	0.109
0.3	0.019	0.045	0.120	–
0.5	0.032	0.077	–	–
0.7	0.057	–	–	–

At certain moments in time, the boundary may move faster than the speed of sound $(L'(\tau) > 1)$. In such cases, the formulated problem becomes incorrect. The inequality $\varepsilon + 2\alpha < 1$ defines the admissible domain. In the cells of the table where this inequality is not satisfied, a dash (—) is used.

Analysis of the Influence of Boundary Motion in the Study of Resonance Properties of Systems with Damping. To answer the question of when it is necessary to take boundary motion into account, let us consider the process of passing through resonance in a system with damping.

In works [10, 28], the resonance properties of two variable-length systems under the influence of damping forces were studied. The expressions for the oscillation amplitude obtained therein take the form:

$$A_n^2(\tau) = E_n^2(\varepsilon\tau) e^{-2\alpha_0(\varepsilon_1\tau)\tau} \{[\int_0^\tau F_n(\varepsilon\zeta) e^{\alpha_0(\varepsilon_1\zeta)\zeta} \sin \Phi_n(\zeta) d\zeta]^2 + [\int_0^\tau F_n(\varepsilon\zeta) e^{\alpha_0(\varepsilon_1\zeta)\zeta} \cos \Phi_n(\zeta) d\zeta]^2\}, \tag{28}$$

where $\alpha_0(\varepsilon_1\tau), E_n(\varepsilon\tau), F_n(\varepsilon\zeta), \Phi_n(\zeta)$ are certain functions.

Omitting some mathematical derivations, we obtain the expression for (28) in the form:

$$A_{0n}^2(\tau_1,\tau_2) = A^2 \frac{2}{|\nu|} A_n^2(z_1,z_2),$$

where

$$A_n^2(z_1,z_2) = e^{-2\alpha Z_2}[I_s^2(z_1,z_2) + I_c^2(z_1,z_2)], \quad (29)$$

$$I_s(z_1,z_2) = \int_{z_1}^{z_2} e^{\alpha z}\sin(\pm z^2)dz,\ \ I_c(z_1,z_2) = \int_{z_1}^{z_2} e^{\alpha z}\cos(\pm z^2)dz, \quad (30)$$

$$\alpha = \alpha_0\sqrt{2/|\nu|},\ z_i = (\nu\tau_i + \omega_0)/\sqrt{2|\nu|},\ i = \overline{1,2}.$$

Here v is a parameter characterizing the speed of resonance passage; α_0 is a coefficient characterizing damping in the system; A is a constant value; τ_1,τ_2 are the boundaries of the resonance region.

Let us analyze expression (29) for its maximum in the vicinity of the point $z_0 = 0$.

As a result of the numerical solution of (29) using the developed software package [27], Table 3 was obtained.

Table 3

Results of the Numerical Solution of Expression (29) for the Maximum

α	0.00	0.10	0.30	0.50	0.70	1.00	1.30	2.00	3.00	7.00
z_1	–1.56	–1.54	–1.49	–1.49	–1.48	–1.48	–1.47	–1.46	–1.35	–1.29
z_2	1.56	1.45	1.30	1.25	1.20	1.15	1.10	1.00	0.70	0.40
$A_n(\alpha)$	2.37	2.06	1.60	1.29	1.07	0.84	0.68	0.47	0.33	0.144

The maximum oscillation amplitude that arises when the boundaries stop at the resonance point is determined by expression (28) at $v = 0$. Performing the calculations, we obtain:

$$A_{0n}^{\max} = A/\alpha_0. \quad (31)$$

When $v \neq 0$ the amplitude is determined by the expression:

$$A_{0n} = A\sqrt{\frac{2}{|\nu|}} A_n\left(\alpha_0\sqrt{\frac{2}{|\nu|}}\right), \quad (32)$$

where the value of the function A_n is taken from Table 3.

The boundary motion should be taken into account when the relative amplitude error

$$\Delta = \frac{A_{0n}^{\max} - A_{0n}}{A_{0n}} \quad (33)$$

is large.

Using the data from the table, it is easy to establish that the error Δ exceeds the value of 0.05 when

$$\alpha_0\sqrt{\frac{2}{|\nu|}} < 2{,}164. \quad (34)$$

Inequality (34) defines the region in the parameter space α_0, v, where boundary motion must be considered. Substituting into (34) and performing the transformations, we obtain the following inequality, which defines the region where boundary motion must be considered:

$$\Delta_A > 3{,}8\sqrt{\gamma\Delta_\ell},$$

where $\Delta_A = 2\pi\alpha_0/\omega_0$ is the relative change in amplitude over one free oscillation; $\Delta_\ell = 2\pi|\upsilon|/\omega_0\ell_0$ is the relative change in length over one free oscillation.

Discussion and Conclusion. The patterns of wave reflection from moving boundaries in systems whose oscillations are described by the wave equation have been investigated. An expression has been obtained for the change in the energy of the reflected wave relative to the incident wave in the case of uniform and periodic boundary motion. It has been established that the system's energy increases when the boundary moves towards the wave and decreases when it moves in the same direction as the wave.

The propagation of longitudinal waves in a rod with a moving boundary has been analyzed. In this case, accounting for deformations renders the problem nonlinear. It has been shown that the amplitude of deformation waves remains unchanged, despite the influence of boundary velocity and deformation magnitude.

The effect of damping forces on the oscillation amplitude during passage through resonance has been studied. Criteria in the form of inequalities have been obtained, defining regions where the boundary motion must be taken into account.

The applied value of the results lies in their potential use for solving a wide range of engineering problems [29–33], including: analysis of longitudinal and bending vibrations of shafts, beams, and rods with movable supports; reliability assessment of ropes in lifting systems and dynamic stability of strings, fibers, and tape transmissions; study of vibrations in tapes used in transport mechanisms, band saws, and flexible transmission elements; analysis of wire oscillations during the fabrication of rotational shells by winding; process control in cable production, rolling; reliability assessment of railway overhead contact systems, etc.

These types of problems are understudied and require further research. The presented results make it possible, already at the design stage, to prevent the occurrence of high-amplitude oscillations in mechanical systems with moving boundaries [34–37].

References

1. Kolosov L.V., Zhygula T.I. Longitudinal and transverse vibrations of the rope string of the lifting installation. *Minerals and Mining Engineering*. 1981;3:83–86. (In Russ.)

2. Zhu W.D., Chen Y. Theoretical and experimental investigation of elevator cable dynamics and control. *J. Vibr. Acoust.* 2006;1:66–78.

3. Shi Y., Wu L., Wang Y. Nonlinear analysis of natural frequencies of a cable system. *J. Vibr. Eng.* 2006;2:173–178.

4. Goroshko O.A., Savin G.N. *Introduction to the mechanics of deformable one-dimensional bodies of variable length*. Kiev, Nauk. dumka; 1971. 290 p. (In Russ.)

5. Anisimov V.N., Litvinov V.L. Transverse vibrations of a rope moving longitudinally. *Izvestia of Samara Scientific Center of the Russian Academy of Sciences*. 2017;19(4):161–165. (In Russ.)

6. Savin G.N., Goroshko O.A. *The dynamics of the thread of variable length*. Kiev, Nauk. dumka; 1962. 332 p. (In Russ.)

7. Liu Z., Chen G. Analysis of plane nonlinear free vibrations of a load-bearing rope taking into account the influence of bending stiffness. *J. Vibr. Eng*. 2007;1:57–60.

8. Palm J., Paredes G.M., Eskilsson C., Pinto F. Simulation of mooring cable dynamics using a discontinuous Galerkin method. In *International Conference on Computational Methods in Marine Engineering*, 2013.

9. Litvinov V.L. Investigation of free oscillations of mechanical objects with moving boundaries using the asymptotic method. *Middle Volga Mathematical Society Journal*. 2014;16(1):83–88. (In Russ.)

10. Anisimov V.N., Litvinov V.L. *Mathematical modeling and investigation of vibrations of one-dimensional mechanical systems with moving boundaries*. Samara, Samar. gos. tekhn. univ., 2017; 149 p. (In Russ.)

11. Uvarova L.A., Fedyanin V.K. Mathematical model of heat transfer in substantially nonlinear coupled media. *Matem. modelirovanie*. 1990;2(6):40–54. (In Russ.)

12. Kudinov V.A., Kudinov I.V. *Methods for solving parabolic and hyperbolic heat conduction equations.* Moscow, Knizhniy dom "Librokom", 2012; 280 p. (In Russ.)

13. Sikhinov A.I., Chistyakov A.E., Nikitina A.V., Atayan A.M., Litvinov V.N. A Method for Solving Grid Equations for Hydrodynamic Problems in Flat Areas. *Mathematical Models and Computer Simulations*. 2023;15(5):35–58. https://doi.org/10.20948/mm-2023-03-03

14. Sukhinov A., Sidoryakina V. Two-dimensional-one-dimensional alternating direction schemes for coastal systems convection-diffusion problems. *Mathematics*. 2021;9(24):3267. https://doi.org/10.3390/math9243267

15. Atayan A.M., Nikitina A.V., Sukhinov A.I., Chistyakov A.E. Mathematical Modeling of Hazardous Natural Phenomena in a Shallow Basin. *Computational Mathematics and Mathematical Physics*. 2022;61(2):269–286. https://doi.org/10.1134/S0965542521120034

16. Vesnitskii A.I. *Waves in systems with moving boundaries and loads*. Moscow, Fizmatlit, 2001; 320 p. (In Russ.)

17. Anisimov V.N., Litvinov V.L., Korpen I.V. A method for obtaining an analytical solution to the wave equation describing the oscillations of systems with moving boundaries. *Journal of Samara State Technical University, Ser. Physical and Mathematical Sciences*. 2012;3(28):145–151. (In Russ.)

18. Vesnitskii A.I. The inverse problem is for a one-dimensional resonator that changes its size over time. *Izvestiya vuzov. Radiophysics*. 1971;10:1538–1542. (In Russ.)

19. Barsukov K.A., Grigorian G.A. Towards the theory of a waveguide with movable boundaries. *Izvestiya vuzov. Radiophysics*. 1976;2:280–285. (In Russ.)

20. Wang L., Zhao Y. Multiple internal resonances and non-planar dynamics of shallow suspended cables to the harmonic excitations. *Journal of Sound and Vibration*. 2009;1–2:1–14.

21. Samarin Yu.P. On a nonlinear problem for the wave equation in one-dimensional space. *Journal of Applied Mathematics and Mechanics*. 1964;26(3):77–80. (In Russ.)

22. Anisimov V.N., Korpen I.V., Litvinov V.L. Application of the Kantorovich-Galerkin Method for Solving Boundary Value Problems with Conditions on Moving Borders. *Mechanics of Solids*. 2018;53(2):177–183.

23. Litvinov V.L., Litvinova K.V. An Approximate Method for Solving Boundary Value Problems with Moving Boundaries by Reduction to Integro-Differential Equations. *Computational Mathematics and Mathematical Physics*. 2022;62(6):945–954.

24. Litvinov V.L., Anisimov V.N. Investigation of patterns of reflection of waves from moving boundaries. *Proceedings of the Sixth All-Russian Scientific Conference (June 1–4, 2009). Math. modeling and boundary value problems*. Samara, SamGTU, 2009;39–43. (In Russ.)

25. Litvinov V.L. Investigation of the interaction of longitudinal waves with a moving boundary. *Scientific and technical creativity: problems and prospects. Collection of articles of the III All-Russian conference-seminar*. Samara, 2008; 31–36. (In Russ.)

26. Litvinov V.L. Accounting for the Influence of Damping Forces on the Resonant Properties of a String with a Moving Boundary. In: *Proceedings of the 5th Anniversary All-Russian Conference-Seminar "Scientific and Technical Creativity: Problems and Prospects"*. Samara: SamSTU Publishing; 2010, pp. 79–80.

27. Litvinov V.L. Certificate of state registration of a computer program. *Automated software package for the study of vibrations and resonant phenomena in mechanical systems with moving boundaries* "*TB-Analysis-7*" No. 2025613649, published on Feb. 13, 2025 (In Russ.)

28. Litvinov V.L. Variational formulation of the problem on vibrations of a beam with a moving spring-loaded support. *Theoretical and Mathematical Physics*. 2023;215(2):709–715. https://doi.org/10.1134/S0040577923050094

29. Litvinov V.L., Litvinova K.V. An Inverse Method for Solving Problems about Oscillations of Mechanical Systems with Moving Boundaries. *Moscow University Mechanics Bulletin*. 2024;3:53–59. https://doi.org/10.3103/S0027133024700122

30. Sandilo S.H., Horssen W.T. van. On variable length induced vibrations of a vertical string. *Journal of Sound and Vibration*. 2014;333:2432–2449.

31. Zhang W., Tang Y. Global dynamics of the cable under combined parametrical and external excitations. *International Journal of Non-Linear Mechanics*. 2002;37:505–526.

32. Faravelli L., Fuggini C., Ubertini F. Toward a hybrid control solution for cable dynamics: Theoretical prediction and experimental validation. *Struct. Control Health Monit*. 2010;17:386–403.

33. Lezhneva A.A. Free bending vibrations of a beam of variable length. *Scientific notes*. Perm, Perm. Univ., 1966; 156:143–150. (In Russ.)

34. Selivanova N.Yu., Shamolin M.V. Local solvability of a one-phase problem with free boundary. *Journal of Mathematical Sciences*. 2013;189(2):274–283.

35. Selivanova N.Yu., Shamolin M.V. Studying the interphase zone in a certain singular-limit problem. *Journal of Mathematical Sciences*. 2013;189(2):284–293.

36. Selivanova N.Yu., Shamolin M.V. Local solvability of the Capillary problem. *Journal of Mathematical Sciences*. 2013;189(2):294–300.

37. Selivanova N.Yu., Shamolin M.V. Quasi-stationary Stefan problem with values on the front depending on its geometry. *Journal of Mathematical Sciences*. 2013;189(2):301–310.

About the Authors:

Aleksey L. Semenov, Academician of the Russian Academy of Sciences, Academician of the Russian Academy of Education, Doctor of Physical and Mathematical Sciences, Professor, Head of the Department of Mathematical Logic and Theory of Algorithms, Faculty of Mechanics and Mathematics, Lomonosov Moscow State University (119991, Russian Federation, GSP-1, Moscow, Leninskie Gory), ORCID, SPIN-code, alsemno@ya.ru

Vladislav L. Litvinov, Candidate of Technical Sciences, Head of the Department of General Theoretical Disciplines (Higher Mathematics), Samara State Technical University (443100, Russian Federation, Samara, Molodogvardeyskaya St., 244), ORCID, SPIN-code, vladlitvinov@rambler.ru

Maksim V. Shamolin, Corresponding Member of RAS, Doctor of Physical and Mathematical Sciences, Professor, Leading Researcher at the Laboratory of General Mechanics, Research Institute of Mechanics, Lomonosov Moscow State University (119991, Russian Federation, GSP-1, Moscow, Leninskie Gory), ORCID, SPIN-code, shamolin@rambler.ru

Contributions of the authors:

A.L. Semenov: General scientific supervision; methodology development; visualization; validation.

V.L. Litvinov: Problem statement; formulation of research ideas, aims and objectives; software development.

M.V. Shamolin: Methodology development; translation; study of the problem's history; literature review; visualization; validation.

Conflict of Interest Statement: **the authors declare no conflict of interest.**

All authors have read and approved the final manuscript.

Об авторах:

Алексей Львович Семенов, академик РАН, академик РАО, доктор физико-математических наук, профессор, заведующий кафедрой математической логики и теории алгоритмов механико-математического факультета Московского государственного университета им. М.В. Ломоносова (119991, Российская Федерация, ГСП-1, г. Москва, Ленинские горы), ORCID, SPIN-код, alsemno@ya.ru

Владислав Львович Литвинов, кандидат технических наук, заведующий кафедрой общетеоретических дисциплин (высшей математики) Самарского государственного технического университета (443100, Российская Федерация, г. Самара, ул. Молодогвардейская, 244), ORCID, SPIN-код, vladlitvinov@rambler.ru

Максим Владимирович Шамолин, член-корреспондент РАН, доктор физико-математических наук, профессор, ведущий научный сотрудник лаборатории общей механики НИИ механики Московского государственного университета им. М.В. Ломоносова (119991, Российская Федерация, ГСП-1, г. Москва, Ленинские горы), ORCID, SPIN-код, shamolin@rambler.ru

Заявленный вклад авторов:

А.Л. Семенов: общее научное руководство; разработка методологии; визуализация; валидация.

В.Л. Литвинов: постановка задачи; формулировка идей исследования, целей и задач; разработка программного обеспечения.

М.В. Шамолин: разработка методологии; перевод; изучение истории задачи; поиск литературы; визуализация; валидация.

Конфликт интересов: ***авторы заявляют об отсутствии конфликта интересов.***

Все авторы прочитали и одобрили окончательный вариант рукописи.

Received / Поступила в редакцию 30.03.2025
Revised / Поступила после рецензирования 25.04.2025
Accepted / Принята к публикации 20.05.2025

MATHEMATICAL MODELLING
МАТЕМАТИЧЕСКОЕ МОДЕЛИРОВАНИЕ

UDC 004.032.26

Original Empirical Research

https://doi.org/10.23947/2587-8999-2025-9-2-44-51

Application of Neural Networks for Solving Elliptic Equations in Domains with Complex Geometries

Alexander V. Galaburdin
Don State Technical University, Rostov-on-Don, Russian Federation
✉ Galaburdin@mail.ru

Abstract

Introduction. Differential equations are often used in modelling across various fields of science and engineering. Recently, neural networks have been increasingly applied to solve differential equations. This paper proposes an original method for constructing a neural network to solve elliptic differential equations. The method is used for solving boundary value problems in domains with complex geometric shapes.

Materials and Methods. A method is proposed for constructing a neural network designed to solve partial differential equations of the elliptic type. By applying a transformation of the unknown function, the original problem is reduced to Laplace's equation. Thus, nonlinear differential equations were considered. In building the neural network, the activation functions are chosen as derivatives of singular solutions to Laplace's equation. The singular points of these solutions are distributed along closed curves encompassing the boundary of the domain. During the training process, the weights of the network are adjusted by minimizing the mean squared error.

Results. The paper presents the results of solving the first boundary value problem for various domains with complex geometries. The results are shown in tables containing both the exact solutions and the solutions obtained using the neural network. Graphical representations of the exact and the neural network-based solutions are also provided.

Discussion and Conclusion. The obtained results demonstrate the effectiveness of the proposed neural network construction method in solving various types of elliptic partial differential equations. The method can also be effectively applied to other types of partial differential equations.

Keywords: elliptic partial differential equations, domain with complex geometry, neural networks

For Citation. Galaburdin A.V. Application of Neural Networks for Solving Elliptic Equations in Domains with Complex Geometries. *Computational Mathematics and Information Technologies*. 2025;9(2):44–51. https://doi.org/10.23947/2587-8999-2025-9-2-44-51

Оригинальное эмпирическое исследование

Применение нейронных сетей при решении эллиптических уравнений для областей сложной формы

А.В. Галабурдин
Донской государственный технический университет, г. Ростов-на-Дону, Российская Федерация
✉ Galaburdin@mail.ru

Аннотация

Введение. При построении моделей в различных областях науки и техники часто используют дифференциальные уравнения. В настоящее время при решении дифференциальных уравнений все чаще применяются нейронные сети. В данной работе предложен оригинальный метод построения нейронной сети для решения эллиптических дифференциальных уравнений. Этот метод применяется при решении краевых задач для областей сложной геометрической формы.

Материалы и методы. Предлагается метод построения нейронной сети, предназначенной для решения дифференциальных уравнений в частных производных эллиптического типа. Используя замену неизвестной функции, исходная задача сводится к уравнению Лапласа. Таким образом, рассматривались нелинейные дифференциальные уравнения. При построении нейронной сети в качестве активационных функций принимаются производные от сингулярных решений уравнения Лапласа. Сингулярные точки этих решений распределены по замкнутым кривым, охватывающим границу области. При настройке весов сети минимизировалась среднеквадратическая ошибка обучения.

Результаты исследования. Представлены результаты решения первой краевой задачи для различных областей сложной геометрической формы. Результаты представлены в виде таблиц, содержащих точные решения задачи и решения, полученные с помощью нейронной сети. Дано графическое представление точного решения и решение, полученное предложенным методом.

Обсуждение и заключение. Полученные результаты доказали эффективность предложенного метода построения нейронной сети при решении различных видов дифференциальных уравнений в частных производных эллиптического типа. Данный метод может эффективно применяться при решении других типов дифференциальных уравнений с частными производными.

Ключевые слова: дифференциальные уравнения в частных производных эллиптического типа, область сложной геометрической формы, нейронные сети

Для цитирования. Галабурдин А.В. Применение нейронных сетей при решении эллиптических уравнений для областей сложной формы. *Computational Mathematics and Information Technologies*. 2025;9(2):44–51. https://doi.org/10.23947/2587-8999-2025-9-2-44-51

Introduction. Differential equations play a crucial role in modelling processes across various fields of science and engineering. Traditional analytical and numerical methods for solving differential equations do not always yield satisfactory results. As a result, different machine learning methods are increasingly being applied to solve differential equations. In particular, artificial neural networks are often used for this purpose.

The theoretical foundations of the neural network method can be traced back to the work of A.N. Kolmogorov [1]. Today, neural networks are widely em-ployed for solving different types of differential equations. In [2], the transition from neural network architecture to ordinary differential equations and the Cau-chy problem is discussed.

Papers [3, 4] focus on the application of neural networks to solve Laplace's equation. In [5], deep learning methods are applied to solve the Poisson equation in a two-dimensional domain. Radial basis function (RBF) neural networks have become particularly widespread in solving partial differential equations [6].

In studies [7, 8], radial basis functions with tunable parameters are used as activation functions. Works [9–11] demonstrate the successful use of neural networks for solving boundary value problems related to the Navier–Stokes equations. Physics-informed neural networks (PINNs) have shown high effectiveness in solving partial differential equations, particularly in classical mechanics problems [12, 13]. In [14], a perceptron-type neural network is applied to a heat and mass transfer problem.

These studies highlight the growing popularity of neural networks for solving differential equations. The present research is devoted to the analysis of boundary value problems for partial differential equations in domains with complex geometries and builds on the approach developed in [15, 16].

Materials and Methods. Let us consider a boundary value problem for a differential equation:

$$U + b_1 \partial_1 U + b_2 \partial_2 U + cU = 0.$$

By representing the solution in the form $U = Ve^{(\lambda x + \alpha y)}$ and appropriately selecting the parameters λ and α, the problem can be reduced to a simpler equation:

$$V + aV = 0.$$

i. e., the Laplace equation.

The resulting equation was solved using a neural network with respect to the function V. The constructed neural networks for solving the Laplace equation can also be used to solve nonlinear elliptic equations, provided they are properly transformed.

As an example, consider the differential equation:

$$U - 2((\partial_1 U)^2 + (\partial_2 U)^2)/(3V) = 0.$$

The original differential equation is reduced to the Laplace equation by introducing a new unknown function $V = U^{1/3}$.

The neural network construction was based on the method described in [15, 16]. This method relies on a formula similar to Green's formula, in which integrals are replaced by sums:

$$V(x) = \sum_{k=1}^{N} w_k f(s_k) U(x, \sigma_k) + \sum_{k=1}^{N} v_k f(s_k) G(x, \tau_k),$$

where $f(s_k)$ is the value of the unknown function u on the boundary of the domain; $U(x, \sigma_k)$ and $G(x, \tau_k)$ are activation functions; σ_k and τ_k are points on closed curves γ_1 and γ_2, which surround the boundary γ of the domain; x is a point inside the domain G.

By requiring that this relation holds at every point on the boundary for all functions in the training set, and applying the least squares method, a system of equations is obtained for determining the weights w_k and v_k.

To improve the conditioning of the matrix in the resulting system of equations, the activation functions were chosen as derivatives of the fundamental solution of the Laplace equation

$$U(x, y, t, s) = \frac{\beta^5 - 10\beta^3\delta^2 + 5\beta\delta^4 + \delta^5 - 10\delta^3\beta^2 + 5\delta\beta^4}{R^{10}},$$

$$G(x, y, t, s) = \frac{\beta^7 - 21\beta^5\delta^2 + 35\beta^3\delta^4 - 7\beta\delta^6}{R^{14}} n_x,$$

$$+\frac{\delta^7 - 21\beta^2\delta^5 + 35\delta^3\beta^4 - 7\beta^6\delta}{R^{14}} n_y,$$

$$\delta = x - t, \beta = y - s, R = \sqrt{\delta^2 + \beta^2}.$$

This increased the singularity of the activation functions. The points σ_k and τ_k were taken on the contours γ_1 and γ_2, which were obtained by shifting each point of the boundary contour γ outward along the external normal to the domain boundary by distances ρ_1 and ρ_2 respectively. During the training process, the weights as well as the values of ρ_1 and ρ_2 were determined. The values ρ_1 and ρ2 were found using a simple brute-force search.

As a training set, a set of functions that are solutions to the Laplace equation in polar coordinates was used:

$$r^k cos(karccos(\frac{x}{r})) + r^k sin(karccos(\frac{x}{r})),\ r = \sqrt{(x^2 + y^2)},$$

where $k = 0, 1, 2, 3, \ldots, M$.

These functions were specified in different coordinate systems, each rotated relative to one another by an angle that is a multiple of $2\pi/5$.

Results. The proposed method was applied to solving problems in domains whose boundary γ is defined by the equation:

$$\begin{cases} x = a\cos(t) + g\cos(\omega t), \\ y = a_1 \sin(t) + g_1 \sin(\omega t), \end{cases} \quad t \in [0, 2\pi],$$

where $t \in [0,2\pi]$; a, a_1, g, g_1, ω are adjustable parameters.

In all cases, the number of functions in the training set was taken as $M = 75$, and the number of neurons in the network was $N = 100$.

Problem 1. As an example, consider the following differential equation:

$$\Delta U - \partial_1 U + 5\partial_2 U + 6.5U = 0.$$

A new unknown function V is introduced, which satisfies the Laplace equation:

$$U = Ve^{(0.5x - 2.5y)}.$$

The first boundary value problem was considered.

Fig. 1 shows the domain whose boundary corresponds to the following parameter values: $a = 1.15$, $g = 1.15$, $a_1 = 0.07$, $g_1 = -0.03$, $\omega = 9$.

The points in the domain where both the exact solution and the neural network solution are evaluated are marked with asterisks in the diagram.

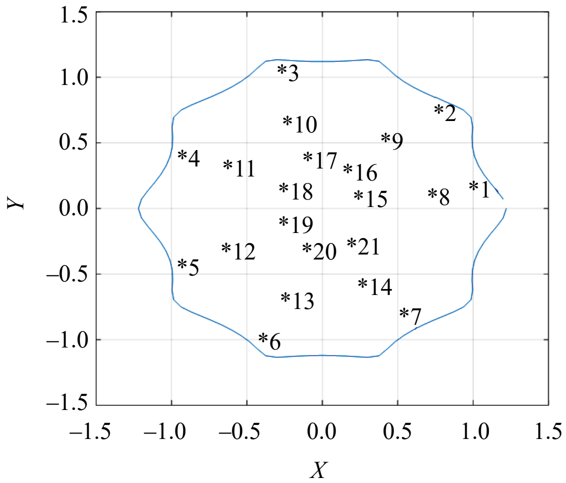

Fig. 1. Shape of the domain for Problem 1

The points in the domain where the exact solution and the neural network solution are computed are marked with asterisks on the diagram. Table 1 presents the computational results corresponding to the solution of the equation:

$$U = xye^{(0.5x-2.5y)}.$$

Table 1

Computation Results for Problem 1

Point Number	1	2	3	4	5	6	7
Exact Solution	0.1158	0.2214	0.1055	0.0241	–0.0142	–0.0473	–0.0835
Neural Network Solution	0.1148	0.2216	0.1054	0.0240	–0.0142	–0.0473	–0.0838
Point Number	8	9	10	11	12	13	14
Exact Solution	0.0385	0.1092	0.0769	0.0244	–0.0157	0.0457	–0.0629
Neural Network Solution	0.0382	0.1090	0.0768	0.0243	–0.0158	0.0458	–0.0630
Point Number	15	16	17	18	19	20	21
Exact Solution	0.0051	0.0213	0.0222	0.0098	–0.0069	–0.0175	–0.0188
Neural Network Solution	0.0047	0.0210	0.0220	0.0096	–0.0071	–0.0177	–0.0190

Problem 2. The following differential equation was considered:

$$\Delta U + 5\partial_1 U + 3\partial_2 U + 8.5U = 0.$$

The introduction of a new unknown function V:

$$U = Ve^{-(2.5x+1.5y)}$$

allows the original differential equation to be reduced to the Laplace equation with respect to the function V. The shape of the domain in this case was determined by the parameters в $a = 1.1$, $g = 1.1$, $a1 = 0.05$, $g1 = 0.1$, $\omega = 4$ (Fig. 2). The first boundary value problem was considered. Table 2 presents the computational results and the exact solution of the differential equation:

$$U = e^{-x} chye^{-(2.5x+1.5y)}.$$

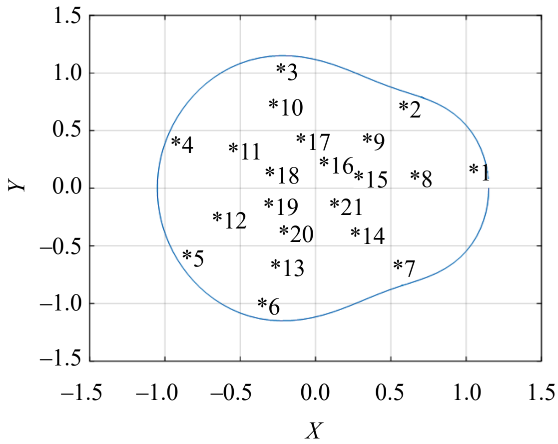

Fig. 2. Shape of the domain for Problem 2

Table 2

Computation Results for Problem 2

Point Number	1	2	3	4	5	6	7
Exact Solution	0.0198	0.0143	0.0245	0.0622	0.1929	1.4682	9.0855
Neural Network Solution	0.0198	0.0143	0.0245	0.0622	0.1928	1.4640	9.0885
Point Number	8	9	10	11	12	13	14
Exact Solution	0.0818	0.0700	0.1163	0.2289	0.4502	1.4325	3.9076
Neural Network Solution	0.0817	0.0700	0.1162	0.2288	0.4499	1.4320	3.9104
Point Number	15	16	17	18	19	20	21
Exact Solution	0.3377	0.3321	0.4896	0.6716	0.7856	1.1957	1.6099
Neural Network Solution	0.3377	0.3320	0.4896	0.6716	0.7857	1.1959	1.6104

Problem 3. The following differential equation was considered:

$$\Delta U - \frac{2((\partial_1 U)^2 + (\partial_1 U)^2)}{3V} = 0,$$

By introducing a new unknown function the original equation is reduced to the Laplace equation. The first boundary value problem was considered. The shape of the domain was defined by the parameters $a = 1.1$, $g = 1.1$, $a_1 = 0.07$, $g_1 = 0.07$, $\omega = 9$ (Fig. 3).

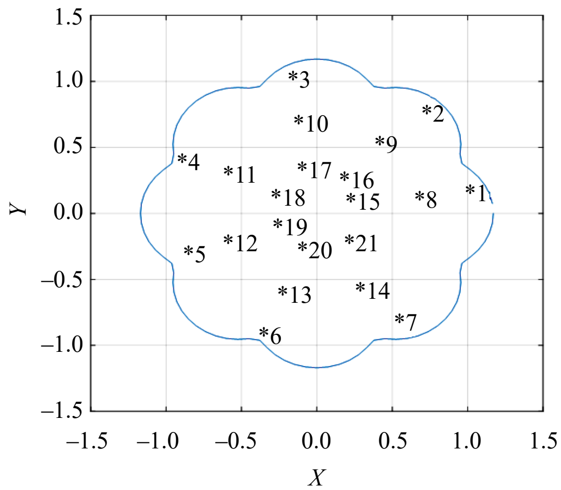

Fig. 3. Shape of the domain for Problem 3

Table 3 presents the computational results and the exact solution of the differential equation:

$$U = (xy + 2.5x + y)^3.$$

Table 3

Computation Results for Problem 3

Point Number	1	2	3	4	5	6	7
Exact Solution	24.613	28.736	32.687	7.2807	0.0363	–2.0562	10.894
Neural Network Solution	24.613	28.878	32.610	7.3419	0.0380	–2.0870	10.834
Point Number	8	9	10	11	12	13	14
Exact Solution	5.7339	5.9627	6.3055	1.4899	0.0169	0.2857	–2.0582
Neural Network Solution	5.7405	5.9727	6.3164	1.4937	0.0169	0.2865	–2.0625
Point Number	15	16	17	18	19	20	21
Exact Solution	0.3331	0.3060	0.2982	0.0754	0.0017	–0.0088	–0.0950
Neural Network Solution	0.3328	0.3058	0.2982	0.0753	0.0017	–0.0089	–0.0957

Fig. 4 and 5 show graphical solutions obtained using the neural network, as well as the exact solution of Problem 3.

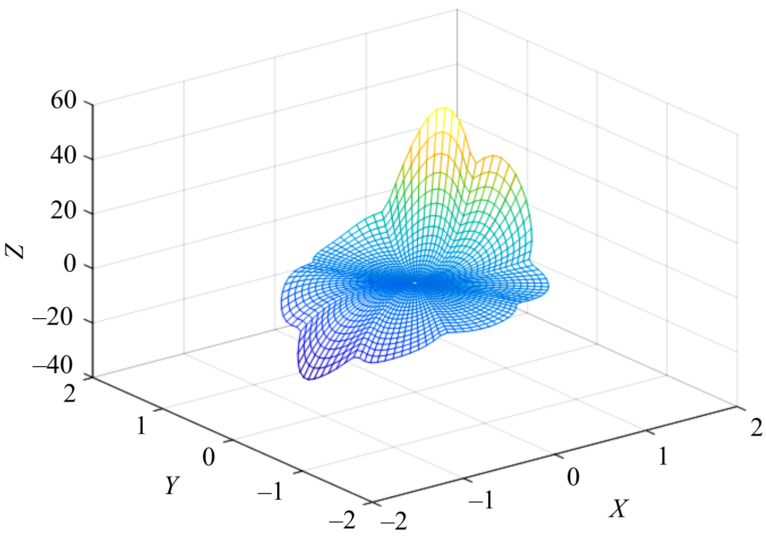

Fig. 4. Solution of Problem 3 obtained by the neural network

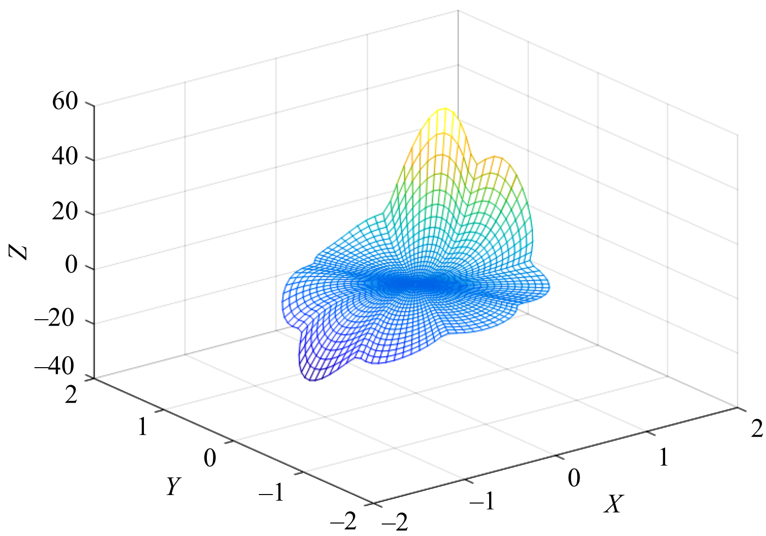

Fig. 5. Exact solution of Problem 3

Discussion and Conclusion. The presented results once again demonstrated the effectiveness of the neural network construction method for solving boundary value problems in domains of complex shape for various types of elliptic partial differential equations. This method can efficiently handle all types of partial differential equations. Future development of the method will focus on expanding the classes of solvable problems and improving training techniques.

References

1. Kolmogorov A.N. On the representation of continuous functions of several variables in the form of superpositions of continuous functions of one variable and addition. *Reports of the USSR Academy of Sciences*. 1957;114(5):953–956. (In Russ.)

2. Margasov O.A. On neural ordinary differential equations and their probabilistic extension. *Izvestiya of the Komi Science Center of the Ural Branch of the Russian Academy of Sciences. Series "Physical and Mathematical Sciences"*. 2021;6(52):14–19. https://doi.org/10.19110/1994-5655-2021-6-14-19 (In Russ.)

3. Varshavchik E.A., Galyautdinova A.R., Sedova Yu.S., Tarkhov D.A. Solution of partial differential equations for domains with constant boundaries. *Artificial intelligence in solving current social and economic problems of the 21st century: collection of articles. Art. based on materials from the Third All-Russian. scientific-practical conf.* Perm, May 14–18, 2018. Perm. state national research univ.; 2018. 294 p. (In Russ.)

4. Tyurin K.A., Bragunets V.V., Svetlov D.D. Solution of the Laplace differential equation using a modified neural network. *Young Scientist*. 2019;27(265):10–12. (In Russ.)

5. Epifanov A.A. Application of deep learning methods for solving partial differential equations. *Advances in cybernetics*. 2020;1(4):22–28. https://doi.org/10.51790/2712-9942-2020-1-4-3 (In Russ.)

6. Kovalenko A.N., Chernomorets A.A., Petina M.A. On the use of neural networks for solving partial differential equations. *Scientific bulletin. The Economics series. Computer science*. 2017;9(258):103–110. (In Russ.)

7. Kansa E.J. *Motivation for using radial basis functions to solve PDEs.* URL: http://uahtitan.uah.edu/kansaweb.html (accessed: 13.04.2025)

8. Kansa E.J. Multiquadrics. A scattered data approximation scheme with applications to computational fluid-dynamics. II. Solutions to parabolic, hyperbolic and elliptic partial differential equations. *Comput. Math. Appl*. 1990;19(89):147–161.

9. Almajid M. Abu-Alsaud M. Prediction of porous media fluid flow using physics informed neural networks. *Journal of Petroleum Science and Engineering*. 2021;208:109205. https://doi.org/10.1016/j.petrol.2021.109205

10. Eivazi H.,Tahani M., Schlatter P., Vinuesa R. Physics-informed neural networks for solving Reynolds-averaged Navier-Stokes equations. *Physics of Fluids*. 2022;34(7):075117. https://doi.org/10.1063/5.0095270

11. Chen J., Viquerat J., Hachem E. *U-net Architectures for Fast Prediction of Incompressible Laminar Flows*. URL: https://arxiv.org/pdf/1910.13532.pdf (accessed: 13.04.2025)

12. Raissia M., Perdikaris P., Karniadakis G.E. Physics-informed neural networks: A deep learning framework for solving forward and inverse problems involving nonlinear partial differential equations. *Journal of Computational Physics*. 2019;378:686–707.

13. Zrelova D.P., Ulyanov S.V. Models of physically informed aware classical Lagrangian Hamiltonian neural networks in deep learning. *Modern information technologies and IT education*. 2022;18(2):310–325. https://doi.org/10.25559/SITITO.18.202202.310-325 (In Russ.)

14. Cai S., Wang Z., Wang S., Perdikaris P., Karniadakis G.E. Physics-informed neural networks for heat transfer problems. *Journal of Heat Transfer*. 2021;143(6):60–80. https://doi.org/10.1115/1.4050542

15. Galaburdin A.V. Application of neural networks to solve the Dirichlet problem for areas of complex shape. *Computational Mathematics and Information Technologies*. 2024;8(2):68–79. https://doi.org/10.23947/2587-8999-2024-8-2-68-79 (In Russ.)

16. Galaburdin A.V. Application of neural networks to solve nonlinear boundary value problems for areas of complex shape. *Computational Mathematics and Information Technologies*. 2024;8(4):35–42. https://doi.org/10.23947/2587-8999-2024-8-4-35-42 (In Russ.)

About the Author:

Alexander V. Galaburdin, Cand. Sci. (Phys. – math.), Associate Professor at the Department Mathematics and informatics, Don State Technical University (1, Gagarin Sq., Rostovon-Don, 344003, Russian Federation), ORCID, SPIN-code, Galaburdin@mail.ru

***Conflict of Interest Statement:* the author declares no conflict of interest.**

The author has read and approved the final version of manuscript.

Об авторе:

Александр Васильевич Галабурдин, кандидат физико-математических наук, доцент кафедры математики и информатики Донского государственного технического университета (344003, Российская Федерация, г. Ростов-на-Дону, пл. Гагарина, 1), ORCID, SPIN-код, Galaburdin@mail.ru

Конфликт интересов: **автор заявляет об отсутствии конфликта интересов.**

Автор прочитал и одобрил окончательный вариант рукописи.

Received / Поступила в редакцию 19.05.2025
Reviewed / Поступила после рецензирования 11.06.2025
Accepted / Принята к публикации 25.06.2025

INFORMATION TECHNOLOGY
ИНФОРМАЦИОННЫЕ ТЕХНОЛОГИИ

Check for updates

Original Empirical Research

UDC 004

https://doi.org/10.23947/2587-8999-2025-9-2-52-64

Automated Processing of Primary Field Data on the Behavior of Natural-Technological Systems under Climate Change and Anthropogenic Impacts in the Far North

Sergey V. Kushukov[1], **Konstantin N. Ivanov**[1], **Sergey P. Levashkin**[1] ✉, **Mikhail V. Yakobovskiy**[2]

[1] Povolzhskiy State University of Telecommunications and Informatics, Samara, Russian Federation

[2] Keldysh Institute of Applied Mathematics of the Russian Academy of Sciences (IPM RAS), Moscow, Russian Federation

✉ ai_lab@psuti.ru

Abstract

Introduction. This work addresses the scientific problem of studying natural-technological systems (NTS) of the Far North under conditions of climate change and anthropogenic impacts. The relevance of ensuring their stability is emphasized, which requires a comprehensive analysis of field data. Problems in automated processing methods of such specific data have been identified. The aim of the study is to develop automated methods for processing field data to reveal patterns. Python libraries for data analysis, processing, and visualization are used as tools.

Materials and Methods. The research object is described — the Main Building of the Yakutsk Thermal Power Plant (TPP) in permafrost conditions. The study materials include field data obtained from engineering-geological boreholes at the Yakutsk TPP, monitoring stations Chabyda and Tuymaada, as well as a section of the Amur-Yakutsk railway (AYR). The data include measurements of soil temperature and moisture, seasonal thaw layer dynamics, snow cover characteristics, and others. A detailed sequence of automated processing of primary data from XLS files using the pandas library is presented, including reading, cleaning, format conversion, filling or replacing missing values, removing duplicates, and saving processed data in CSV, JSON, and XLSX formats.

Results. Specific results of automated processing and systematization of primary field data are presented. Heterogeneous measurements were successfully unified into a single format, ensuring their proper use. A unique data array was formed based on empirical observations under the specific conditions of the Far North. The practical application of Python libraries for executing key stages of preprocessing and data preparation is demonstrated.

Discussion and Conclusion. It is shown that the application of a systematic approach and automated data processing significantly improves the quality and reliability of natural-technological system data analysis. Handling missing data and normalization enhance accuracy, and the final data formats are convenient for further modeling. The universality of Python is highlighted. Prospects for further research include applying machine learning, clustering, and modeling methods aimed at uncovering patterns and forecasting the behavior of natural-technological systems in the Far North under climate and anthropogenic influences.

Keywords: data analysis, Python libraries, data preparation, data preprocessing, information technologies.

Funding. This work was supported financially by the Russian Science Foundation (grant No. 23–61–10032).

For Citation. Kushukov S.V., Ivanov K.N., Levashkin S.P., Yakobovsky M.V. Automated Processing of Primary Field Data on the Behavior of Natural-Technological Systems under Climate Change and Anthropogenic Impacts in the Far North. *Computational Mathematics and Information Technologies*. 2025;9(2):52–64. https://doi.org/10.23947/2587-8999-2025-9-2-52-64

Оригинальное эмпирическое исследование

Автоматическая обработка первичных данных натурных исследований поведения природно-технических систем при изменении климата и антропогенных воздействиях в условиях Крайнего Севера

С.В. Кушуков[1], К.Н. Иванов[1], С.П. Левашкин[1]✉, М.В. Якобовский[2]

[1] Поволжский государственный университет телекоммуникаций и информатики, г. Самара, Российская Федерация

[2] Институт прикладной математики имени М.В. Келдыша РАН, г. Москва, Российская Федерация

✉ ai_lab@psuti.ru

Аннотация

Введение. Рассматривается научная проблема изучения природно-технических систем (ПТС) Крайнего Севера в условиях изменения климата и антропогенных воздействий. Отмечается актуальность задачи обеспечения их устойчивости, что требует комплексного анализа натурных данных. Выявлены проблемы в методах автоматизированной обработки таких специфических данных. Целью работы является разработка автоматизированных методов обработки натурных данных для выявления закономерностей. В качестве инструментов используются библиотеки Python для анализа, обработки и визуализации данных.

Материалы и методы. Описан объект исследования — Главный корпус Якутской ТЭЦ в условиях вечной мерзлоты. В качестве материалов исследования использованы натурные данные, полученные из инженерно-геологических скважин Якутской ТЭЦ, стационаров Чабыда и Туймаада, а также железнодорожного участка Амуро-Якутской магистрали (АЯМ). Данные включают измерения температуры и влажности грунтов, динамики сезонноталого слоя, характеристик снежного покрова и др. Представлена детальная последовательность автоматизированной обработки первичных данных из XLS-файлов с использованием библиотеки pandas, включая чтение, очистку, преобразование форматов, заполнение или замену значений, удаление дубликатов, а также сохранение обработанных данных в форматах CSV, JSON и XLSX.

Результаты исследования. Представлены конкретные результаты автоматизированной обработки и систематизации первичных натурных данных. Успешно выполнено приведение разнородных измерений к единому формату, обеспечивающему их корректное использование. Сформирован уникальный массив данных на основе эмпирических наблюдений в специфических условиях Крайнего Севера. Продемонстрировано практическое применение библиотек Python для выполнения основных этапов предобработки и подготовки данных.

Обсуждение и заключение. Доказано, что применение системного подхода и автоматизированной обработки данных существенно повышает качество и надежность анализа натурных данных ПТС. Устранение пропусков и нормализация данных улучшают точность, а итоговые форматы данных удобны для дальнейшего использования в моделировании. Подчеркивается универсальность применения Python. Обозначены перспективы исследования — применение методов машинного обучения, кластеризации и моделирования, предназначенных для выявления закономерностей и прогнозирования поведения природно-технических систем в условиях Крайнего Севера под воздействием климатических и антропогенных факторов.

Ключевые слова: анализ данных, библиотеки Python, подготовка данных, предобработка данных, информационные технологии

Финансирование. Работа выполнена при финансовой поддержке РНФ (грант № 23–61–10032).

Для цитирования. Кушуков С.В., Иванов К.Н., Левашкин С.П., Якобовский М.В. Автоматическая обработка первичных данных натурных исследований поведения природно-технических систем при изменении климата и антропогенных воздействиях в условиях Крайнего Севера. *Computational Mathematics and Information Technologies*. 2025;9(2):52–64. https://doi.org/10.23947/2587-8999-2025-9-2-52-64

Introduction. The study of natural-technological systems (NTS) under climate change and anthropogenic impacts, especially in the challenging conditions of the Far North, represents an important scientific problem. These systems are formed as a result of interactions between natural processes and technical objects, and their stability largely depends on the dynamics of external factors. To identify patterns of NTS functioning and predict possible changes, a comprehensive data analysis is required.

Information processing obtained during field studies involves several stages: collection of primary data, their preliminary processing, analysis, and interpretation of results. The goal of this work is to develop methods for automated processing of field data, which will allow identification of key trends and patterns in the interaction between natural and technogenic factors [1–3].

The relevance of the research is driven by the need to make informed decisions to ensure sustainable functioning and management of natural-technological systems under increasing climatic and anthropogenic impacts [2–8].

First, we present algorithmic libraries [4] that provide diverse tools for data processing, analysis, and modelling [5]:

• scikit-learn: a universal machine learning toolkit covering the entire process from data preparation to model evaluation. This library includes all necessary functions to solve machine learning and statistical analysis tasks [9, 10];

• statsmodels: a library for estimating statistical models, offering tools for statistical tests, regression analysis, and time series analysis.

Next, we list visualization libraries that enable effective data presentation:

• matplotlib: helps create static, interactive, and animated graphs in Python. It provides a broad arsenal of tools for visualizing data in various formats, revealing a wide range of possibilities for illustrative information presentation [11–14];

• seaborn: a data visualization library built on top of matplotlib, offering a high-level interface for creating informative statistical graphics.

Additionally, we mention scientific computing libraries used for mathematical calculations and data processing:

• pandas: a framework for data manipulation and analysis. It provides powerful tools including data structures like DataFrame, which simplify working with tabular data. The library is widely used in loading, cleaning, analyzing, and preparing data before integration into machine learning algorithms;

• numpy: a library designed for manipulating multidimensional arrays and matrices, as well as performing mathematical operations on them. It offers a variety of functions optimized for efficient numerical data processing;

• scipy: a highly efficient library for scientific and technical computations, extending functionalities for optimization, integration, interpolation, and many other scientific tasks.

Materials and Methods

Review of Existing Research. In recent years, there has been a growing interest in studying the influence of climatic and anthropogenic factors on natural-technological systems (NTS). Various studies emphasize the necessity of a comprehensive approach to managing these systems to ensure their stability and functionality.

R.S. Rozhkov and co-authors, in their work "Management of Natural-Technological Systems through the Concept of Sustainable Development and Acceptable Risk" [15], highlight the importance of considering environmental, economic, and social factors in the management of NTS. The authors propose using systems analysis and risk assessment to develop optimal strategies aimed at reducing anthropogenic load and improving the ecological state of the environment.

N. Dregulo investigates the impact of climatic factors on the operation of NTS related to wastewater treatment. In [16], it is emphasized that increased atmospheric precipitation can adversely affect the operational and environmental performance of such systems, necessitating the revision of regulatory criteria and adaptation to changing climatic conditions.

The article "Impact of Anthropogenic Factors on Urban Heat Pollution" [17] presents a comprehensive assessment of human activity's effects on atmospheric heat pollution. It is noted that a significant share of heat pollution is contributed by heat consumption and transportation, underscoring the need to develop measures to reduce anthropogenic thermal impact in urbanized areas.

A study published on the website of LLC "Biochem-TL" analyzes the influence of anthropogenic factors on agricultural development [18]. Particular attention is given to soil changes caused by prolonged use of fertilizers and livestock waste, which affect the ecological condition of agricultural landscapes.

Taken together, these studies highlight the necessity of a comprehensive and adaptive approach to managing natural-technological systems amid changing climate and increasing anthropogenic pressure. Accounting for the specifics of each NTS component and continuous monitoring of their condition are key elements to ensure their sustainable functioning.

Research Subject Area. The object of the study is the Main Building of the Yakutsk Thermal Power Plant (Yakutsk TPP) — a unique engineering structure constructed on permafrost (cryolithozone) conditions. This facility is particularly interesting because it was the first industrial building in the USSR erected on permafrost soils following the pioneering principle of construction. This means that during construction, measures were taken to preserve the frozen soils as a reliable foundation for the power plant. Construction began in 1933, with active participation from scientists specializing in permafrost studies. In 1937, the TPP was commissioned and has since been supplying electricity to Yakutsk, and since 1961 — also heat.

To understand how the TPP operates under permafrost conditions and how it is affected by various external factors, a computational model was developed. This model covers an area of 180 by 150 meters and extends to a depth of up to 30 meters, enabling analysis of the permafrost soils (multi-year frozen ground, MYFG) on which the plant stands. The model is based on data from engineering-geological boreholes. These data allow determining the behavior of soils under varying temperature and external conditions, which is crucial for ensuring the stable operation of the TPP.

Special attention in the study is given to the thermal regime of the surrounding environment. Average monthly air temperature data for the Yakutsk region over the past 10 years were collected and analyzed. These data are significant for understanding how climatic conditions change and how these changes may affect the state of frozen soils and the operation of the TPP. It is important to note that these data differ from those provided by the Hydrometeorological Service based on norms established since 1966. Normative data are statistical indicators obtained by long-term averaging of climatic observations (usually over a 30-year period). These indicators serve as reference values for assessing the climatic conditions of the region. However, under current climate change conditions, if these norms are not regularly updated, they may not reflect modern trends and often underestimate temperature values, limiting their applicability in analyzing the current climate state.

For studying thermodynamic processes in permafrost soils, field data obtained from engineering-geological boreholes and stationary observation sites were used. These data represent detailed time series covering multi-year measurements of key parameters of permafrost soils in various regions of Yakutia.

Data were collected from three main sources:

• Yakutsk Thermal Power Plant (TPP) — 8 engineering-geological boreholes where systematic measurements of soil temperature and moisture are conducted, as well as studies of the lithological composition, physical, and thermophysical properties of frozen soils;

• Chabyda and Tuymaada observation stations — 16 sites where soil temperature and moisture, seasonal dynamics of thaw depth, interannual variability of the seasonally thawed layer (STS), snow cover height, snow density, and physical-mechanical soil properties are recorded;

• Railway section of the Amur-Yakutsk railway line — 41 engineering-geological boreholes collecting data on soil temperature and moisture, variability of the STS, snow cover height, and other geocryological parameters.

Unlike generalized climatic norms presented in official sources, these data reflect the actual processes occurring in permafrost soils, with high resolution in depth and time. This makes them a unique source of information for studying the stability of natural-technical systems of the Far North under conditions of climate change and anthropogenic impacts.

Data Processing and Preliminary Analysis. Consider the preprocessing of data using the example of a monitoring dataset from sixteen sites in Yakutia, provided by the Permafrost Institute of the Siberian Branch of the Russian Academy of Sciences (SB RAS). Each site contains its own observational data. For example, "Site 9_Chabyda" includes information on soil temperature, moisture, seasonal dynamics of thaw depth, interannual variability of the seasonally thawed layer, monthly snow height, interannual dynamics of snow density, seasonal dynamics of snowpack density and height, lithological profile, and physical and thermophysical properties of soil and surface covers.

The objective of the study is to prepare data analysis using machine learning methods and to find relationships between their attributes. It should be emphasized that the processes automated by the authors are usually performed manually or using interactive methods. As a result of this interaction, structured and analysis-ready datasets are formed, transformed from the raw data initially provided.

The structural scheme of the automatic data processing workflow is shown in Fig. 1.

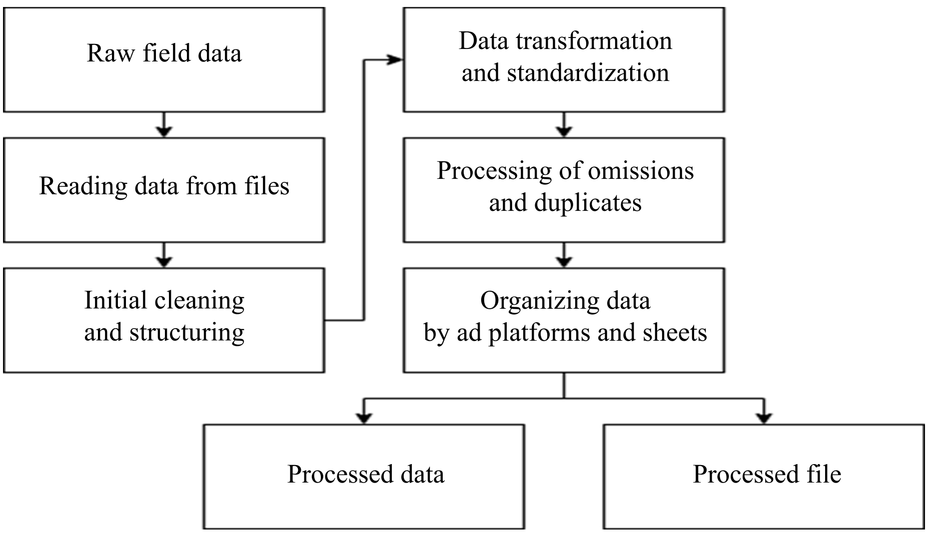

Fig. 1. Structural scheme of automated primary data processing

For data preprocessing, it is necessary to read data from XLS files (the original format of the monitoring data) and load them into a DataFrame object using the pandas library. This stage includes detecting and handling missing values, choosing a strategy for filling gaps in columns, as well as removing irrelevant features.

To analyze the dataset, all relevant data should be prepared and the described Python modules applied in practice [7–8]. The first stage is extracting data from the XLS file. Efficient storage and processing of tabular data are critical aspects when analyzing data.

We obtain information about the number of files per site:

```
def get_excel_files_info(folder_path: str):
""" """
excel_files_info = []
for filename in tqdm(os.listdir(folder_path)):
if filename.endswith('.xls') or filename.endswith('.xlsx'):
file_path = os.path.join(folder_path, filename)
if filename.endswith('.xls'):
xls_workbook = xlrd.open_workbook(file_path)
number_sheets = xls_workbook.nsheets
else:
workbook = load_workbook(file_path)
number_sheets = len(workbook.sheetnames)
name_for_directory, extension = os.path.splitext(filename)
file_info = {
'file_path': file_path,
'name_file': filename,
'type_file': 'xls' if filename.endswith('.xls') else 'xlsx',
'number_sheets': number_sheets,
'name_for_directory': name_for_directory,
}
excel_files_info.append(file_info)
return excel_files_info[::-1]
raw_data = get_excel_files_info(data_cache)
print(f'Number files: {len(raw_data)}\n\nList files:\n')
pprint.pprint(raw_data).
```

After executing the code, the variable raw_data will contain information about the files located in the directory, which allows for easy viewing of the contents of these files (Fig. 2).

```
Number files: 16

List files:

[{'file_path': '/home/user/data_farm/projects/rnf_yakutia/data_cache/monitoring_data/Площадка '
               'Луг_Туймаада.xlsx',
  'name_file': 'Площадка Луг_Туймаада.xlsx',
  'name_for_directory': 'Площадка Луг_Туймаада',
  'number_sheets': 9,
  'type_file': 'xlsx'},
 {'file_path': '/home/user/data_farm/projects/rnf_yakutia/data_cache/monitoring_data/Площадка '
               'Лес_Туймаада.xlsx',
  'name_file': 'Площадка Лес_Туймаада.xlsx',
  'name_for_directory': 'Площадка Лес_Туймаада',
  'number_sheets': 9,
  'type_file': 'xlsx'},
 {'file_path': '/home/user/data_farm/projects/rnf_yakutia/data_cache/monitoring_data/Площадка '
               '(Скважина) 1_Чабыда.xlsx',
  'name_file': 'Площадка (Скважина) 1_Чабыда.xlsx',
  'name_for_directory': 'Площадка (Скважина) 1_Чабыда',
  'number_sheets': 9,
  'type_file': 'xlsx'},
 {'file_path': '/home/user/data_farm/projects/rnf_yakutia/data_cache/monitoring_data/Площадка '
               '10_Чабыда.xlsx',
  'name_file': 'Площадка 10_Чабыда.xlsx',
  'name_for_directory': 'Площадка 10_Чабыда',
  'number_sheets': 9,
  'type_file': 'xlsx'},
 {'file_path': '/home/user/data_farm/projects/rnf_yakutia/data_cache/monitoring_data/Площадка '
               '11_Чабыда.xlsx',
  'name_file': 'Площадка 11_Чабыда.xlsx',
  'name_for_directory': 'Площадка 11_Чабыда',
  'number_sheets': 9,
  'type_file': 'xlsx'},
 {'file_path': '/home/user/data_farm/projects/rnf_yakutia/data_cache/monitoring_data/Площадка '
```

Fig. 2. File information

Next, we analyze the number of sheets in each dataset file:

```
def read_non_empty_excel(file_path, sheet_name):
""" """
df = pd.read_excel(file_path, sheet_name=sheet_name)
return df if not df.empty else None
raw_file = raw_data[15]
state_name = raw_file.get('name_for_directory')
df = pd.ExcelFile(raw_file.get('file_path'))
dfs = {name_sheet: read_non_empty_excel(df, name_sheet) for name_sheet in df.sheet_names
if read_non_empty_excel(df, name_sheet) is not None}
key_list = list(dfs.keys())
print(f'Name file: {state_name}\n\nNumber sheets: {len(key_list)}\n\nNames all sheets in
this file:\n\n{key_list}').
```

After running the code, we will have information about the number of sheets in the dataset, as well as the name of each sheet, which allows us to directly access a specific sheet by its name (Fig. 3).

```
Name file: Площадка 9_Чабыда

Number sheets: 9

Names all sheets in this file:

['Температура грунтов', 'Влажность грунтов', 'Сезон.дина
м.глубины протаивания', 'Межгодовая изменчивость СТС', 'М
есячная высота снега', 'Межгод.динамика плотн.снега', 'Се
зон.динамика плотн.выс.снега', 'Литологический разрез',
'Физические и теплофизические...']
```

Fig. 3. Output of sheet information

However, it should be noted that some datasets contain errors in the sheet names that need to be corrected to avoid problems in further analysis:

```
# Naming errors 1
if 'Interannual snow density dynamics' in dfs:
   dfs['Interannual snow density dynamics'] = dfs.pop('Interannual snow dnamics density')
if 'Interannual snow density dynamics ' in dfs:
   dfs['Interannual snow density dynamics'] = dfs.pop('Interannual snow density dynamics ')
if 'Interannual snow density dynamics' in dfs:
   dfs['Interannual snow density dynamics'] = dfs.pop('Interannual snow density dynamics')
# Naming errors 2
if 'Seasonal dynamics of thaw depth' in dfs:
    dfs['Seasonal thaw depth dynamics'] = dfs.pop('Seasonal dynamics of thaw depth')
if 'Seasonal thaw depth dynamics' in dfs:
    dfs['Seasonal thaw depth dynamics'] = dfs.pop('Seasonal thaw depth dynamics')
if 'Seasonal dynamics of snow density and height' in dfs:
    dfs['Seasonal snow density and height dynamics'] = dfs.pop('Seasonal dynamics of
snow density and height')
if 'Seasonal snow density and height dynamics' in dfs:
    dfs['Seasonal snow density and height dynamics'] = dfs.pop('Seasonal snow density
and height dynamics')
# Naming errors 3
if 'Physical and thermophysical...' in dfs:
    dfs['Physical and thermophysical'] = dfs.pop('Physical and thermophysical...')
if 'Physical and thermophysical (typo)...' in dfs:
   dfs['Physical and thermophysical'] = dfs.pop('Physical and thermophysical (typo)...')
key_list = list(dfs.keys())
```

```
print(f'Updated sheet names:\n\n{key_list}').
```

After executing the code, all the sheet names in the document were corrected (Fig. 4).

```
Update sheets names:

['Температура грунтов', 'Влажность грунтов', 'Сезон.дина
м.глубины протаивания', 'Межгодовая изменчивость СТС', 'М
есячная высота снега', 'Межгод.динамика плотн.снега', 'Се
зон.динамика плотн.выс.снега', 'Литологический разрез',
'Физические и теплофизические']
```

Fig. 4. Updated sheet names

Now we can proceed to processing the Excel sheets themselves.

The first sheet is titled "Soil Temperature", which contains information about the measurement date and depth, as well as the measurement values themselves (Fig. 5).

	Температура грунтов, оС	Unnamed: 1	Unnamed: 2	Unnamed: 3	Unnamed: 4	Unnamed: 5	Unnamed: 6	Unnamed: 7	Unnamed: 8	Unnamed: 9	Unnamed: 10	Unnamed: 11	Ur
0	NaN	Глубина, м	NaN	NaN	NaN	NaN	NaN	NaN	NaN	NaN	NaN	NaN	
1	Дата	0	п/п	0.15	0.3	0.5	1.0	1.25	1.5	1.75	2.0	3.00	
2	1985-06-01 00:00:00	NaN	NaN	NaN	NaN	NaN	-2.1	NaN	NaN	NaN	-2.8	-3.00	
3	1985-06-05 00:00:00	NaN	NaN	NaN	NaN	NaN	-2.2	NaN	NaN	NaN	-2.8	-2.90	
4	1985-06-10 00:00:00	NaN	NaN	NaN	NaN	NaN	-1.5	NaN	NaN	NaN	-2.3	-2.70	
...	...	...	...	...	...	...	...	...	...	...	...	...	

Fig. 5. Sheet "Soil Temperature"

For successful data processing, it is necessary to take into account the specifics of how the data are presented. In particular, in some entries of the column containing the depth of the temperature sensors, the designation "п/п" appears. This is not a missing value (NaN – Not a Number), but a special marker indicating that the sensor is located directly under the snow cover. During data preparation, the "п/п" values should be replaced with the corresponding numerical depth values according to the characteristics of the sites.

It should also be noted that the table contains missing values denoted as NaN. In this context, NaN means that a specific parameter was not measured at a given time and depth. Additionally, the column containing dates needs to be converted to a unified format, and the data should be checked for duplicate records, which should be removed if found. A universal code was written to perform all of the above tasks, applicable to all the "Soil Temperature" sheets in the dataset as a whole.

```
df1 = dfs['Soil Temperature']
# Dictionary for replacing «п/п» values for specific sites
dict_pp_values = {'Site 9_Chabyda': 0.08,
                  'Site 10_Chabyda': 0.03,
                  'Site 11_Chabyda': 0.02}
if state_name in dict_pp_values:
    df1.replace({'п/п': dict_pp_values[state_name]}, inplace=True)
dict_pkr_values = {'Site 8_Chabyda': 0.06}
if state_name in dict_pkr_values:
    df1.replace({'под пкр': dict_pkr_values[state_name]}, inplace=True)
date_indices = df1[df1.apply(lambda row: row.astype(str).str.contains('Date').any(),
axis=1)].index[1:]
df1 = df1.drop(date_indices)
df1 = df1.iloc[1:]
df1 = df1.reset_index(drop=True)
df1.columns = df1.iloc[0]
df1 = df1.iloc[1:]
df1 = df1.reset_index(drop=True)
df1 = df1.rename(columns={'Date ': 'Date'})
df1['Date'] = pd.to_datetime(df1['Date'])
```

```
for column in df1.columns:
    if column != 'Date':
        df1[column] = df1[column].astype(float)
def drop_duplicate(df, sort_columns):
    """ Remove duplicate rows and sort the dataframe. """
    duplicate_df = df[df.duplicated()]
    if not duplicate_df.empty:
        print(f'Duplicate rows:\n{duplicate_df}\n')
        df = df.drop_duplicates(keep='last')
    else:
        print('No duplicate rows found')
    df = df.sort_values(by=sort_columns)
    df = df.reset_index(drop=True)
    return df
df1 = drop_duplicate(df1, 'Date')
df1
```

After executing the code, the variable df1 contains the processed sheet «Soil Temperature,» which is easy to read and understand (Fig. 6).

	Дата	0	0.08	0.15	0.3	0.5	1.0	1.25	1.5	1.75	2.0	3.0	4.0	5.0	6.0	7.0	8.0	9.0	10.0
0	1985-06-01	NaN	NaN	NaN	NaN	NaN	-2.1	NaN	NaN	NaN	-2.8	-3.00	NaN	-2.8	-1.7	-1.6	-1.4	-1.4	-1.4
1	1985-06-05	NaN	NaN	NaN	NaN	NaN	-2.2	NaN	NaN	NaN	-2.8	-2.90	NaN	-2.8	-1.6	-1.6	-1.4	-1.4	-1.4
2	1985-06-10	NaN	NaN	NaN	NaN	NaN	-1.5	NaN	NaN	NaN	-2.3	-2.70	NaN	-2.8	-1.7	-1.6	-1.5	-1.5	-1.4
3	1985-06-15	NaN	NaN	NaN	NaN	NaN	-1.3	NaN	NaN	NaN	-2.5	-2.70	NaN	-2.7	-1.6	-1.6	-1.5	-1.5	-1.4
4	1985-06-19	NaN	NaN	NaN	NaN	NaN	-1.1	NaN	NaN	NaN	-2.4	-2.70	NaN	-2.7	-1.6	-1.6	-1.5	-1.5	-1.4
...	...	...	...	...	...	...	...	...	...	...	...	...	...	...	...	...	...	...	...
497	2022-08-19	NaN	NaN	NaN	NaN	NaN	4.1	NaN	NaN	NaN	-1.2	-1.60	-2.1	-2.5	-2.7	-2.5	-2.4	-2.4	NaN
498	2022-09-18	NaN	NaN	NaN	NaN	NaN	1.9	NaN	NaN	NaN	-0.9	-1.30	-1.8	-2.2	-2.4	-2.3	-2.3	-2.5	NaN
499	2022-10-18	NaN	NaN	NaN	NaN	NaN	0.7	NaN	NaN	NaN	0.9	0.60	0.0	-0.2	-0.3	-0.3	-0.4	-0.4	NaN
500	2022-11-16	NaN	NaN	NaN	NaN	NaN	-1.5	NaN	NaN	NaN	-0.1	0.00	0.0	-0.2	-0.3	-0.3	-0.4	-0.4	NaN
501	2022-12-14	NaN	NaN	NaN	NaN	NaN	-5.3	NaN	NaN	NaN	-1.1	-0.04	-0.1	-0.2	-0.3	-0.3	-0.3	-0.4	NaN

502 rows × 19 columns

Fig. 6. Processed data of the "Soil Temperature" sheet

The second sheet, "Soil Moisture", contains similar information to the "Soil Temperature" sheet. However, more transformations are required, such as removing empty rows, renaming the column "Date of determination" to "Date" and converting it to date format, replacing letter values like "Ice" with numeric values, searching for duplicates, and removing them (Fig. 7).

	Влажность грунтов, %	Unnamed: 1	Unnamed: 2	Unnamed: 3	Unnamed: 4	Unnamed: 5	Unnamed: 6	Unnamed: 7	Unnamed: 8	Unnamed: 9	...	Unnamed: 17	Unnamed: 18	Unnamed: 19	Unnamed: 20
0	NaN	Глубина, м	NaN	NaN	NaN	NaN	NaN	NaN	NaN	NaN	...	NaN	NaN	NaN	NaN
1	Дата определения	0.05	0.1	0.2	0.3	0.4	0.5	0.6	0.7	0.8	...	1.6	1.7	1.8	1.9
2	1985-06-09 00:00:00	31.5	22.9	15.6	19.6	20.0	16.0	16.7	17.0	19.6	...	27.4	33.0	30.5	44.2
3	1985-08-30 00:00:00	46.4	17.4	16.0	NaN	12.8	NaN	8.7	NaN	11.2	...	NaN	NaN	NaN	NaN
4	1985-09-16 00:00:00	35	9.7	7.5	NaN	12.6	NaN	13.9	NaN	10.0	...	NaN	NaN	NaN	NaN
5	1986-06-16 00:00:00	21.9	19.4	14.2	15.2	20.9	NaN	19.4	NaN	NaN	...	NaN	NaN	NaN	NaN
6	1986-07-17 00:00:00	12.3	13.8	15.3	18.9	18.6	NaN	15.8	NaN	22.9	...	NaN	NaN	NaN	NaN
7	1986-08-27 00:00:00	7.8	5.8	6.6	12.2	15.2	15.2	11.7	NaN	14.4	...	NaN	NaN	NaN	NaN
8	1986-09-28 00:00:00	23.2	16.1	17.2	13.7	13.4	16.0	17.9	NaN	18.8	...	NaN	NaN	NaN	NaN
9	1990-10-02 00:00:00	16.1	11.2	10.8	NaN	16.3	NaN	20.4	NaN	23.0	...	28.6	NaN	NaN	NaN
10	1991-04-04 00:00:00	48.5	22.5	22.4	NaN	21.5	NaN	26.0	NaN	28.9	...	46.1	NaN	NaN	NaN
11	2002-09-13 00:00:00	NaN	NaN	15.8	NaN	11.5	NaN	12.0	NaN	8.3	...	NaN	NaN	NaN	NaN

12 rows × 27 columns

Fig. 7. The "Soil Moisture" sheet

To accomplish this, code was written that performs all these transformations for the “Soil Moisture” sheets:

```
df2 = dfs['Влажность грунтов']
df2 = df2.iloc[1:]
df2 = df2.reset_index(drop=True)
df2.columns = df2.iloc[0]
df2 = df2.iloc[1:]
df2 = df2.reset_index(drop=True)
df2 = df2.rename(columns={'Дата определения': 'Дата'})
df2 = df2.dropna(how='all')
df2 = df2.dropna(thresh=2)
if state_name == 'Площадка Лес_Туймаада':
df2['Дата'] = df2['Дата'].astype(str)
df2['Скважена'] = df2['Дата'].apply(lambda x: 1 if '*' in x else 2)
df2['Дата'] = df2['Дата'].astype(str).str.replace(' *', '')
df2['Дата'] = df2['Дата'].astype(str).str.replace('*', '')
df2['Дата'] = df2['Дата'].apply(lambda x: x + ' 00:00:00' if len(x) == 10 else x)
for index, row in df2.iterrows():
try:
df2.at[index, 'Дата'] = pd.to_datetime(row['Дата'], format='%d.%m.%Y %H:%M:%S').
strftime('%Y-%m-%d %H:%M:%S')
except ValueError:
pass
if state_name == 'Площадка Луг_Туймаада':
df2['Дата'] = df2['Дата'].astype(str)
df2 = df2[~df2['Дата'].str.contains('Дата')]
def fill_skvazhena(row):
if '*' in row['Дата']:
return '2'
elif row['Дата'].count(' ') == 0 and not row['Дата'].isdigit():
return '3'
else:
return '1'
df2['Скважена'] = df2.apply(fill_skvazhena, axis=1)
df2['Дата'] = df2['Дата'].astype(str).str.replace(' *', '')
df2['Дата'] = df2['Дата'].astype(str).str.replace('*', '')
df2['Дата'] = df2['Дата'].apply(lambda x: x + ' 00:00:00' if len(x) == 10 else x)
for index, row in df2.iterrows():
try:
df2.at[index, 'Дата'] = pd.to_datetime(row['Дата'], format='%d.%m.%Y %H:%M:%S').
strftime('%Y-%m-%d %H:%M:%S')
except ValueError:
pass
months_dict = {'Январь': 'January',
               'Февраль': 'February',
               'Март': 'March',
               'Апрель': 'April',
               'Май': 'May',
               'Июнь': 'June',
               'Июль': 'July',
               'Август': 'August',
               'Сентябрь': 'September',
               'Октябрь': 'October',
               'Ноябрь': 'November',
               'Декабрь': 'December'}
months_dict_number = {'January': '01',
                      'February': '02',
                      'March': '03',
```

```
                      'April': '04',
                      'May': '05',
                      'June': '06',
                      'July': '07',
                      'August': '08',
                      'September': '09',
                      'October': '10',
                      'November': '11',
                      'December': '12'}
df2['Год'] = np.where(df2['Скважена'] == '3', '1979', np.nan)
df2['Дата'].replace(months_dict, inplace=True, regex=True)
df2['Дата'].replace(months_dict_number, inplace=True, regex=True)
df2.loc[df2['Скважена'] == '3', 'Дата'] = df2['Год'] + '-' + df2['Дата'] + '-01 00:00:00'
df2 = df2.drop(['Год'], axis=1)
df2 = df2.sort_values(by='Дата')
df2 = df2.reset_index(drop=True)
df2['Дата'] = pd.to_datetime(df2['Дата'])
# Замена значения «Лед» на «-1.0»
df2.replace('Лед', -1.0, inplace=True)
for column in df2.columns:
if column != 'Дата':
df2[column] = df2[column].astype(float)
if 'Скважена' in df2.columns:
df2['Скважена'] = df2['Скважена'].astype(int)
df2 = drop_duplicate(df2, 'Дата').
```

After running the code, the variable df2 contains the processed sheet «Soil Moisture,» presented in a human-readable format (Fig. 8).

	Дата	0.05	0.1	0.2	0.3	0.4	0.5	0.6	0.7	0.8	...	1.6	1.7	1.8	1.9	2.0	2.2	2.4	2.6	2.8	3.0
0	1985-06-09	31.5	22.9	15.6	19.6	20.0	16.0	16.7	17.0	19.6	...	27.4	33.0	30.5	44.2	71.1	31.4	28.3	18.5	19.2	20.9
1	1985-08-30	46.4	17.4	16.0	NaN	12.8	NaN	8.7	NaN	11.2	...	NaN	NaN	NaN	NaN	NaN	NaN	NaN	NaN	NaN	NaN
2	1985-09-16	35.0	9.7	7.5	NaN	12.6	NaN	13.9	NaN	10.0	...	NaN	NaN	NaN	NaN	NaN	NaN	NaN	NaN	NaN	NaN
3	1986-06-16	21.9	19.4	14.2	15.2	20.9	NaN	19.4	NaN	NaN	...	NaN	NaN	NaN	NaN	NaN	NaN	NaN	NaN	NaN	NaN
4	1986-07-17	12.3	13.8	15.3	18.9	18.6	NaN	15.8	NaN	22.9	...	NaN	NaN	NaN	NaN	NaN	NaN	NaN	NaN	NaN	NaN
5	1986-08-27	7.8	5.8	6.6	12.2	15.2	15.2	11.7	NaN	14.4	...	NaN	NaN	NaN	NaN	NaN	NaN	NaN	NaN	NaN	NaN
6	1986-09-28	23.2	16.1	17.2	13.7	13.4	16.0	17.9	NaN	18.8	...	NaN	NaN	NaN	NaN	NaN	NaN	NaN	NaN	NaN	NaN
7	1990-10-02	16.1	11.2	10.8	NaN	16.3	NaN	20.4	NaN	23.0	...	28.6	NaN	NaN	NaN	NaN	NaN	NaN	NaN	NaN	NaN
8	1991-04-04	48.5	22.5	22.4	NaN	21.5	NaN	26.0	NaN	28.9	...	46.1	NaN	NaN	NaN	NaN	NaN	NaN	NaN	NaN	NaN
9	2002-09-13	NaN	NaN	15.8	NaN	11.5	NaN	12.0	NaN	8.3	...	NaN	NaN	NaN	NaN	NaN	NaN	NaN	NaN	NaN	NaN

10 rows × 27 columns

Fig. 8. Processed data of the "Soil Moisture" sheet

In a similar way, the remaining seven sheets for "Site 9_Chabyda" and the other fifteen sites, each containing nine sheets of data, were processed. To save the results of this work, a function was written that creates a directory with subfolders to store the processed data by site and corresponding sheets (Fig. 9) in the following formats:

• CSV (Comma-Separated Values) — one of the most common formats for representing tabular data, a simple and universal format used for storing data as text files based on comma-separated values;

• JSON (JavaScript Object Notation) — a standard text format for storing and transmitting structured data;

• XLSX — the Microsoft Excel file format used for storing spreadsheets.

```
 11%|████                                       | 1/9 [00:00<00:00,  9.31it/s]
Directory /home/user/data_farm/projects/rnf_yakutia/data/monitoring_data/Площадка 9_Чабыда/csv/ create
Directory /home/user/data_farm/projects/rnf_yakutia/data/monitoring_data/Площадка 9_Чабыда/json/ create
Directory /home/user/data_farm/projects/rnf_yakutia/data/monitoring_data/Площадка 9_Чабыда/xlsx/ create
100%|███████████████████████████████████████████| 9/9 [00:00<00:00, 42.49it/s]
```

Fig. 9. Saving processed data in CSV, JSON, and XLSX formats

A script was also written to create an XLSX file containing summary information about the sites:

```
xlsx_files = [f for f in os.listdir(f'{folder_path}/xlsx/') if f.endswith(«.xlsx»)]
xlsx_dfs = {}
# Reading data from each file and adding it to a dictionary
for file in xlsx_files:
file_path = os.path.join(f'{folder_path}/xlsx/', file)
xl = pd.ExcelFile(file_path)
for sheet_name in xl.sheet_names:
df = xl.parse(sheet_name)
if sheet_name not in xlsx_dfs:
xlsx_dfs[sheet_name] = []
xlsx_dfs[sheet_name].append(df)
with pd.ExcelWriter(f'{folder_path}/xlsx/{state_name}.xlsx', engine='xlsxwriter') as
writer:
for sheet_name, dataframes in xlsx_dfs.items():
for i, df in enumerate(dataframes):
df.to_excel(writer, sheet_name=sheet_name, index=False).
```

After running it, a file with summary information for each of the sites is generated (Fig. 10).

Площадка	Широта_дмс	Долгота_дмс	Широта_дд	Долгота_дд	Количество_метрик	Тип_местности	Условия	Первая_дата	Последняя_дата
Площадка Луг_Туйм...	62° 00' 49" с.ш.	129° 39' 24" в.д.	62.0136	129.6567	9		Сливающейся мерзл...	1967-08-14	2022-12-14
Площадка Лес_Туйм...	61° 00' 46" с.ш.	129° 39' 11" в.д.	61.0128	129.6531	8		Сливающейся мерзл...	1967-08-16	2022-12-14
Площадка (Скважин...	61° 57' 27" с.ш.	129° 24' 50" в.д.	61.9575	129.4139	9	Мелкодолинный	Сливающейся и не с...	1980-09-12	2022-12-14
Площадка 10_Чабыда	61° 57' 10" с.ш.	129° 25' 46" в.д.	61.9528	129.4294	9	Склонный	Сливающейся и не с...	1982-11-01	2022-12-14
Площадка 11_Чабыда	61° 57' 00" с.ш.	129° 25' 48" в.д.	61.9500	129.4300	9	Склонный	Сливающейся и не с...	1982-11-01	2022-12-14
Площадка 3_Чабыда	61° 57' 36" с.ш.	129° 24' 53" в.д.	61.9600	129.4147	9	Склонный	Сливающейся и не с...	1981-01-01	1989-01-01
Площадка 3а_Чабыда	61° 57' 26" с.ш.	129° 25' 17" в.д.	61.9572	129.4214	9	Склонный	Сливающейся и не с...	1982-11-01	2022-12-14
Площадка 4_Чабыда	61° 57' 24" с.ш.	129° 25' 27" в.д.	61.9567	129.4242	9	Склонный	Сливающейся и не с...	1980-07-02	1989-01-01
Площадка 5_Чабыда	61° 57' 28" с.ш.	129° 25' 03" в.д.	61.9578	129.4175	9	Склонный	Сливающейся и не с...	1980-07-02	2022-12-14
Площадка 6_Чабыда	61° 57' 36" с.ш.	129° 24' 53" в.д.	61.9600	129.4147	9	Склонный	Сливающейся и не с...	1982-10-01	1992-04-01
Площадка 6б_Чабыда	61° 57' 24" с.ш.	129° 25' 27" в.д.	61.9567	129.4242	9	Склонный	Сливающейся и не с...	1982-11-01	2022-12-14
Площадка 7_Чабыда	61° 57' 36" с.ш.	129° 24' 53" в.д.	61.9600	129.4147	9	Склонный	Сливающейся и не с...	1982-10-01	1991-04-02
Площадка 7б_Чабыда	61° 57' 26" с.ш.	129° 25' 17" в.д.	61.9572	129.4214	9	Склонный	Сливающейся и не с...	1982-11-01	2022-12-14
Площадка 8_Чабыда	61° 57' 17" с.ш.	129° 25' 13" в.д.	61.9547	129.4203	9	Мелкодолинный	Сливающейся и не с...	1982-10-01	2022-12-14
Площадка 8а_Чабыда	61° 57' 14" с.ш.	129° 25' 09" в.д.	61.9540	129.4192	9	Мелкодолинный	Сливающейся и не с...	1982-11-01	2022-12-14
Площадка 9_Чабыда	61° 57' 03" с.ш.	129° 05' 56" в.д.	61.9508	129.0989	9	Склонный	Сливающейся и не с...	1982-11-01	2022-12-14

Fig. 10. File with summary information on the sites

Results. The processing and systematization of data made it possible to unify disparate measurements into a consistent format, ensuring their correct use in subsequent calculations. As a result, a unique dataset was obtained that has no analogs, since it is based on direct empirical observations and covers the specific conditions of the studied area.

Data analysis using Python is a highly demanded skill in the modern world. This language is characterized by relative ease of learning, making it accessible for beginners. The work considered the main stages of data processing using Python libraries: preprocessing and data preparation. Using the example of the dataset "Site 9_Chabyda," key preprocessing techniques were demonstrated, such as detection and handling of missing values, data transformation, optimization, as well as removal of insignificant attributes.

Discussion and Conclusion. The results demonstrate that applying a systematic approach to data processing significantly improves the quality and reliability of the analysis. Addressing missing data and normalizing the dataset improves the reliability of the dataset. The final processed data is provided in convenient formats for further use in modelling, including CSV, JSON, and XLSX formats. This highlights the versatility of Python in solving data processing tasks.

Future research plans include expanding the study by incorporating data analysis methods such as clustering, machine learning model development, and result visualization [12, 14, 19]. These methods will not only help uncover hidden patterns within the data but also enable the prediction of the behavior of natural-technical systems under changing external conditions. Special attention will be given to modelling the impact of climatic factors and anthropogenic loads on natural-technical systems, providing a more comprehensive understanding of processes occurring in the conditions of the Far North.

References

1. Poruchikov M. A. *Data analysis*. Samara: Samara University Press; 2016. 88 p. (In Russ.)
2. *Introduction to Data Analysis*. URL: https://mipt-stats.gitlab.io/courses/ad_fivt/titanik.html (accessed: 08.08.2024)
3. Leskovec Yu. *Analysis of Large Datasets.* Moscow: DMK; 2016. 498 p. (In Russ.)

4. McKinney W. *Python and Data Analysis*. Moscow: DMK; 2015. 482 p. (In Russ.)
5. Makshanov A.V. *Data Mining Technologies*. Saint Petersburg: Lan; 2018. 212 p. (In Russ.)
6. Mirkin B.G. *Introduction to Data Analysis*. Lyubertsy: Yurayt; 2016. 174 p. (In Russ.)
7. Rafalovich V. *Data Mining, or Data Analysis for the Busy: Practical Course*. Moscow: SmartBook; 2018. 352 p. (In Russ.)
8. Chashkin Yu.R. *Mathematical Statistics. Data Analysis and Processing*. Rostov-on-Don: Feniks; 2017. 236 p. (In Russ.)
9. Gron A. *Machine Learning and Data Analysis with Python*. Saint Petersburg: Piter; 2019. 460 p. (In Russ.)
10. Vorontsov K.V. *Machine Learning and Data Mining*. Moscow: MIPT Publishing; 2018. 328 p. (In Russ.)
11. Algozina E.R. *Data Processing and Analysis with Python and Pandas: Beginner's Guide*. Moscow: DMK; 2020. 312 p. (In Russ.)
12. Troyan I.V. *Data Analysis and Machine Learning in Python*. Saint Petersburg: BHV-Peterburg; 2019. 320 p. (In Russ.)
13. McKinney W. *Python Programming and Data Analysis*. Saint Petersburg: Piter; 2020. 504 p. (In Russ.)
14. Mueller A.C., Guido S. *Introduction to Machine Learning with Python*. Saint Petersburg: Piter; 2017. 420 p. (In Russ.)
15. Rozhkov R.S., Molchanova E.S., Fadeev M.K., Pimenov N.A. Managing Natural-Technical Systems through the Concept of Sustainable Development and Acceptable Risk. *Bulletin of Eurasian Science*. 2024;16(5):1–10. (In Russ.)
16. Dregulo N. Influence of Climatic Factors on the Operation of Natural-Technical Systems for Wastewater Treatment. URL: https://pureportal.spbu.ru/ru/publications/---------%28a9c91d8e-c5e0-43d9-98b5-8aac39cc4a61%29.html (accessed: 13.01.2025) (In Russ.)
17. Impact of Anthropogenic Factors on Thermal Pollution of the Urban Environment. URL: https://www.abok.ru/for_spec/articles.php?nid=7635 (accessed: 13.01.2025) (In Russ.)
18. Impact of Anthropogenic Factors on Agricultural Development. URL: https://biohim.com.ru/articles/page2 (accessed: 13.01.2025) (In Russ.)
19. Levashkin S.P., Ivanov K.N., Kushukov S.V. Data Farm: An Information System for Collecting, Storing, and Processing Unstructured Data from Heterogeneous Sources. *Proceedings of the Institute for System Programming of the RAS (Proceedings of ISP RAS)*. 2023;35(2):57–72. https://doi.org/10.15514/ISPRAS-2023-35(2)-5 (In Russ.)

About the Authors:

Sergey V. Kushukov, Engineer, Povolzhskiy State University of Telecommunications and Informatics, Research Laboratory "Artificial Intelligence" (77, Moskovskoe Shosse, Samara, 443090, Russian Federation), ORCID, SPIN-code, s.kushukov@psuti.ru

Konstantin N. Ivanov, Engineer, Povolzhskiy State University of Telecommunications and Informatics, Research Laboratory "Artificial Intelligence" (77, Moskovskoe Shosse, Samara, 443090, Russian Federation), ORCID, SPIN-code, k.ivanov@psuti.ru

Sergey P. Levashkin, Candidate of Physical and Mathematical Sciences, Associated Professor, Povolzhskiy State University of Telecommunications and Informatics, Head of Research Laboratory "Artificial Intelligence" (77, Moskovskoe Shosse, Samara, 443090, Russian Federation), ORCID, SPIN-code, ai_lab@psuti.ru

Mikhail V. Yakobovskiy, Corresponding Member of the Russian Academy of Sciences, Doctor of Physical and Mathematical Sciences, Director, Keldysh Institute of Applied Mathematics of the Russian Academy of Sciences (IPM RAS), (4, Miusskaya pl., Moscow, 125047, Russian Federation), ORCID, SPIN-code, lira@imamod.ru

Contributions of the authors:
S.V. Kushukov: development, testing of existing code components; writing a draft of a manuscript.
K.N. Ivanov: formal analysis.
S.P. Levashkin: problem statement; formulation of research ideas; goals and objectives.
M.V. Yakobovskiy: review and editing of the manuscript.

Conflict of Interest Statement: **the authors declare no conflict of interest.**

All authors have read and approved the final manuscript.

Об авторах:

Сергей Владимирович Кушуков, инженер Поволжского государственного университета телекоммуникаций и информатики, Научно-исследовательской лаборатории «Искусственный интеллект» (443090, Российская Федерация, г. Самара, Московское ш., 77), ORCID, SPIN-код, s.kushukov@psuti.ru

Константин Николаевич Иванов, инженер Поволжского государственного университета телекоммуникаций и информатики, Научно-исследовательской лаборатории «Искусственный интеллект» (443090, Российская Федерация, г. Самара, Московское ш., 77), ORCID, SPIN-код, k.ivanov@psuti.ru

Сергей Павлович Левашкин, кандидат физико-математических наук, доцент Поволжского государственного университета телекоммуникаций и информатики, заведующий Научно-исследовательской лаборатории «Искусственный интеллект» (443090, Российская Федерация, г. Самара, Московское ш., 77), ORCID, SPIN-код, ai_lab@psuti.ru

Михаил Владимирович Якобовский, член-корреспондент РАН, доктор физико-математических наук, директор Института прикладной математики имени М.В. Келдыша РАН (ИПМ РАН), (125047, Российская Федерация, г. Москва, Миусская пл., 4), ORCID, SPIN-код, lira@imamod.ru

Заявленный вклад авторов:
С.В. Кушуков: разработка, тестирование существующих компонентов кода; написание черновика рукописи.
К.Н. Иванов: формальный анализ.
С.П. Левашкин: постановка задачи; формулировка идей исследования, целей и задач.
М.В. Якобовский: рецензирование и редактирование рукописи.

Конфликт интересов: ***авторы заявляют об отсутствии конфликта интересов.***

Все авторы прочитали и одобрили окончательный вариант рукописи.

Received / Поступила в редакцию 15.05.2025
Revised / Поступила после рецензирования 02.06.2025
Accepted / Принята к публикации 18.06.2025